

The Caledonian tectonomagmatic evolution of the Orkney Islands, Scotland

*A new interpretation based on
geochronological, geochemical and field
data*

Audun Dalene Bjerga



Master thesis at the department of geosciences

UNIVERSITY OF OSLO

[01.06.2017]

A new interpretation based on geochronological, geochemical and field data

© Audun Dalene Bjerga

2017

The Caledonian tectonomagmatic evolution of the Orkney Islands, Scotland

Audun Dalene Bjerga

Abstract

The geology of the Orkney Islands is dominated by well-studied Devonian sedimentary rocks deposited in the Orcadian basin. However, on the islands of Mainland Orkney and Graemsay there are small, relatively poorly studied outcrops of the underlying basement. Based on comparison with rocks in mainland Scotland this basement has been suggested to comprise pre-Caledonian para-gneisses and Caledonian granites. This has, however, never been documented. Here the contact relationships in the basement have been documented and through geochronological, geochemical and structural geologic studies the Caledonian tectono-magmatic history of the Orkneys is unraveled.

Two granites intruded the metasedimentary gneiss at $431\pm$ Ma and $430\pm$ Ma, during the Scandian phase of the Caledonian Orogeny. Inherited zircon grains in the granites, most likely derived from the host rock, give ages that are typical of Moine schist. Both the granite and gneiss are observed to be cut by mylonite zones, later overprinted by phyllonites and brittle faults. In total, three shear zones are observed, all overprinted by phyllonites and brittle faults: a northern one at Yesnaby showing top-to-the-north sense of shear and two southern ones at Stromness and Graemsay showing top-to-the-south sense of shear.

Above the basement complex east of Stromness an intraformational rhyolite occurring in the basal Devonian Hara Ebb formation date the onset of Devonian deposition and probably initiation of the Orcadian basin at $390,\pm 0.41$ Ma. The Hara Ebb formation contains clasts of the local granites and gneisses, showing that the Orkney basement was exposed during its formation.

Based on these new results I present a model for the tectono-magmatic evolution of the Orkneys summed up by: 1) initial formation of high Ba-Sr melts due to slab breakoff during the start of continental collision and melt ascension through crustal scale shear zones associated with the Great Glen Fault system; 2) intrusion of granites into gneisses (probably of the Moine Group) in a pull-apart strike-slip setting controlled by large scale movement on the Great Glen Fault and an associated more local Riedel shear zone; 3) progressive exhumation of the basement on shear zones and subsequently brittle faults; 4) uplift of the basement above sea level before eruption of the subaerial Quoyelsh rhyolite at ca. 390 Ma; 5) probable initiation of the Orcadian basin marked by eruption of the intraformational Quoyelsh rhyolites at the base of the Hara Ebb Formation.

Acknowledgements

First I would give a warm and sincere thanks to my supervisor! Professor Anders Mattias Lundmark was the main supervisor for this thesis. I thank him for proposing the study area and for the enthusiastic supervising during the field work and the continued enthusiasm during the writing of the thesis. He is always ready for questions and discussions related to this thesis. His thorough review is also highly appreciated.

Post-doctor Lars Eivind Augland is also thanked for enthusiastic and excellent supervising during the field work, and even more for the patient supervising during work in the geochronology lab. He is always positive and helpful, even during my bad moments of losing zircons while doing chemistry. His thorough review is also highly appreciated.

DPhil John F Brown is thanked for interesting discussions during the stay on Orkney, and his willingness to share his work, particularly his excellent geological map of Stromness, and his intimate knowledge of the geology of Orkney. Also, thanks to Cynthia for the hospitality and delicious cooking after a long hard days work (and for the generous amounts of Scottish national brew).

Gunborg Bye Fjeld is thanked for teaching me crushing procedures and mineral separation. And Salahalldin Akhavan was of great help using the rock saw.

My fellow students at the Department of Geoscience, University of Oslo are thanked for hanging around, keeping the spirit up with nice lunches and cheering on each other.

Then a thanks goes to all my friends, for example Ingrid Handegard that took time to proofread, and my family for support and comfort during the long process of writing a master thesis. Most importantly I thank my wife, Elen Andrea, for sticking out with late days at school, and for dinners and cookies waiting for me when I finally come home.

Finally, a thanks goes to that post-office woman in Stromness, who spent two hour helping me wrap and ship off 60 kg of rock samples to the University of Oslo!

Contents

1	Introduction and aim of study	1
2	Geological background	2
2.1	Introduction	2
2.2	Pre-Caledonian geology of Scotland	4
2.2.1	Geological evolution	4
2.2.2	The Moine Group	5
2.3	British Isles Caledonides	6
2.3.1	The Caledonian basement cover relationships	6
2.3.2	Caledonian tectonic evolution	8
2.3.3	The Great Glen Fault	10
2.3.4	Tectonic environments for granite formation	11
2.3.5	Syn-collisional magmatism	13
2.3.6	Petrogenesis of magmatic plutons in the Northern Highlands	13
2.3.7	High Ba-Sr granite	14
2.3.8	The slab breakoff model for granite formation	17
2.3.9	Devonian evolution	20
2.4	Regional geology of the Orkney Islands	21
2.4.1	Introduction	21
2.4.2	Previous work on Orkney	23
2.4.3	Comparison to granitic rocks in East Sutherland	25
2.4.4	Devonian evolution on Orkney	26
3	Methods	28
3.1	Field work	28
3.1.1	Introduction	28
3.1.2	Study areas	29
3.2	Laboratory methods	32
3.2.1	Introduction	32
3.2.2	Sample preparation	32
3.3	Analytical method	40
3.3.1	Thermal induced mass spectrometer	40
4	Results	44

4.1	Introduction	44
4.2	Granite and gneiss	44
4.2.1	Exposure of the rocks	44
4.2.2	The grey granite	45
4.2.3	The pink granite	47
4.2.4	Relation between the granites	49
4.2.5	Different phases in the granite	50
4.2.6	Contact between the gneiss and the granite	54
4.3	Mylonites and phyllonites in shear zones.....	57
4.3.1	Mylonite zone at Stromness	57
4.3.2	Mylonite zone at Yesnaby.....	59
4.3.3	Thin section of granite from the Yesnaby shear zone area	63
4.3.4	Shear zone at Graemsay	64
4.4	Volcanic rocks: felsite layers.....	66
4.4.1	Introduction	66
4.4.2	Promontory with felsite.....	66
4.5	Hara Ebb formation	70
4.6	Old Red Sandstone east of Stromness bay	72
4.6.1	Exposures at Stromness beach	72
4.7	Structural geology.....	75
5	Geochronology and geochemistry.....	79
5.1	U/Pb geochronology; results and interpretations of data.....	79
5.1.1	Introduction	79
5.1.2	Grey granite.....	79
5.1.3	Pink granite	81
5.1.4	Pegmatite.....	84
5.1.5	Felsite	85
5.2	Geochemistry.....	1
5.2.1	Classification diagrams	1
5.2.2	Tectonic discrimination diagrams	3
5.2.3	Multi-element diagrams	7
5.2.4	REE-patterns	9
6	Discussion	12

6.1	Introduction	12
6.2	Orkney granite complex	12
6.2.1	Age relation between the grey and the pink granite.....	12
6.2.2	Deformation	13
6.3	Geochemical signature	13
6.3.1	Tectonic discrimination diagram.....	14
6.3.2	REE patterns.....	14
6.3.3	High Ba-Sr granite	14
6.3.4	Fractionation mechanisms.....	16
6.4	Regional comparisons.....	17
6.4.1	Tectonic movements – Scandian phase.....	17
6.4.2	Magma emplacement during the Scandian phase	18
6.4.3	Other plutons emplaced during the Scandian phase.....	18
6.4.4	Tectonic model for magma emplacement of the Orkney granite complex	19
6.4.5	Exhumation history	20
6.5	Tectonic setting during Rhyolite formation.....	23
7	Conclusions	25
	Reference list.....	27

1 Introduction and aim of study

The focus of this thesis is the outcrops of basement found at the Orkney Islands (Figure 1). These outcrops are located at the islands Mainland Orkney and Graemsay. The basement is interpreted to have formed as part of the Caledonian orogeny (Strachan, 2003). Due to the geographical position of the Orkney Islands this basement forms a link between the Norwegian and the Scottish Caledonides, offering a glimpse of the basement presently hidden beneath the North Sea. Despite the long history of geological investigations in Scotland, not much is known about the basement on Orkney. The age of the rocks, their relationship to the Precambrian gneisses and Caledonian granites in Scotland, their structural evolution and exhumation, and their tectonic significance remain conjectural.

The present thesis work was designed to address these issues. Fieldwork was conducted to map out the different rock types encountered in the basement and the relations between them. Structural evidence was sought out to shed light on the pre-, syn- and post-Caledonian basement evolution. Samples of granites, rhyolites and pegmatites were collected for age determinations, geochemical analyses and thin section investigation.

The aims of this study were to:

- 1) document the basement rocks, measure structural properties and map out their relations
- 2) sample and analyse (geochronology/geochemistry) rocks that can shed light on the basement evolution
- 3) investigate an area with outcrops of felsic volcanic rocks of uncertain age to determine their relation, if any, to the Caledonian evolution of the Orkney Islands
- 3) attempt a large scale interpretation of the tectonic evolution of the Orkney basement complex informed by the new data gathered during the course of the thesis work

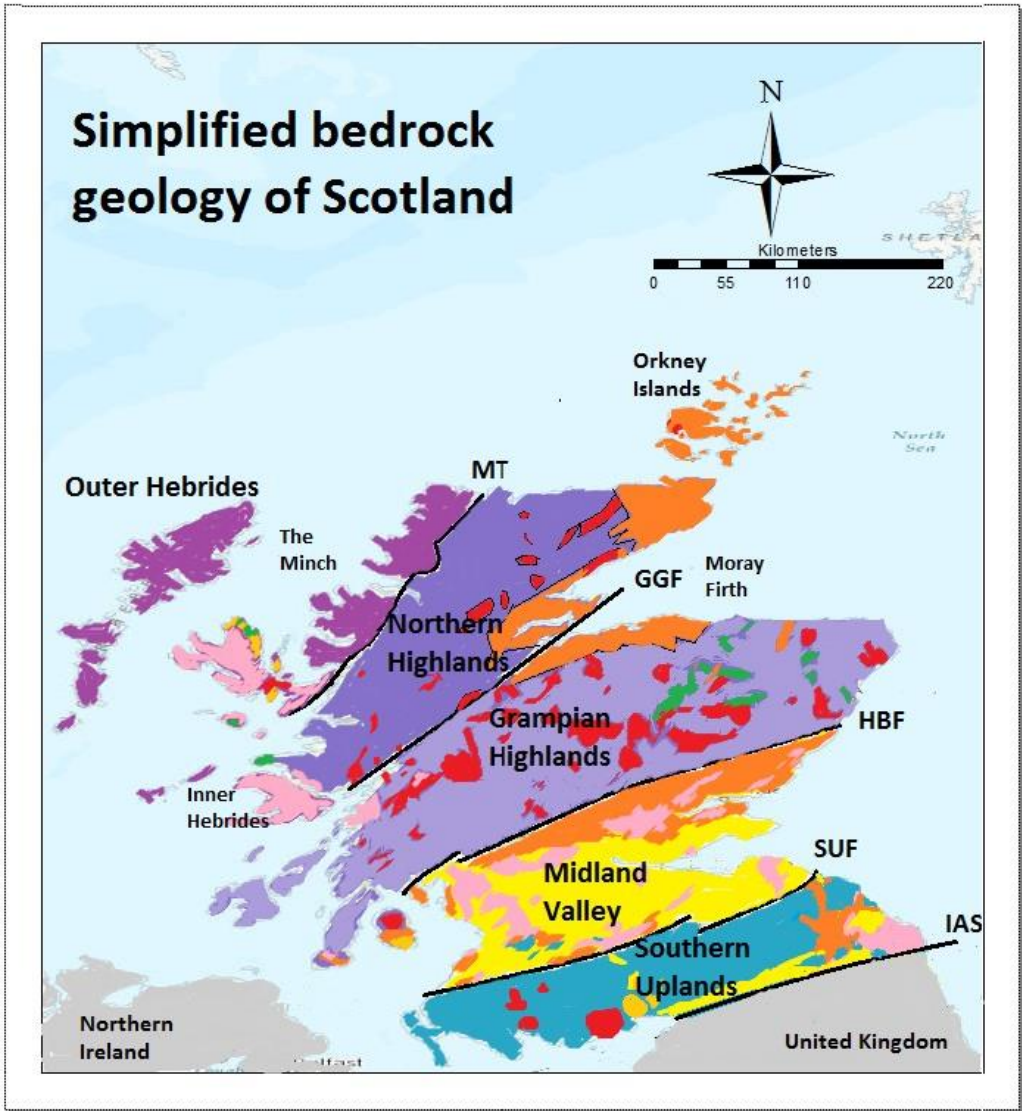
2 Geological background

2.1 Introduction

Scotland has overall a wide variation in landscapes, rock types and structures. It is marked by a long history of tectonic activity, sedimentation, magmatic intrusions and metamorphism. Most geological eras are represented, from the oldest, crystalline rocks of the Outer Hebrides and northern parts of Scotland, to the younger and softer sedimentary rocks in the central and southern Scotland (Gillen, 2003). Scotland has been part of several orogenic events. The latest being the Caledonian orogeny, that had a large impact on Scotland's geological and geomorphological appearance, shaping the way it looks today (the basement of Orkney as well as any other part). Further, the Caledonian orogeny has given a NE-SW direction to faults and foldaxes in the rocks, stacking tectonic units in a NW-SE direction (Gillen, 2003). Before the Caledonian orogeny there have been other orogenic events, as well as extensional phases and periods with deposition of sediments.

This master thesis focuses on the basement on the islands of Mainland Orkney and Graemsay off the Scottish coast (cf. Figure 8), which were chosen as the areas for field work. These areas have some outcrops of pre-Caledonian para-gneisses. The rest of the rocks however, are granites formed as a result of magmatic and tectonic activity during the Caledonian orogeny (Strachan, 2003). There are also outcrops of volcanic rocks that according to Strachan (2003) are related to later tectonic movements. The granites and the volcanic rocks are the focus of this thesis.

The pre-Caledonian geological evolution will be described briefly, followed by a more thorough description of the geologic evolution during and after the Caledonian orogeny and its impact on Scotland.



Legend

- | | |
|---------------------------------------------------|--------------------------------------------------------------|
| The Lewisian complex & Torridonian Supergroup | Non-metamorphosed sedimentary rocks from Carboniferous |
| Moine Supergroup | Weakly metamorphosed sedimentary rocks |
| Dalradian Supergroup | Intrusion of basic (silica poor) igneous rocks |
| Caledonian granites (Newer and older granites) | Non-metamorphosed sedimentary rocks from Devonian |
| Non-metamorphosed sedimentary rocks from Devonian | Non-metamorphosed sedimentary rocks from Triassic & Jurassic |
| Thick and extensive lava flows | Unspecified bedrock geology |

Figure 1 – Simplified geological map of Scotland, with the main geological regions. Abbreviations; MT, Moine Thrust; GGF, Great Glen Fault; HBF, Highland Boundary Fault; SUF, Southern Uplands Fault; IAS, Iapetus Suture. Map modified from Bridge (2016)

2.2 Pre-Caledonian geology of Scotland

2.2.1 Geological evolution

Scotland's oldest rocks are found in the northernmost part of Scotland (Figure 1), and are called Lewisian gneisses. These rocks are high-grade metamorphic rocks formed over 3 billion years ago. Two main episodes of deformation at 2900 and 1800 Ma respectively have led to intense deformation of the rocks. The Lewisian gneiss complex is a fragment of deep-level continental crust that belonged to the Laurentian plate, prior to the Caledonian orogeny (Gillen, 2003).

During the Grenvillian Orogeny, a series of continent collisions that led to formation of the supercontinent Rodinia between 1100-900 Ma (Li et al., 2008), the uplift and erosion of the crust led to exposure of Lewisian basement rock at ca. 1200 Ma. East facing rivers in Greenland and Canada were at the time situated much closer to Scotland. From these, thick continental sediments were deposited in fault-bounded basins in the northwest part of Scotland. Sedimentary rocks formed from these are known as "the Torridonian" and are the oldest sedimentary rock sequences in Great Britain. In basal conglomerates above the non-conformity separating the sedimentary rocks and the gneisses, blocks of Lewisian gneiss can be found. Only a few isolated mountains of Torridonian sandstone remain (Gillen, 2003).

Between 1000-870 Ma, shallow marine sand and clay were deposited in a slowly subsiding basin stretching across Scotland. These deposits now form the Moine rocks, a series of pale gray schists that dominate the Northern Highlands (Figure 1; Gillen, 2003). Previous workers have proposed that Moine form part of the basement of the Orkney Islands (Strachan, 2003, Mykura et al., 1976). The Moine rocks are further described in section 2.2.2.

The Grampian Highlands are dominated by the Neoproterozoic Dalradian rocks, mainly consisting of siliciclastic metasediments, which form a broad belt from Shetland and southwestwards through Scotland (Figure 10)(Prave et al., 2009). The rocks are similar to the Moine rocks, which suggest continuous depositions. However the Dalradian rocks are 25 km thick (Moine rocks being about half the thickness of this (Strachan et al., 2010)) and much more varied than the Moine rocks, especially in the upper parts. In addition to schist and

quartzite the Dalradian rocks also include limestone, slate, phyllite, volcanic rocks and glacial deposits (Prave et al., 2009).

The Dalradian sediments were deposited between 750-600 million years ago in subsiding fault-bounded basins. This created accommodation space for large amounts of sediments. These shallow marine basins formed when Rodinia started to break up, reflecting rifting and opening of the Iapetus Ocean (Gillen, 2003). The Dalradian rocks include several formations recording glacial conditions. The oldest glacial unit, the Port Askaig Formation is suggested to represent one of the Sturtian glacial episodes that occurred between 750-690 Ma. Crustal thickening probably affected some Dalradian rocks prior to 590 Ma (Dempster et al., 2002).

Dempster et al. (2002) have interpreted parts of the history of the Dalradian rocks, based on U-Pb zircon ages, concluding that the Dalradian stratigraphy is broken into smaller units and rejecting models that assume continuous deposition of Dalradian sediments from pre-750 Ma to 470 Ma.

When the Iapetus Ocean started to close in the Ordovician, chains of volcanic arcs started to form (Macdonald et al., 2014). This was the beginning of the Caledonian orogeny that would have a huge impact on the geology of Scotland, and the Orkney Islands.

2.2.2 The Moine Group

The Moine Supergroup is found in the northwest part of Scotland and includes the Morar, the Loch Eil and the Glenfinnan Groups (Dewey et al., 2015). It is a thick sequence of early Neoproterozoic sedimentary rocks. Throughout the sequence there is evidence of several phases of regional metamorphism (Strachan et al., 2010). The group is exposed across large areas in the Caledonides north of the Great Glen Fault (Soper et al., 1998).

The Moine Supergroup is characterized by structural complexity and monotonous siliciclastic lithologies. There is no biostratigraphic control of the sequence, but it is possible to combine locally defined successions into a regional stratigraphy. This permits an evaluation of the tectonic setting for the depositions that formed the Moine Supergroup. The sediments are inferred to have been deposited in two large Riphean (1400-800 Ma) half grabens (Soper et al., 1998).

The Morar Group and the Glenfinnan Group are related to the first of these basins. Recent work, by Krabbendam et al. (2008) has led to a significant reappraisal of the sedimentary environment of the Morar Group. In contrast to previous work that viewed these sediments as mainly shallow marine (Soper et al., 1998), Krabbendam et al. (2008) interpreted these rocks as high-energy, braided fluvial deposits. Structural analysis showed that this fluvial sequence was at least 3km, and possibly 5 km, thick (Krabbendam et al., 2008). Bonsor and Prave (2008) re-examined the Upper Morar Psammite in Ardnamurchan and similarly concluded that it was deposited in an alluvial braidplain.

The Glenfinnan group is partly interpreted as a distal equivalent to the Morar Group and partly interpreted as a post-Morar transgressive thermal re-equilibration sequence (Soper et al., 1998).

The second of the main basins was placed further to the east. Here the Loch Eil Group was deposited. The group is dominated by marine arkosic and quartz-rich metasandstones. These were subsequently emplaced adjacent to the Morar basin during the Caledonian orogeny (Soper et al., 1998).

2.3 British Isles Caledonides

2.3.1 The Caledonian basement cover relationships

The Caledonian orogeny occurred from 540-400 Ma (McKerrow et al., 2000). Within this timeframe the process can be divided into different phases where some of the phases have had a huge impact on the geology of Scotland.

In addition to the Caledonian mountain ranges in the Scottish Highlands there are also north-east trending Caledonian faults that cut wide across Scotland. From north to south the main faults are named “the Moine thrust”, “the Great Glen Fault”, “the Highland Boundary Fault” and “the Southern Uplands Fault” (Figure 2).

The faults divide Scotland into geological regions. From north to south the regions are the Outer Hebrides, the Northern Highlands, the Grampian Highlands, the Midland Valley and the Southern Uplands (Figure 2) (Gillen, 2003). The full collage of regions was assembled during the Caledonian orogeny.

The Southern Uplands is interpreted as a lower Paleozoic accretionary prism, thus, the rocks that are found in the Southern Uplands were deposited along a subduction zone on the NW margin of the Iapetus Ocean during the lower palaeozoic (Leggett et al., 1979). The stratigraphy can be simplified into 3 belts; one with early Ordovician basalt and cherts underlying thick greywacke, the next with late Silurian and early Ordovician graptolitic shales also underlying thick greywacke, and finally a belt of graptolitic shale that are interbedded with greywacke (Leggett et al., 1979).

The Midland Valley has been interpreted by Bluck (1983) as an arc-interarc region during the Ordovician and Devonian periods. The arc is inferred to be made up of mainly plutonic rocks, some with basic and some with granitic composition. At the final Silurian-Devonian stage of the arc it was dominated by effusive rocks that contributed to the Devonian sediments (Bluck, 1983). Today, the Midland Valley is covered in large areas by Carboniferous sedimentary rocks. In many of the sedimentary groups there are extensive lava flows (Waters et al., 2011).

The Grampian Highlands are mostly covered by the Dalradian Supergroup (see section 1.2.1). Between 428-385 Ma it was displaced 500 km or more to its position relative to the Moine rocks (in the Northern Highlands) to its present position (Dewey et al., 2015), by sinistral strike slip movement along the Great Glen Fault. Granites have intruded during the Ordovician and Silurian, and are divided into The Older granites and The Newer granites; these are further described in Section 1.3.6.

The Northern Highlands are mostly covered by the Moine Supergroup (see section 1.2.2), which was intruded by both Older and Newer granites in the Ordovician and Silurian periods, analogous to the development in the Grampian Highlands to the south of the great Glen Fault (Fowler et al., 2008).

Main faults and geological regions Scotland

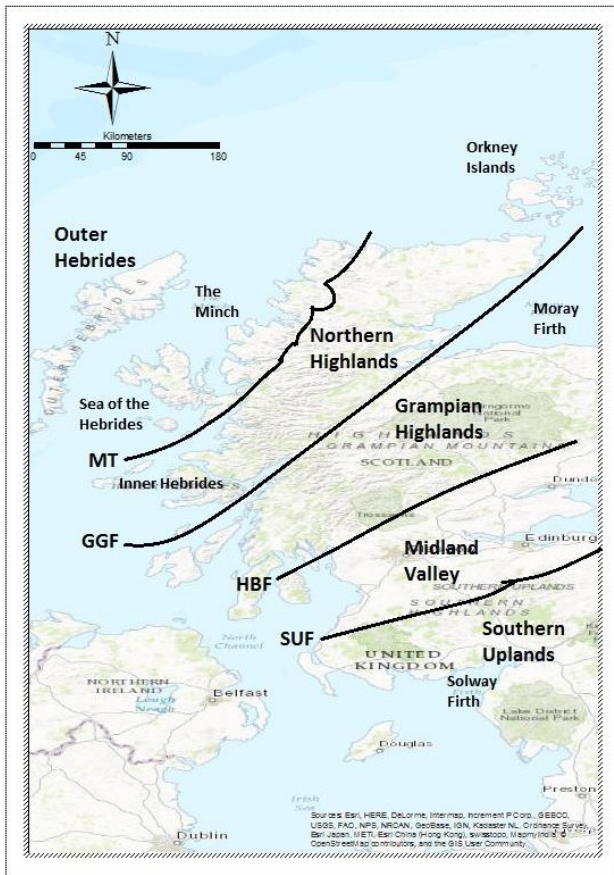


Figure 2 Topographic map of Scotland with the main geological regions and boundaries shown. Abbreviations, from north to south: MT, Moine Thrust; GGF, Great Glen Fault; HBF Highland Boundary Fault; SUF, Southern Uplands Fault.

The areas on the Orkney Islands studied during this master thesis are placed within the the Northern Highlands (Figure 2). This region is delimited by the Great Glen Fault to the south and the Moine Thrust to the north.

2.3.2 Caledonian tectonic evolution

Scotland has been situated along the margin of a continental plate through several cycles of collision and break-up of plates, with the Caledonian orogeny as the latest collision phase. If an orogeny is defined as “a series of tectonic processes that forms mountains”, the Caledonian orogeny must be a series of orogenic phases, each with its characteristic set of time and space-features (Gillen 2003). The Caledonian orogeny includes the early Paleozoic areas of the British Isles and Scandinavia. These areas went through sequences of mountain-range forming events during the closure of the Iapetus Ocean. Areas adjacent to it underwent the same processes, for example Svalbard, Greenland, Ireland and the northern parts of the Appalachians (a mountain chain in North-America). Therefore the Caledonides include the

continental margins of Laurentia, Baltica and Avalonia that collided as the Iapetus, and Tornquist oceans, were closed in Ordovician and Silurian (Figure 3) (Torsvik et al., 1996).

Avalonia was formed in a late Neoproterozoic juvenile volcanic arc setting. It was accreted to the margin of Gondwana and subsequently rifted and transferred to eastern Laurentia during the Caledonian orogeny (Nance et al., 2002).

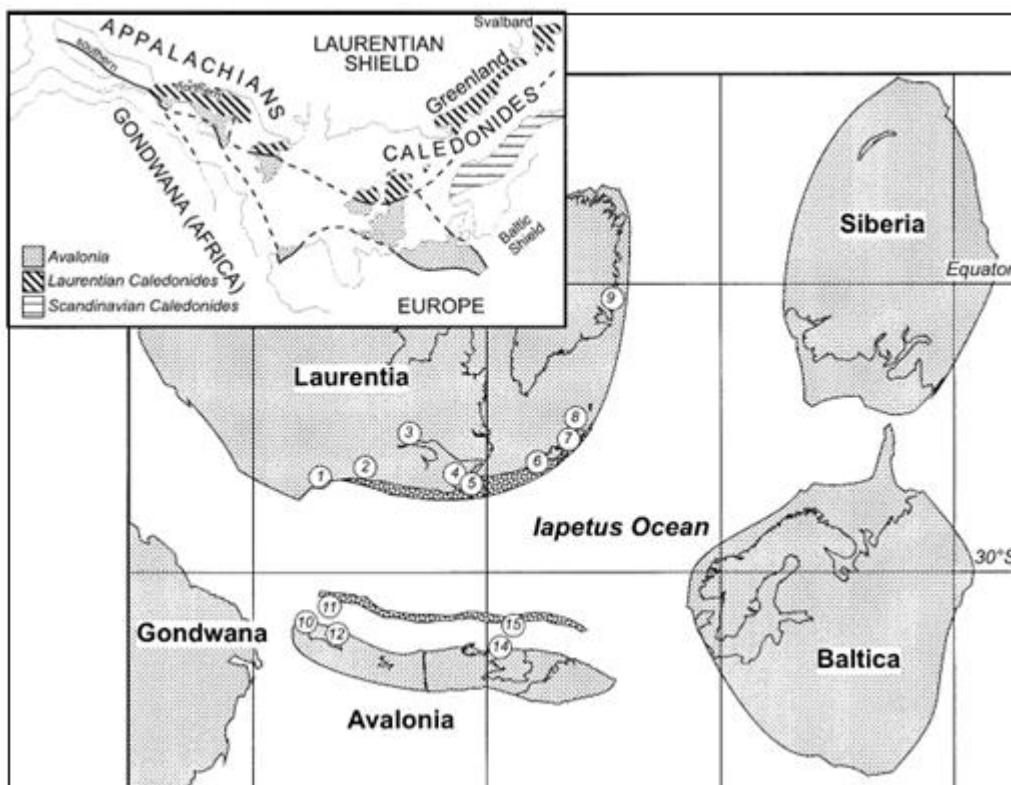


Figure 3 - Map of the continental plates surrounding the Iapetus Ocean during the Caradoc (c 455 MA) (McKerrow et al. 2000)

600 million years, the Northern- and the Grampian Highlands in Scotland were situated at the margin of the continent Laurentia. As the Iapetus Ocean started closing, it caused three continental plates, Laurentia, Eastern Avalonia and Baltica, to move towards each other (Torsvik et al., 1996). The collision itself is divided into several phases. To understand the tectonic setting of the Silurian-Devonian magmatism occurring in the Orkney Islands during the Caledonian orogeny (this thesis), the Grampian and the Scandian phases are especially important.

In the British Caledonides, the first orogenic phase is named “The Grampian phase”. This was a short-lived orogenic event when a chain of volcanic arcs collided with a rifted part of the

Laurentian margin from 470 to 460 Ma (McKerrow et al., 2000, Dewey and Shackleton, 1984). The Grampian phase is observed as deformation of late Precambrian and Cambrian rocks, and emplacement of Older Granites. The Taconian phase in the Mainland Maritimes and New England is also related to arc-continent collision and is viewed as an equivalent to the Grampian phase (McKerrow et al., 2000). A change in subduction direction before or after the Grampian phase would have led to the seafloor of Iapetus Ocean and a newly assembled arc being subducted under Laurentia by Caradocian time. This subduction continued until the closing of Iapetus Ocean in Silurian (McKerrow et al., 2000).

The second phase of particular interest for the evolution of Orkney is the Scandian phase. It occurred around 440 Ma as an oblique collision between Baltica and Laurentia. During this phase, the Northern Highlands was thrust towards the west, followed by a phase of sideways movement along faults, included the Great Glen Fault and the Boundary Fault in Shetland. The Scandian phase covers the emplacement of large nappes in Scandinavia (Stephens and Gee, 1989).

The third and last phase of the Caledonian orogeny in Britain happened when Eastern Avalonia collided around 425 Ma across the Iapetus suture (Figure 1). Unlike the Grampian phase and the Scandian phase, this collision was relatively soft, and did not cause as large amounts of deformation. However, it did complete the joining together of Scotland and England (McKerrow et al., 2000).

2.3.3 The Great Glen Fault

The Great Glen Fault is a major strike slip fault with occurrence within the Caledonian belt of the British Isles (Figure 1) (Stewart et al., 1999). It cuts across Scotland from east coast to the west coast, separating the widespread and thick succession of Neoproterozoic siliciclastic deposits referred to as the Grampian Group of the Grampian Highlands from the Moine metasediments of the Northern Highlands (Figure 2; Leslie et al. 2013). The sediments of the Grampian Group were deposited in basins formed during a phase of Neoproterozoic rifting that led to NE- to SW-trending marine basins. The group has lithological similarities with the Moine metasediments, and was earlier referred to as the younger Moine (Leslie et al., 2013). The relation between the rocks of the Northern Highlands and the Grampian terrane still represents a major challenge in the understanding of the geology of the Northern and Grampian Highlands (Leslie et al., 2013).

Winchester (1974) showed that the metamorphic patterns in the Moine schist are displaced by the Great Glen fault. Intrusion of numerous syn-collisional magmatic rocks occurred during the formation of the Great Glen Fault. The Ratagain granite is an example of this. Field evidence from the Ratagain granite demonstrate that emplacement was synchronous with sinistral displacement along a major fault, the Strathconan Fault, associated with the Great Glen Fault movement (Stewart et al., 1999).

The amount of displacement that has taken place along the Great Glen Fault has been the subject of debate. According to Briden et al. (1984) palaeomagnetic data from north of the Great Glen Fault forms a polar wander path that cannot be recognized south of Great Glen fault. Thus, Briden et al. (1984) conclude that there is no reason to believe that displacement that happened before the early Paleozoic time was more than 100 km. This is also indicated by the lithological similarities across the fault. On the other hand, theories of larger of displacements have been proposed by several authors. Storetvedt (1974) argued for 200-300 km displacement, based on comparison of Old Red Sandstone paleomagnetic data from Norway, with Orkney lava and Caithness Old Red Sandstone. However the data from Norway do not corresponded with data from Britain *south* of Great Glen Fault. Unfortunately, the data correlations are not sufficiently precise to determine the relative movement between them. The idea that the movement along the Great Glen Fault have been up to several thousand kilometers are heavily criticized by Smith and Watson (1983).

2.3.4 Tectonic environments for granite formation

Granitic magmatism can occur in several different tectonic environments. Since Chappell and White (1974) introduced their concept of I- and S-type granites, the idea that granite composition reflects the type of material *present in the source*, has been widely accepted (a view also claimed by for example Pearce et al. (1984)). However, the tectonic conditions also affect the types and occurrence of granite, and the extent of this effect has been discussed over decades. Pearce et al. (1984) examined the relationship between chemical composition of granites and the tectonic setting in which they occur. Based on this, Pearce et al. (1984) divided the granite formed in different tectonic environments into 4 main groups: syn-collision granites (SYN-COLG), Volcanic arc granites (VAG), Within plate granites (WPG) and Oceanic ridge granites (ORG) (cf. Figure).

Syn-Collisional Granites

Syn-collisional granites are formed in collision settings. This is the most complex tectonic setting. Thus, granites formed under collision settings are the most difficult to discriminate based on their geochemical properties. Contributing to the complexity is the fact that there are many different types of collisional settings. Pearce et al. (1984) subdivided collisional granites into continent-continent, arc-continent and arc-arc collision. However, the latter two are not easy to distinguish from the continental arc setting (see VAG section).

Continent-continent collision proceeds in stages which can be seen in terms of the Wilson cycle. Continents can only collide when the intervening oceanic or arc crust has been consumed from *arc-arc collision* or *arc-continent collision*. Continental collision settings can produce distinctive granites, namely highly evolved, peraluminous granites with high contents of Rb and other lithophile elements. Typical associated minerals are biotite, muscovite, hornblende and garnet (Barbarin, 1990).

Volcanic Arc Granites

Volcanic arcs granites form in ocean arcs or continental arcs (Pearce et al., 1984).

Granites forming an oceanic arcs may lack continental source material (i.e., be juvenile, these are called immature arcs) but there are also many cases of oceanic arcs with a mixed or transitional character. This can occur in areas where, continental crust form part of an island arc, or an oceanic arc is located adjacent to a continental margin (Pearce et al., 1984). Typical associated minerals with oceanic island arcs are hornblende and lesser amounts of biotite (Barbarin, 1990).

At continental arcs, the magmatism on the active continental margins is complex. Arc-arc and arc-continent collision (accretion) *in addition to* subduction-related magmatism is one of the reasons for the complexity. Another reason is the potential overlap of arc, back-arc, and continental rift magmas of diverse compositions, if the region of melting or emplacement shifts with time. Magmatism related to subduction can be active several hundreds of kilometers inland from the margin This means that arc magmas may be emplaced across different crustal domains. Thus the continental arc setting is much more heterogeneous than the oceanic arc settings (Pearce et al., 1984). Typical associated minerals in a volcanic arc granites are hornblende and biotite (Barbarin, 1990).

Within-plate granitoids

Within-plate granites are formed by processes that are more enigmatic than those at plate margins because there are no obvious mechanisms behind the magmatism. In addition, the mechanisms are poorly constrained by geophysical and field data and the products are spatially scattered and chemically diverse (Winter John, 2010).

The dominant magma type for oceanic intraplate volcanism is basaltic, and the most familiar products of oceanic intraplate volcanism are the numerous islands in the world oceans. The melting mechanism for Within-plate Granites are hotspot and/or adiabatic mantle rise, causing partial melting of mantle and/or the lower crust (Barbarin, 1990).

Oceanic Ridge Granite

Oceanic Ridge Granite is subdivided in two main groups, namely subduction-unrelated and subduction-induced groups (Pearce et al. 1984). Subduction-unrelated conditions are divided into normal ocean ridges (associated basalts are N-MORB; i.e. normal mid-oceanic ridge basalt), and anomalous ocean ridges. Subduction related granites are divided into back arc basin ridges and supra-subduction zone ridges (Pearce et al. 1984).

An important note when distinguishing different tectonic environments is that the tectonic settings are not static. Tectonic settings can move in space (for example due to arc migration), and time (for example as an intracontinental rift evolves into an oceanic basin). Also, the distance between the source and the site of emplacement may be many kilometers (Förster et al., 1997).

2.3.5 Syn-collisional magmatism

An orogenic event with continent collisions causes not only metamorphic processes, but also syn-collisional magmatic activity. Syn-collisional magmatism is triggered by different mechanisms that lead to different characteristics and appearance. The traditional method to categorize granite is to use S-type and I-type designations (Fowler et al., 2001). I-type granites form from an igneous protolith, and S-type from a sedimentary protolith (Fowler et al., 2008).

2.3.6 Petrogenesis of magmatic plutons in the Northern Highlands

Granites that intruded the Northern highlands of Scotland during the Caledonian orogeny have been divided into «Older Granite» and «Newer granite» (Read, 1961).

Older granite are typically S-type, two-mica granites. They are usually associated with areas with a high grade of Grampian regional metamorphism. The magmatic climax is at ca. 470 Ma (Dewey and Mange, 1999).

Newer granites form a large intrusive group that intruded 40-50 Ma after the Grampian phase events, that is, during the Scandian phase and at the end of the Caledonian orogeny. These are mainly granodioritic plutons of essentially calc-alkaline I-type-character. In Scotland, the Newer granites (Figure 1) are formed between 435-390 Ma (Soper, 1986). The Newer granites are found in the Caledonian metamorphic belt, and have been interpreted to be a result of the collision between Baltica and the Scoto-Greenland margin that followed the closure of the Iapetus. There are two chemically, isotopically and geographically separate Newer granite suites in the metamorphic belt of Scotland, *The Argyll suite and the Cairngorm Suite* (Dewey et al., 2015).

Rock types ranging from appinite to granodiorite and granite are the typical occurrence of plutons in the Argyll suite. The typical chemical signatures are a calc-alkaline character, high Na₂O compositions, and high enrichment in Sr and Ba with low Th, Nb and Rb- values (Jacques and Reavy, 1994). Some of these granites are classified as “High Ba-Sr granites” (Fowler et al., 2008) these rocks are further described in section below.

The plutons of the Cairngorm suite are different in chemical composition from the High Ba-Sr granites of the Argyll suite. The Cairngorm suite Newer granites are relatively low in Ba-Sr content and there are few appinites (Stephens and Halliday, 1984, Halliday et al., 1985, Fowler et al., 2001) .

There are also found Newer granites in Southern Uplands. However, these are unrelated to, and younger than, the Newer granites that outcrop further north (Brown et al., 2008) and is not covered further in this thesis.

2.3.7 High Ba-Sr granite

The characteristics of the High Ba-Sr granites are given by Tarney and Jones (1994). The main features are the unusual trace element characteristics. High amounts of Ba, Sr and light

REEs, and low amount of Nb, Ta and heavy REEs. The Caledonian granites and syenites of the Northern Highland of Scotland (that belongs to the “Argyll suite” of Stephens and Halliday (1984)) are typical high Ba-Sr plutons (Tarney and Jones, 1994). These granites and syenites have been the subject of research since the studies of Read (1961). The plutons that intruded the Northern Highlands display a great range in composition from ultramafic, mafic to granitic and syenitic compositions. Most of the plutons are intruding Neoproterozoic Moine metasediments (Fowler et al., 2008).

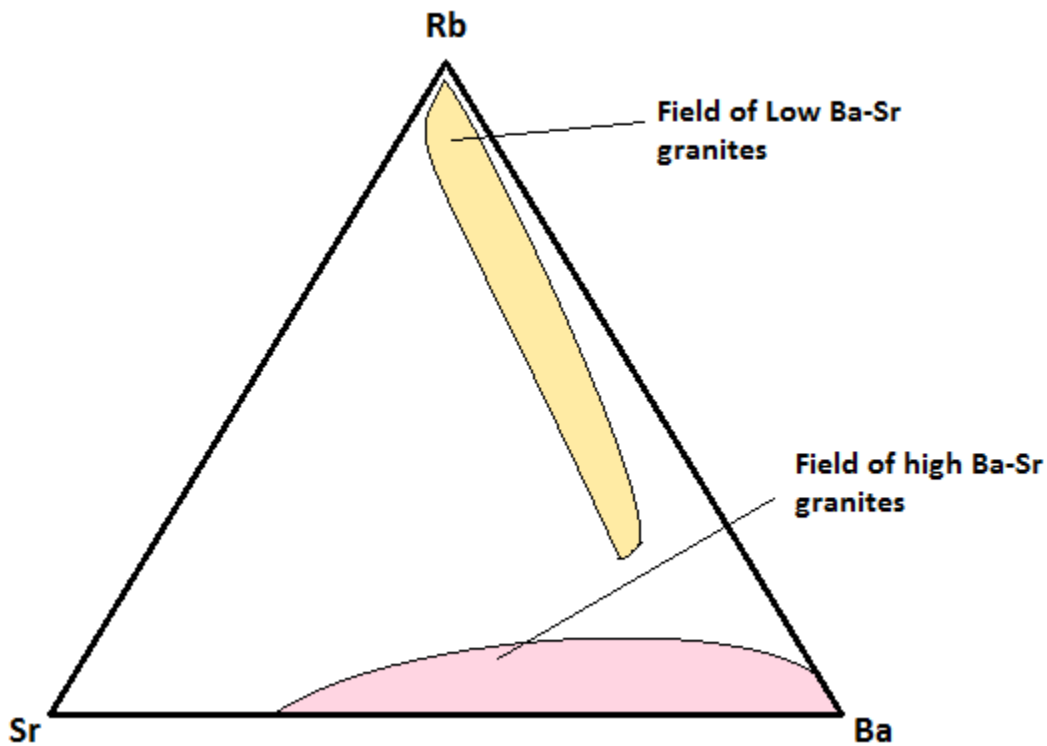


Figure 4 – Sr-Rb-Ba plot with data from O’Brien (1985) that shows field areas for High Ba-Sr granites and other (low Ba-Sr) granites. Field areas are marked based on data from Tarney and Jones (1994)

Fowler et al. (2008) presented element and Sr-Nd-O isotope data for six High Ba-Sr complexes in the Northern Highlands. The locations of the plutons are shown in Figure 5.

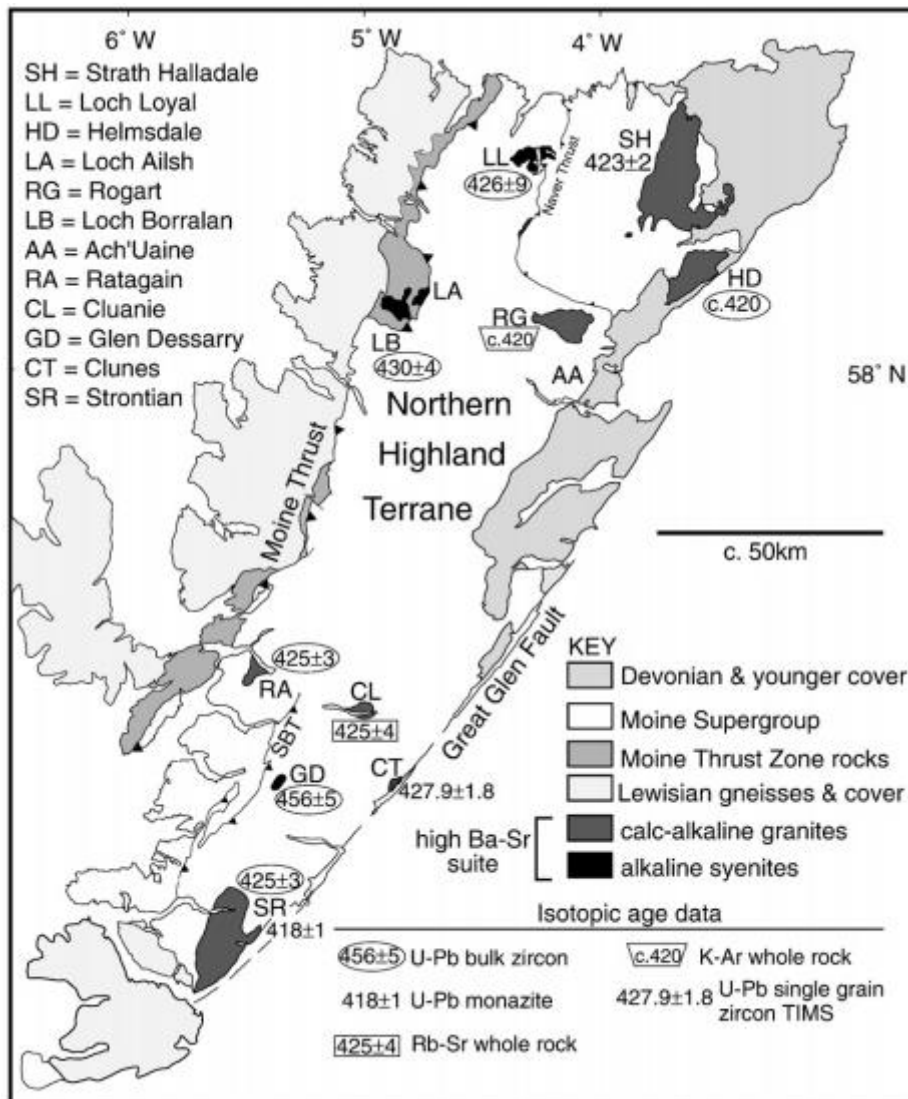


Figure 5 - Geological sketch map of the Northern Highlands, showing the Caledonian high Ba-Sr plutons, with age data collated by Fowler et al. (2008). Figure and age data from Fowler et al. (2008) and reference therein

The magmatic genesis and the relation between the alkaline syenites and the calc-alkaline granites are much debated topics. Isotope Sr-Nd-O data, points to both types being derived from mantle sources, which include small fractions of subducted pelagic sediments. Most of the volume is made up of juvenile material, though the evolution of the magmas has involved contamination with local continental crust in addition to crystal fractionation. Direct derivation from a mafic underplate crust is not likely, due to the a) absence of HREE and Y-depletion, and b) main-element differences from adakitic magma, and c) the typical presence of a geochemically continuous array of mantle-derived rocks of the same age (Fowler et al., 2008).

The parent magmas to the plutons are derived from a Caledonian Parent Magma Array of isotopically depleted to strongly enriched compositions. The enriched compositions have high $\delta^{18}O$. Oxygen isotope values and the high Ba-Sr signatures are strong indications of a mantle contaminated with subducted pelagic sediments and carbonates to form the Crustal Parent Magma Array. The Nd-Sr isotopes limit this sediment contribution to less than 10 %. (Fowler et al., 2008).

Caledonian syenites developed by extensive pyroxene-dominated fractionation, in some cases accompanied by assimilation/contamination of Lewisian granulite. The granites however, fractionated amphibole and plagioclase, and were typically assimilating local Moine metasediments. The extended time interval of the formation of the syenites (30 Ma) corresponds with the continuous Iapetus-subduction under the Laurentian margin. The late pulse of appenites and granites are formed around 425 Ma (Fowler et al., 2008). The formation of the late pulse is suggested to coincide with a slab breakoff (Atherton and Ghani, 2002). A model of rock formation during slab breakoff is described in the section below.

2.3.8 The slab breakoff model for granite formation

A complete model to explain the formation of the Late Caledonian granites must accommodate granite and syenite magmatism long after the Grampian Ordovician orogeny in the Ordovician. Also, it must be consistent with the closure of the Iapetus Ocean immediately followed subduction of Baltica under Laurentia. Atherton and Ghani (2002) argue that slab breakoff as a model can account for all of these observations.

In the slab breakoff model a sequence of partial melting from new lamprophyric underplated-crust, and then from more shallow and older crust when heat is conducted upwards through the crust after the slab breakoff is envisioned (Figure 6). This gives the magmas characteristic of the Argyll and the Cairngorm suites (Atherton and Ghani, 2002).

According to Miles et al. (2016) the slab breakoff models of Atherton and Ghani (2002) and Neilson et al. (2009) are consistent with the timing, compositions and volumes of magmatism across the Grampian Highlands. However, Miles et al. (2016) have identified similarities between magmas emplaced across all of northern Britain. Thus Miles et al. (2016) propose that the northwest dipping Iapetus slab did not only breakoff below Laurentia, but peeled back below the Iapetus Suture for about 100 km to the southeast below Avalonia. This break off

began at about 430 Ma (mid-Wenlock) when the soft collision of Avalonia with the Laurentian accretionary prism began (Miles et al., 2016)

If a slab breakoff occurs, the expected outcome would be a linear belt of high-K, calc-alkaline magmas, some with characteristic trace elements-signatures (especially high Ba, Sr and Zr contents). The linear heat pulse from the breakoff is geographically-, intensity, and time-limited and provides a small volume of melt, emplaced in separate plutons over a short time-interval (Atherton and Ghani, 2002). According to Von Blanckenburg and Davies (1996) “Syncollisional-basaltic” (Iamprohyric high-K calc-alkali) and “granitoid”-magmatism are the most critical evidence for slab breakoff .

The Newer granites has for a long time been regarded as a good example of calc-alkaline orogenic magmatism (Soper, 1986). Therefore they have been assumed to have compositions comparable to batholites in modern magmatic arcs formed by subduction (Brown et al., 1984). However, according to Atherton and Ghani (2002), the problems with subduction as an explanation for the syn-collisional magmatism are:

- 1) The peak in the Newer granite-magmatism is *after* the subduction
- 2) The plutons do not have a progressive space/time-change in chemistry and isotopic character in the magmatism towards the plate margin (Halliday et al., 1985).
- 3) The variation in chemistry is not typical for a subduction situation but can appear post-subduction and at ridge-subduction (Rogers and Saunders, 1989). The chemistry involves an enhancement of Na, Ba Sr, Ce/Y and decrease in Th, Rb and K in a northwesterly direction and Pb has no trend (Halliday et al., 1985).

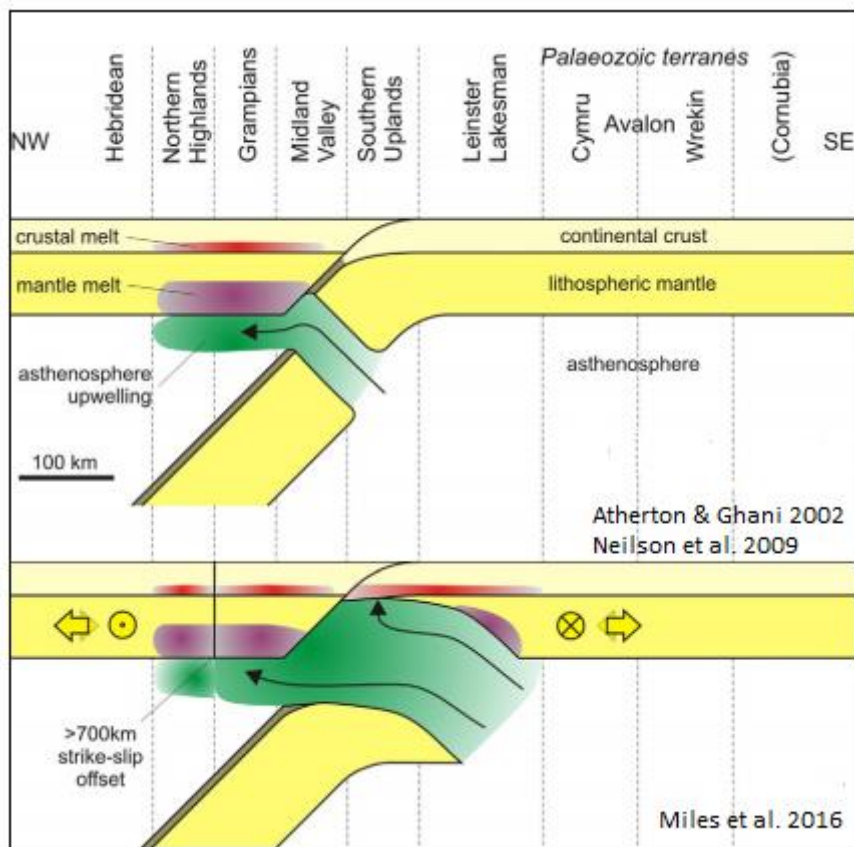


Figure 6 – Slab breakoff models. The upper model is from Atherton & Ghani (2002) and Neilson et al (2009). The lower model is a modified model proposed by Miles et al (2016). The lower model includes strike and slip along the Great Glen Fault that separates Northern Highlands and the Grampian highlands. Modified from Miles et al. (2016).

Other features to the slab breakoff are for example rapid uplift after slab breakoff, this would be consistent with the observed unroofing of granites from the lower Devonian. This uplift causes erosion and formation of extensive Old Red Sandstone extension molasses basins.

According to Atherton and Ghani (2002), the genetic relation between the magmatic activity and the tectonic environment at the end of the oblique closure of the Iapetus Ocean (Watson, 1984, Soper and Hutton, 1984, Hutton, 1987) can be explained by slab breakoff. The melt produced weakens the lithosphere and the crust that overlies the slab breakoff can more easily deform (Von Blanckenburg and Davies, 1996) and thus accommodate the oblique convergence of Baltica with Laurentia. The sinistral NE-SW trending transpressional strike slip faults in Scotland are parallel with the postulated slab breakoff model of Atherton and Ghani (2002).

In this model, the high Ba-Sr pluton forms a curved belt (80-100 km wide) from Donegal to Shetland, and is closely connected to the Great Glen fault system (Watson, 1984). Atherton and Ghani (2002) suggest that this connection can be used to mark the slab breakoff area at the surface.

2.3.9 Devonian evolution

The syn-collisional magmatism was followed by the deposition of the «Old Red Sandstone» in the Northern Highlands (Friend et al., 2000).

The Old Red Sandstone is formed in basins at the margins of the Atlantic Ocean. These deposit ranges in age from mid-Silurian to Carboniferous time and ranges in areal distribution from the Appalachians at 40° N to the northernmost of Spitsbergen at 80° N (Friend et al., 2000). The Old Red Sandstone has long been regarded as a response to the Caledonian mountain building, a post-orogenic belt of deposits that is homogeneous in lithological and paleontological characteristics (Friend et al., 2000). A modern overview of the basins has been provided by Friend et al. (2000), who interpreted the Old Red Sandstone basin geodynamics in relation to plate-scale forces related to the temporally and spatially overlapping Caledonian, Variscan and Ellesmerian orogenies.

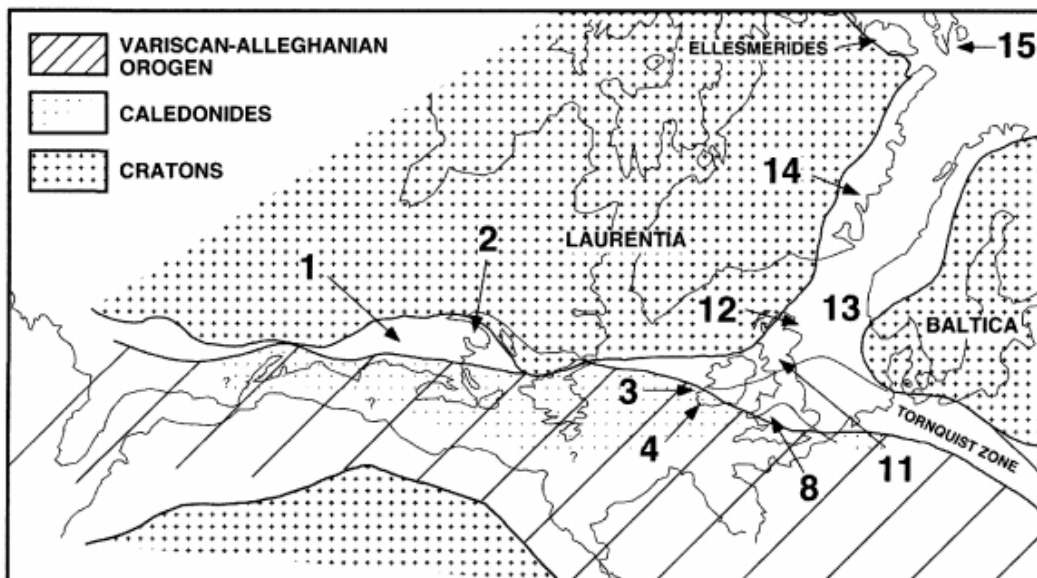


Figure 7 – illustration of the The Caledonian Appalachian, Variscan and Ellesmerian orogens and cratonic block with included basins. 1, Catskills; 2, Maritime Canada; 3, Dingle Basin; 4, Munster Basin; 8, Isle of Man-Lake District; 11, Midland Valley, Scotland; 12, Orcadian Basin (*of the Northern & Grampian highlands*); 13, West Norway; 14, East Greenland; 15 Spitsbergen. Illustration from Friend et al. (2000)

In the Orcadian basin, (number 12 in Figure 7), the Devonian sandstone in the Northern and the Grampian Highlands were formed. The present distribution of Devonian sandstone in Scotland is shown in Figure 1.

2.4 Regional geology of the Orkney Islands

2.4.1 Introduction

The Orkney Islands are a part of the northern Isles of Scotland along with Shetland. The Orkney Islands lie about 125 km SW of Shetland, and are separated from the mainland of Scotland by a narrow firth (Figure 8). Mainland is the largest island of the group. The land area is 956km² and the islands extend for 80 km from north to south and 47 km from west to east (Mykura et al., 1976).

Geographical position of the studied areas at the Orkney Islands

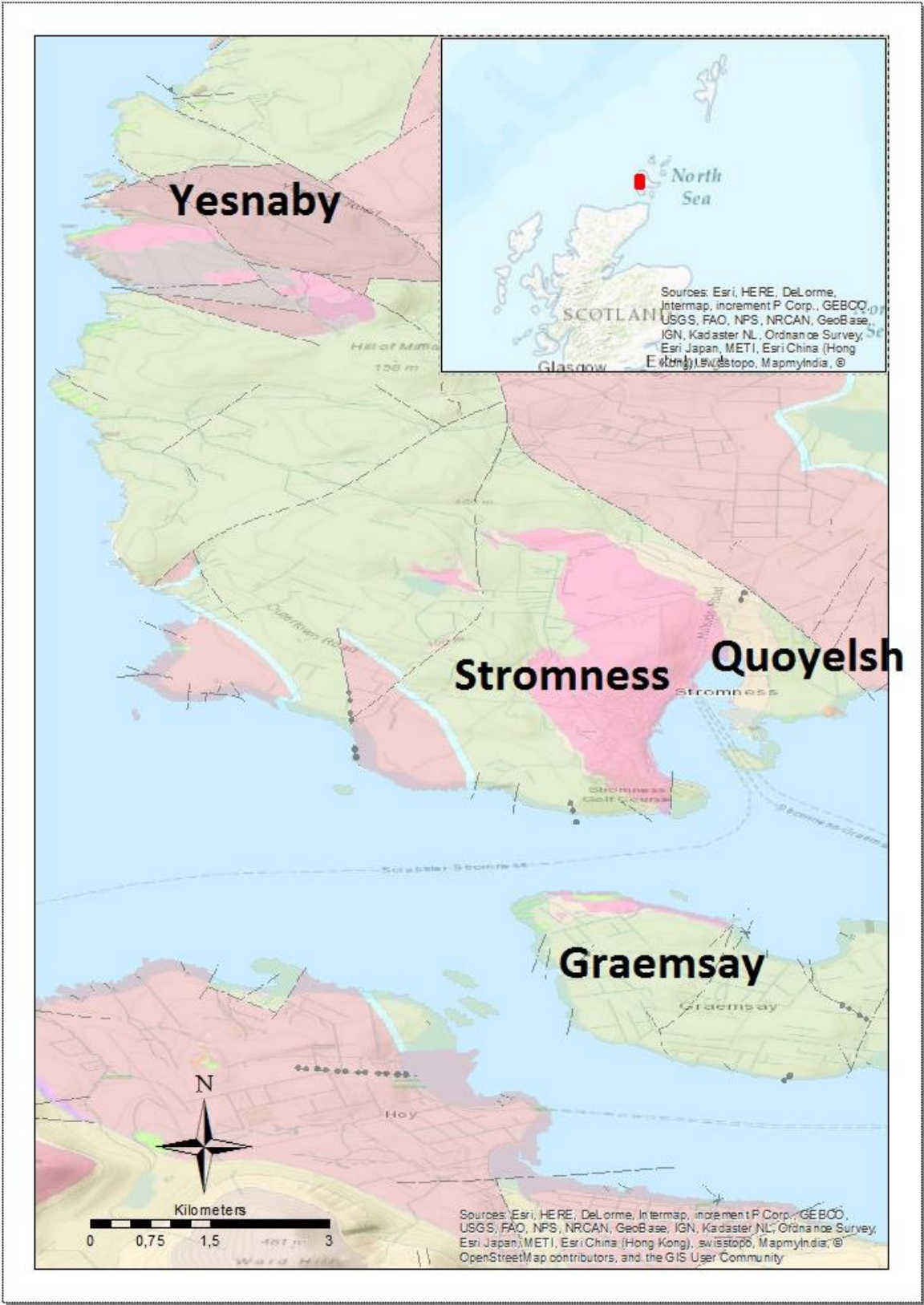


Figure 8 – Simplified geological map from BGS 1:50000 and locations referred to in text.

The Orkney Islands are dominated by extensive outcrops of post-Caledonian sedimentary rocks, predominantly the Old Red Sandstone. However, pre-Devonian rocks are exposed in small areas on the south-western part of Mainland between Stromness and Yesnaby, and on the north tip of the small island Graemsay, just south of Mainland (Strachan, 2003). All previous fieldwork on the basement of Orkney has been done in these areas, which is also the case with the field work presented in this master thesis.

2.4.2 Previous work on Orkney

Previous field work on the basement of Orkney is presented in Wilson et al. (1935), Mykura et al. (1976) and Strachan (2003).

Mykura et al. (1976) presented the basement complex of Orkney as crystalline basement rocks that form a number of small inliers near Stromness, Yesnaby and Graemsay. All the inliers lie along a north-northwest trending belt that extends from Yesnaby to Graemsay with the largest outcrop situated at the hilly ground north of Stromness. Mykura et al. (1976) describes the basement to be composed of a high portion of coarse pink and greyish colored granite that is weakly foliated. In some areas it is claimed that it locally grades into granite-gneiss, thus an anatexite formed from the gneiss. In addition, enclaves of biotite-gneiss and smaller masses of siliceous, micaceous and hornblende schist, is described to occur throughout the granite outcrops. Both the granite and included country rock xenoliths are cut by fine grained pink granite and pegmatite.

An outcrop with felsite is observed at the promontory at the Quoyelsh promontory (Figure 10). It is described as a pale grey flow banded porphyritic felsite. Lying unconformably on top of this is a thin breccia, which contain clasts of the felsite. Mykura et al. (1976) states that whether the *felsite is underlain by Stromness Flagstone*, or forms a part of the basement that the *Stromness Flagstone overlies* is not known.

Wilson et al (1935) suggested that the granite forms part of a deep seated mass, where only the top is seen. The metamorphic rocks are compared with inliers of Lewisian rocks found in the Moine of the Altnaharra district. The coarse granite, which is slightly foliated and partly pass into granite-gneiss were suggested to form a part of the suite of the Older G (ca. 490-460 Ma, associated with the Grampian orogeny). Further, Wilson et al. (1935, p. 49) regarded the

felsite at Quoyelsh as a pre-Middle Old Red Sandstone rock. Other studies, for example by Gallagher et al. (1971), has suggested it to be an ignimbrite of Lower Old Red Sandstone age.

Strachan (2003) separated the pre-Devonian metamorphic rocks into three groups; Paragneisses, foliated meta-granites, and late, undeformed granitic and aplitic veins.

He interpreted the Paragneisses to belong to the Moine supergroup, based on lithological correlations with the high-grade Moine rocks of east Sutherland. These have later been deformed and metamorphosed during the Ordovician-Silurian Caledonian orogeny. Strachan (2003) also suggested that inliers in the basement could correlate with the Lewisian complex to the Caledonian foreland west of the Moine thrust zone.

Further, Strachan (2003), proposes that outcrops of the granites in Stromness, Yesnaby and Graemsay probably form a series of separate intrusive sheets, rather than one major body, with the main intrusive sheet being around 250-300 m thick and exposed at Stromness. The granites are described to have a strong foliation that is defined by the alignment of biotite and recrystallized grains and aggregates of quartz and feldspar. Thus, the granites are interpreted as meta-granites.

Contacts between the intrusive meta-granites and the gneissic wall rock is described at the coast west of Yesnaby and at the northern part of Graemsay (Strachan, 2003). Strachan (2003) claims that the contact between the granites and the gneiss *in most cases are concordant*, with the exception of some contacts at Graemsay, where the granite locally is seen to cut obliquely ($<10^\circ$) across the gneiss layering.

Finally Strachan (2003) describes a network of fine-grained granite and aplite that cuts through both the gneiss and granites, with no preferred orientation.

Strachan (2003) suggests that there is evidence for three deformational events. D1 and D2 are the two main events, followed by a weakly developed D3.

D1 resulted in a gneissic foliation within the metasedimentary rocks. The metamorphic processes are associated with migmatization under mid- to upper amphibolite facies conditions.

D2 is associated with intrusion of the meta-granites. The meta-granites are unmigmatized, this indicates that the granites must have been emplaced following D1, but prior to, or during, D2. The metamorphic grade during D2 was probably within the lower amphibolite facies.

D3 resulted in gentle, upright folding of earlier foliations and a braided network of undeformed, fine-grained granites and aplites. The thickness ranges from a few centimeters to a meter. The veins intrude the metasedimentary gneisses and the foliated meta-granites. The lithological properties of the paragneisses could be argued to correlate with high-grade Moine rocks from east-Sutherland.

Strachan (2003) compares the geology in the area to the better known Moine rocks of East Sutherland in order to define a possible geochronology. Based on Kinny et al. (1999), migmatization and deformation of the Moine rocks in East Sutherland is thought to have occurred during mid-Ordovician Grampian orogenic event (ca.-470-450 Ma). These deformation processes are linked to the collision of the Laurentian margin with a volcanic arc in the Iapetus Ocean (Dallmeyer et al., 2001). Thus, Strachan (2003) suggests that the *D1 and migmatization in the Orkney Islands could be assigned to the Grampian event.*

2.4.3 Comparison to granitic rocks in East Sutherland

Two types of granitic rocks are observed in the Moine rocks of East Sutherland. First, a trondhjemitic crustal melt that were formed during regional migmatization. This is petrologically very different from the Orkney rocks. The second type however, a quartz-plagioclase-feldspar bearing granite that belongs to the Newer granite suite, is petrologically very similar to the Orkney granites. These were emplaced during the late Silurian to early Devonian (Strachan et al., 2002).

In east Sutherland, the earliest members of the suite has been related to the collision of Laurentia and Baltica (Kinny et al., 2003). The suite has been intruded as concordant sheets (some of them gently inclined) during regional thrusting. For example, the Rogart granite were emplaced after thrusting and during late-orogenic strike-slip displacements (Kocks, 2002). According to Strachan (2003) the granites of Orkney seems likely to correlate with early, syn-thrusting plutons. This implies that the interpreted D2 and D3 *are Silurian* in age. However, Strachan (2003) proposes that *geochemical and isotopic data* should be collected to confirm these inferences.

2.4.4 Devonian evolution on Orkney

The basins of the Old Red Sandstone found at Orkney are part of the Orcadian Basin (Figure 7; Friend et al. 2000). The Orcadian Basin extends from the north of Shetland Islands, and southeastwards to the southern shores of the Moray Firth with Caithness and the Orkneys in between as the center. The basin fill overlies Northern Highland (Moine) and Grampian (Dalradian) crustal terranes juxtaposed by the Great Glen Fault (Friend et al., 2000).

The Old Red Sandstone is divided into three groups; The Lower Old Red Sandstone, the Middle Old Red Sandstone and the Upper Old Red Sandstone.

According to Rogers et al. (1989) The Lower Old Red Sandstone in this basin is Emsian (407-394 Ma) in age and is mainly restricted to the western Moray Firth region. There are outcrops that provide evidence for a number of small, fault-defined basins. Dispersal in the main outcrops was east directed, toward the Great Glen Fault (Bluck et al., 1992). Field relationships to onshore faults indicate an extensional origin for the Lower Old Red Sandstone subsidence (Friend et al., 2000).

The Middle Old Red Sandstone succeeds the Lower mainly with conformable relationships (Mykura et al., 1976). However, locally there are minor angular unconformable relationships that are interpreted to occur from extensional fault-block tilting (Rogers et al., 1989) or from an increase in extension rate-accelerated subsidence (Scotland, 1987).

The fluvial Upper Old Red Sandstone accumulated in the time period between 387-382 Ma (Rogers et al., 1989), in geographically restricted regions of the basin, e.g. the island Hoy in the Orkneys where thick calc-alkaline lavas were erupted (Friend et al., 2000).

The lower Old Red Sandstone was dominated by sedimentation in a rift environment (Friend et al., 2000). In the middle Old Red Sandstone however, the onshore geology shows a phase of quiescent lacustrine deposition. During this period, a thick sequence of organic-rich carbonate sands and sand (now comprising “flagstones”) were deposited over large areas of the Orcadian basin (Mykura et al., 1976).

Astin (1990) separated the Middle Old Red Sandstone on Orkney into the Lower Stromness flagstone formation, the Upper Stromness Flags and the Rousay Formation. He estimated the thickness of the Upper Stromness Flagstone Formation and Rousay Flagstone Formation to

around 325 m and 220 m respectively. Illustration of the stratigraphic record is presented in Figure 9.

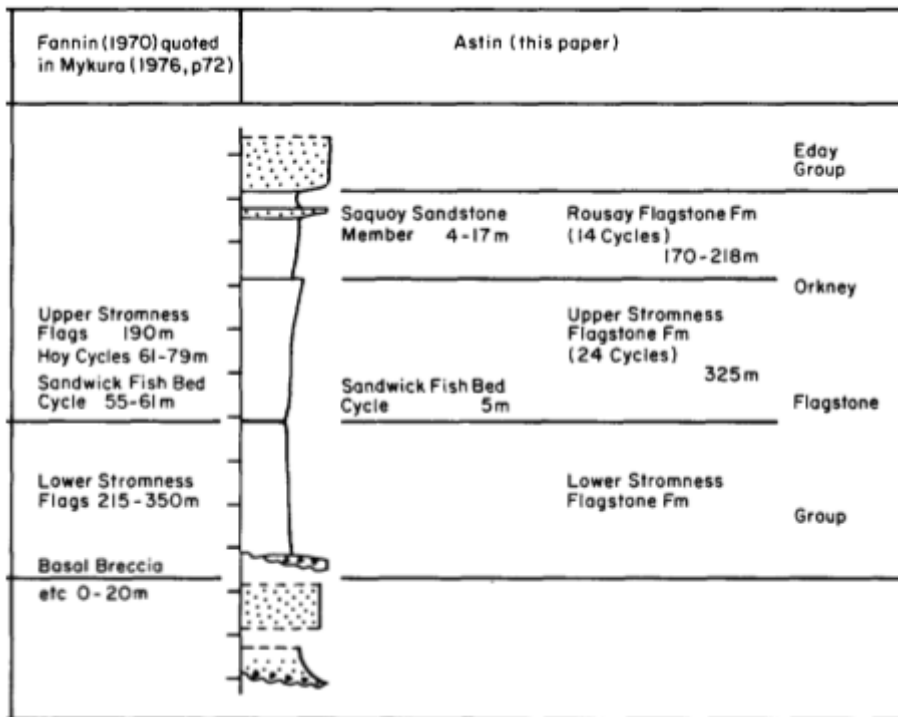


Figure 9 – Illustration of stratigraphy on Orkney. To the left, stratigraphic record based on Mykura (1976). To the right; stratigraphic record based on Astin (1990)

The lateral thickness varies and the detailed paleogeography of the alluvial sandstones shows the importance of active extensional half-graben basins during sedimentation. The relatively thin sequence, coupled with the evidence for early maturation of hydrocarbons in the basin, indicates a high heat flow through the Orcadian basins early in its history (Astin, 1990).

3 Methods

3.1 Field work

3.1.1 Introduction

Fieldwork for the thesis was conducted in the period from August 1 to August 10 on the Orkney Islands. Three days of field work was done with nice weather, and the remaining field work was done at days with some wind and periods with heavy rain. The four areas that were the subjects of observations was Stromness (along the water front and at the hill behind), at the Quoyelsh promontory, on the other side of the cove of Stromness, an area at Yesnaby, and finally, the north tip of the small island Graemsay (Figure 10). These locations were selected because they provide good exposures of the granite, gneiss, conglomerate and felsites, and because it is possible to observe the relation between these rocks. Key factors to understand important aspects of the tectonomagmatic evolution on Orkney, is therefore likely to be provided at these areas. The introduction to get to know the areas was done with help and guidance from supervisors Anders Mattias Lundmark and Lars Eivind Augland.

The rest of the days were used to follow up the observations. All outcrops with features thought to be significant were photographed and sketched. Rocks showing foliation were measured with a clinometer compass. At locations where new types of rock were encountered or a similar type of rock was observed at a different area, samples were collected.

Rock samples were collected to undertake:

- 1) Microscope studies of thin section from hand pieces of the different rock types.
- 2) Geochemical analyses. A laboratory in Sweden, ALS geochemistry, provides full chemistry. This allows comparison to other studied rocks in the areas around Orkney.
- 3) Geochronological studies.

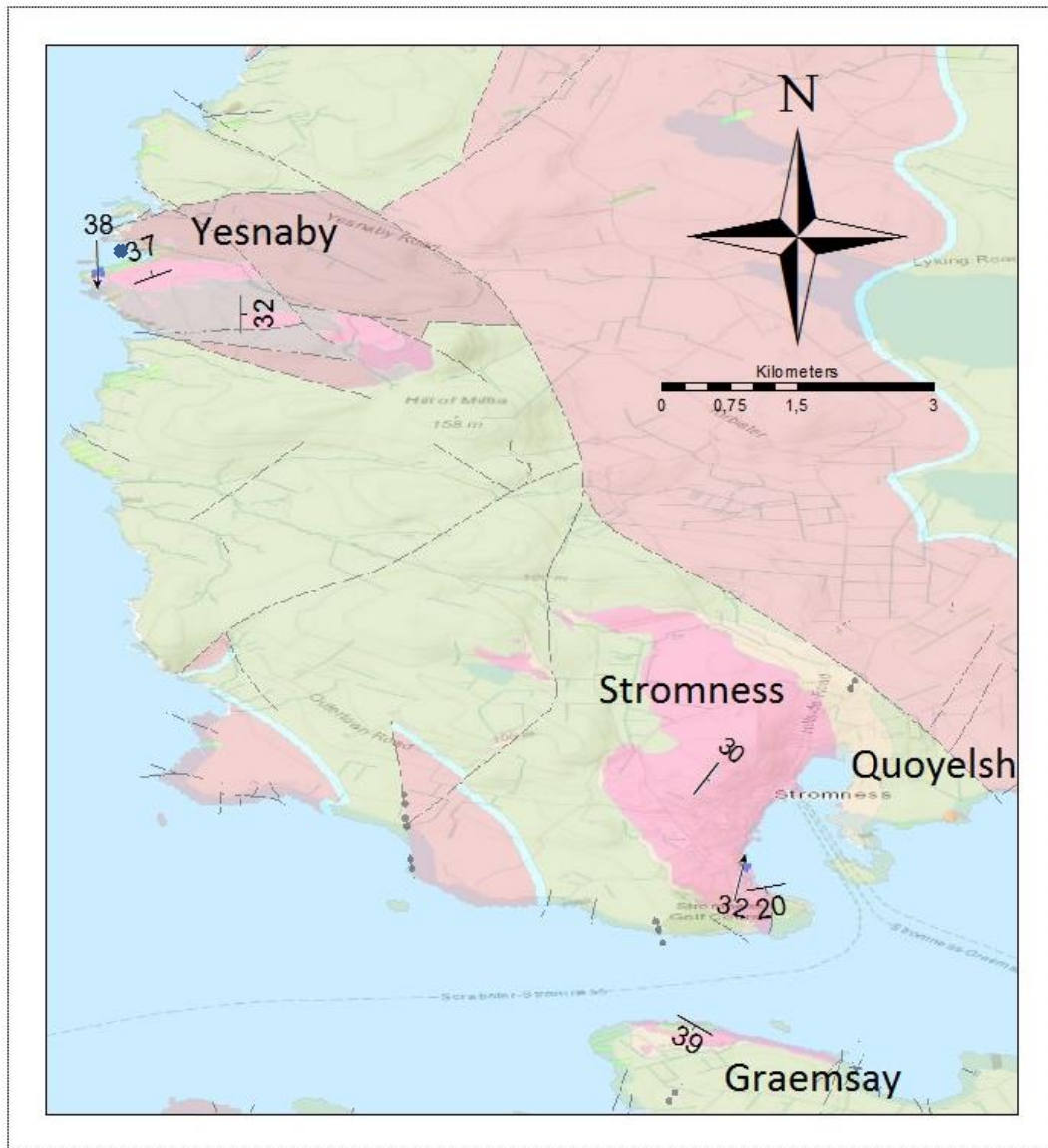
The two types of granite that were observed were sampled from both Yesnaby and Stromness; in order to compare the same rocks from two different geographical areas. All the observed

felsite layers were sampled, as were all observed mylonites. The psammitic gneiss, often observed in close relation with the granites, was also sampled.

3.1.2 Study areas

An overview over the study areas with the main structural measurements is given in Figure 10. An overview over position for the samples taken and utilized in this master thesis is presented in Figure 11.

Overview- study areas



Legend


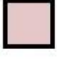

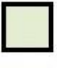





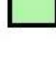
	Granite with xenoliths of gneiss		Yesnaby sandstone group
	Mylonite		Lower Stromness Flags
	Felsite		Sandwick Fish Bed
	Basal breccia and conglomerate		Upper Stromness Flags
	Basal breccia and conglomerate		Mafic intrusion

Figure 10 – Geological map of Mainland and northern part of Graemsay in the Orkney Islands. The locations that were observed during the field work are shown in the map. Structural measurements of the main structural grain are shown. Blue X marks the Yesnaby Castle landform.

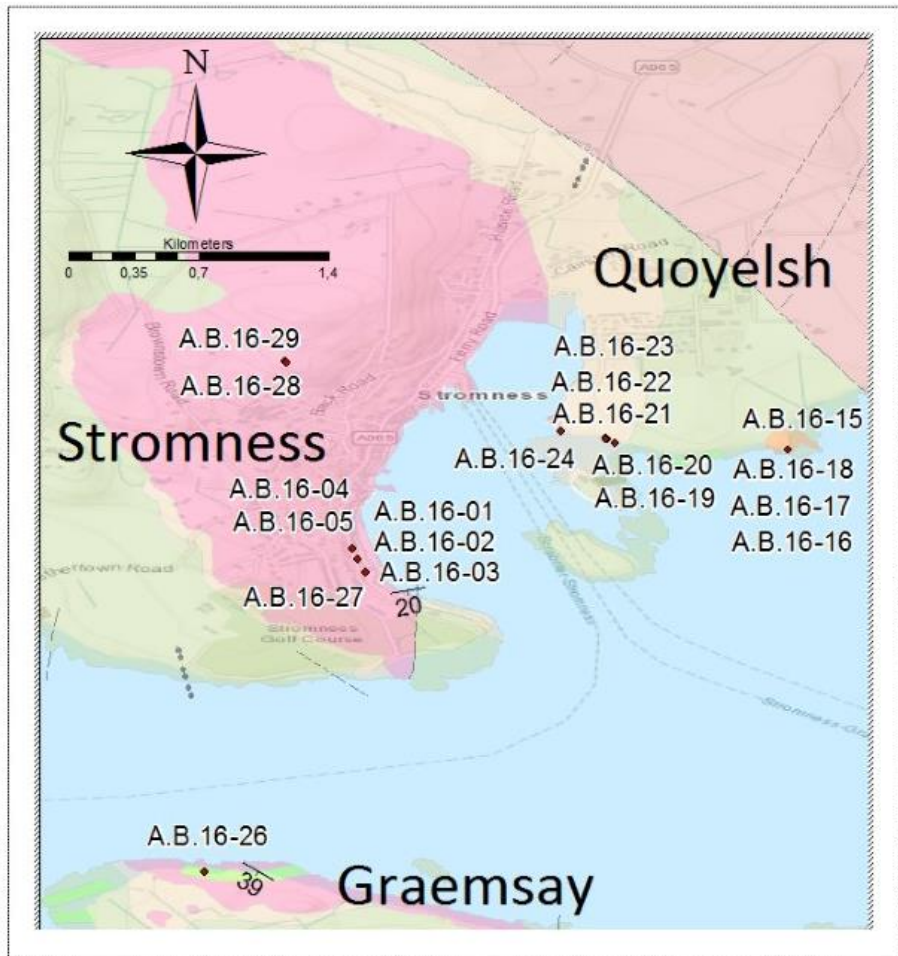
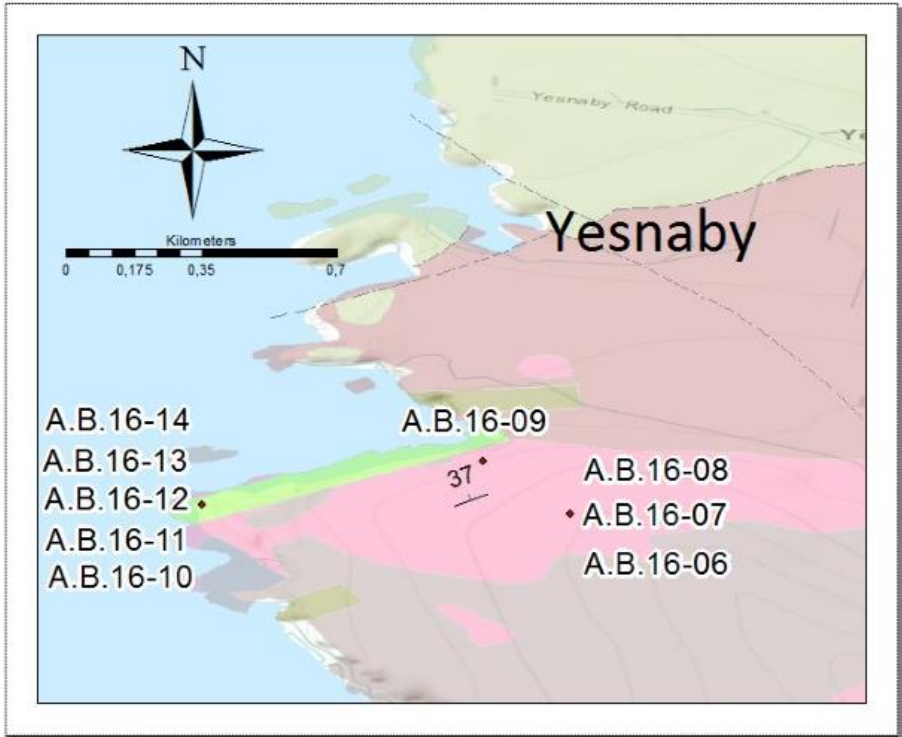


Figure 11 – Geological map showing sample localities with sample numbers at Stromness, Yesnaby and Graemsay

3.2 Laboratory methods

3.2.1 Introduction

During the field work at Stromness, Yesnaby and Graemsay, several rocks were sampled. Size of the rock-sample depended on grain size in the rock, and the purpose of this particular sample. When sampled, the rocks were placed and sealed in plastic bags, labelled and the location where the samples were picked was listed. At the end of the field work, all samples were emplaced in two large plastic boxes, and shipped off to the University of Oslo. At the University, the laboratory work was done.

Five samples were selected for geochronology by the Isotope Dilution Thermal Ionization Mass Spectrometry (ID-TIMS) method. The rocks taken for geochronology had to be crushed, prepared and washed, until finally the selected grains could be analyzed and dated.

15 samples were chosen for geochemistry. A rock saw was used to cut away all potentially weathered surfaces of the rock. Samples (now cut to have only fresh surfaces) were sent to ALS geochemistry for analysis of the geochemistry in the rock.

The rest of the samples were intended for thin section and hand sample studies. The wanted surface of the sample were exposed with the rock saw, and samples were made thin sections of.

3.2.2 Sample preparation

The five samples were selected for geochronology was crushed and sorted in order to extract the wanted grains (zircon) for analysis. This is achieved through a series of processes.

3.2.3 Sample crushing

Initial crushing is done with a machine named “Jawcrusher” (Figure 12). Its function is to crush the rocks samples from hand pieces into somewhat fine-grained gravel. The jawcrusher consists of two plates with grooves. These are called crushing plates. A clean plastic bag is placed between the plates. In this



Figure 12 – “Jawcrusher”. In the middles is the bag that collects the sample. In front f the bag are the crushing plates that crush the rock

bag the rock will be placed, and it will collect all the pieces when it is crushed. After the crushing process, the grain size will be under 1 cm and the gravel will be collected in the bag.

The gravel collected in the bag from the Jawcrusher process will be further milled down to < 0.3-0.5 mm particles in a Retsch crusher. The gravel is emplaced in a funnel with the opening towards a plate. This plate vibrates the sample out piece by piece to the end of the plate and into the machine. Inside the machine there are three crushing plates that swirl with a high speed. The sample is crushed and collected in a bucket in the bottom of the machine.

3.2.4 Wilfley table

The Wilfley-table is used for separating heavy minerals from the lighter ones. This is the first step in the process of removing grains that are not zircon grains. The Wilfley-table use water, and separates the grains by gravitation. The sample is placed in the upper right corner, at the end of a one meter long washboard. The board is rinsed continuously by water that flows down. The water is gradually stirred to the left and bit by bit, pieces of the sample are rinsed out on the board. The lightest material is spilled out with the water that rinses downward. Quartz and feldspar are examples of minerals that in large numbers will be separated out. The heaviest minerals will remain; they end up in two cups at the end of the board. The cups with the samples are cleaned in alcohol, and dried, ready for the next step.

3.2.5 Free fall, screening and Frantz

Dried samples are ready for further mineral separation processes. Every sample is collected in two cups (or more if the sample is big). The cup marked W1 is the one that is primarily used in the next steps.

The first process, “Free fall”, separates the most magnetic material from the sample. It could be magnetic grains, and it could be pieces that have followed from the crushing processes. Zircon-grains are not highly magnetic and will not be separated out. A magnet is placed vertically at a table and a plastic bag is attached tightly with the one side of the bag up to the magnet. Inside the plastic bag, two cups are placed to collect the sample. Then, a funnel is placed over the cups.

The sample is poured slowly into the funnel. Most of the sample will end up in the cup, while the most magnetic material will attach to the side of the funnel towards the magnet. This magnetic material is regularly poured into the other cup. When the whole sample has run through, the process starts over again. The strength of the magnet is turned somewhat higher, until the magnet is at its highest at 1.5 A.

The material that is not caught up by the magnet is brought to the next process of separation. A bowl, in two parts, is screwed together with a net placed in between. The net has a mesh size of 250 μm . The sample is poured out in top of the net, and then stirred. The material that passes through will have a grains size less than 250 μm , and will be taken for further separation by the Frantz magnetic separator.

The sample is poured in a can. Magnetic grains are separated with use of a magnet. The sample will fall along a rail with two tracks. The one track is placed closest to the magnet, and it will extract the magnetic grains. This provides further separation of magnetic grains that could have ended up alongside the zircon-grains. The samples run through this magnetic separation method in one step.

3.2.6 Heavy liquid separation

The last step at the separation lab is to separate the heaviest grains that still has not been sorted out. Zircon grains will be a part of these grains. The last separation process is done with heavy liquid.

The heavy liquid has a density of 3 kg/m^3 . This is poured over in a funnel with an opening in the top, and a stopper in the bottom. The stopper can be turned to allow extraction of the liquid. When the sample is mixed with the liquid, the whole funnel is shaken to thoroughly mix it. After all movement in the liquid has ended, the lightest grains will remain floating in the top of the liquid, while the some of the heaviest grains sink to the bottom. When the stopper is turned, a part of the liquid will flow out, with some of the heavier grains. The liquid ends up in a bottle placed



Figure 13 – picture of the heavy liquid bottle. Underneath is a bottle to collect the liquid the liquid that flows out. On top of this the paper that collects the heavy grain.. To the left is the bottle containing the heavy liquid.

underneath the funnel, while the grains are picked out from the liquid by a paper, placed on the top of the bottle (Figure 13).

The process is repeated 4-5 times, until enough material is collected. The rest of the material is also collected, in case it will be used again later on.

The paper with the heavy grains is put at a hot plate to dry. Then, the grains are shaken off the paper, into a petri dish. Now, the sample is reduced enough so that it is ready to be studied in microscope.

3.2.7 Preparation for ID-TIMS analysis

After the crushing processes, wash at Wilfley-table and the mineral separation processes, the sample is ready for microscope and picking of zircon grains. Below follows a description of how to prepare the zircon for analysis in the ID-TIMS-machine.

ID-TIMS is a method used for U-Pb geochronology. Isotopes from certain minerals are ionized and measured in a mass spectrometer. This is one of the most accurate and precise isotopic methods for dating of rocks (Parrish and Noble, 2003).

The most common mineral to use in ID-TIMS are zircons. Zircon is a refractory mineral that is difficult to destroy, both in nature and in a laboratory. They can survive several rounds of sedimentation, metamorphism and rock-melting. The crystal structure incorporates uranium and thorium in moderate amounts (10-1000 ppm U, and 1-100 ppm Th). Pb is almost completely excluded from the crystal lattice during formation. This gives high U/Pb- ratio at formation of the mineral (Parrish and Noble, 2003).

The uranium – isotopes ^{238}U og ^{235}U will, over time, decay to ^{206}Pb and ^{207}Pb .

^{232}Th decays into ^{208}Pb . The isotope ^{204}Pb is not formed by any form of radioactive decay and its abundance in the Earth is therefore constant through time. This isotope system gives the frame work for U-Th-Pb geochronology by using U and Th bearing accessory minerals in a rock. This will often be zircons (Parrish and Noble, 2003).

Different crystal quality can lead to different degree of Pb-loss between the zircon grains (Parrish and Noble, 2003). The two U-Pb decay constants will not always give the same age estimation, such data are called discordant. Parrish and Noble (2003) states that «Relatively

low-U zircons» has less radiogenic Pb, but also that there are less radiation damage and less Pb-loss in general. The fact that they have less radiation damage and Pb-loss outweigh the disadvantage of radiogenic Pb. Therefore, these types of grains are better suited for analysis, and gives better concordance in the measurements. Since the study of Silver and Deutsch (1963) it is generally accepted that pre-selection of zircon grains are necessary.

3.2.8 Microscope

To pre-select the best zircon grains, the sample is studied in a microscope. When studied under a microscope, the zircon grains will often be clear, with a high relief. The zircon grains appear in many different shapes from long, prismatic grains to shorter and more rounded varieties. Also, the grains can be broken and fragmented. If the grains are highly rounded, it could mean that these are xenocrysts from sedimentary host rocks.

If Uranium-content is high, the grains will usually have a more red and brownish color. It could also have more cracks, and a foggy texture. These types of grains are called metamict, and metamictisation is the consequence of radiation damage in the crystal. If zircons are too metamict, they may be too destroyed so that they could not be used in the next steps. If metamictisation is more moderate however, the grains can be used.

15-30 grains are picked (dependent on how good the sample seems to be). These are extracted with a pipette, and transferred to a small vial, made of quartz. These types of vials can take temperatures up to 1000 °C

Every sample that is to be analyzed is placed in separate quartz vials.

3.2.9 Annealing of the grains

The process of restoring the crystal lattice is called annealing. If the crystal structure is too damaged, it will not be restored during annealing, and those unrestored parts will therefore be dissolved during the following chemical abrasion. The selected grains are placed in an oven that holds 900 °C for three days. The chemical abrasion method (section 2.2.10) utilizes high temperatures treatment to anneal damages in the zircon lattice caused by alpha recoil, and spontaneous fission processes

After three days, the zircon grains are removed from the oven. With use of alcohol and a tweezer, the grains are transferred to a new petri dish.

3.2.10 Chemical abrasion

Partially open system behavior (Pb loss) has been recognized as a major factor limiting the accuracy of zircon age determination. Pb-loss will cause discordance in the results. Therefore, various methods have been developed over the years to deal with this problem. In this master thesis, the chemical abrasion method follows the development by Mattinson (2005). The chemical abrasion is capable of completely removing domains of the zircon that have lost Pb. Thus, the residual will be closed-zircon systems. (Mattinson, 2005).

Selected grains are picked and placed in the first bombs that are to be used. One bomb is used for each sample. To each bomb 10 drops of HF and 1 drop of 6HNHO_3 is added, and it is then placed in the oven at 195°C .

After a day, the bombs are removed from the oven and cooled. Then, the bombs are placed on a hot-plate and the HF is converted to 6NHCL , and after two hours on a hotplate again converted to H_2O .

3.2.11 Air abrasion

An earlier method for abrasion of the grains was developed by Krogh (1982). It is an air-abrasion method to remove the outer part of the grain. This step is important in the preparation process and is done because most of the Pb-loss will probably happen in the outer part of the grain. This procedure was performed on grains that were to metamict to be chemically abraded.

The grains are placed in a container, and mixed with a larger amount of pyrite. Then the container is sealed and air-pressure makes the grains swirl inside the container. The process continues for some hours to a day (depending on the quality of the zircon grains).

When the zircon grains are well rounded, the outer parts of the grains will be removed. The outer parts are the areas where most of the Pb-loss occurs. To separate the zircon grains from

the pyrite, all material is placed in a dish, and HNO_3 is added. Then the material is warmed on a hot plate. The pyrite grains will be dissolved and the zircon grains remain.

3.2.12 Picking suitable grains

During the abrasion, grains that are too metamict will be (almost) fully dissolved and thus impossible to analyze. Grains with crystal shapes, or fragments that are still intact will be ready for further use. These can be picked out, one by one. The numbers of grains that are selected depend on the sample.

When the wanted grains are selected they are transferred with the use of a pipette over to small glass vials. One grain is placed in each of the vials. The vials are marked, both on the top and in the bottom. The mark at the bottom is drawn where the grain assumingly has fallen down. When all the grains are picked and placed in each of the vials, it is ready for the cleaning process.

First, nitric acid (HNO_3 (+ H_2O)) is added to the vials. The vials are filled about two-thirds full. Then, they are placed at a hotplate for 20-30 minutes. Then the vials are held obliquely in an ultrasonic bath. The vials are carefully put on the table, still held obliquely, and the edge is knocked to ensure that the grain is shaken off to the wanted side of the cup. The liquid is extracted from the other side of the vial, to ensure that the grains remain in the vials.

This is done in several steps with and water acetone. The zircon-grains are then fully cleaned and ready for analysis.

3.2.13 Weighing

One by one, the cups are studied under microscope. When the zircon grain is observed, the cups are placed over a piece of aluminum foil, with rolled edges. The grains are shaken out of the cup into the foil. The foil is placed under the microscope, and the grain is observed to ensure that it has been successfully transferred. The foil is placed on a sensitive weight. This can observe weight over 0.001 mg. If the grains are smaller than this, is registered as <0.001 mg.

Then, the foil is placed underneath the microscope again to check that the grain is still present. A Teflon bomb is opened, and a drop of nitric is added. The sample is transferred from the foil into the bomb. Finally, twelve drops of HF is added, and the lid is placed on top.

This method is repeated until all the zircon grains are placed in separate bomb. Generally it is 12 bombs in total.

3.2.14 Spike

The last step before the grains are put in the oven is to add a specific quantity of spike to each of the bomb. The spike contains a known quantity of uranium and lead. It is a mixed of ^{202}Pb - ^{205}Pb - ^{235}U tracer that has recently been calibrated to the Earthtime (ET) 100 Ma solution (Svensen et al., 2015), to allow direct comparison with ages obtained with the ET tracer solutions (Earthtime). ^{205}Pb is an isotope that does not occur naturally.

The Pb blank of the laboratory is generally below 1 pg and the measured blank composition is:

18.59 ± 0.77 15.24 ± 0.38 35.8 ± 1.2

After the spike is added, the bombs are closed. Teflon bombs with little traces of Pb were developed by Mattinson (1972). Then, all the bombs are put in the oven for 6 days at 195 °C. This dissolves the grains, and then it is possible to extract uranium and lead from the samples.

3.2.15 Preparation

Preparing of columns

Chromatographic columns to separate the different remaining ions in the zircon grains are placed in line. In the bottom of the column it is placed an ion exchange resin. The purpose of the resin is to separate the remaining materials in the sample. The wanted material is the uranium and lead. Before the sample is added, the resin is cleaned in several steps with water, HNO_3 and 6N HCl.

Extracting uranium and lead

After the last round of water has run through the columns, they are ready for use. The sample is placed in the columns. Drops of 3 N HCl are added in several rounds to extract Hf and REE's from the sample. Then, 1 ml of 6N HCl is added; this will extract the lead from the column and add it to the bombs that are now placed underneath to collect it. Then 1 ml of H₂O is added to extract the uranium. Finally in the bomb, there will be a solution with lead and uranium. A drop of H₃PO₄ is added. Then the liquid is evaporated. Remaining in the bomb will be the uranium and lead, and the remains of the added H₃PO₄.

3.3 Analytical method

3.3.1 Thermal induced mass spectrometer

The TIMS-machine is shown in Figure 14.



Figure 14 – TIMS machine. To the left is the source where the samples are introduced and the following pipes that the ionized elements will run through. To the right is the computer used to control all the processes in the machine.

Every sample (in drops) is placed on a filament in silica gel on the turret that is to be placed in the TIMS-machine (Figure 15). The first filament is loaded with a standard that is used to

check that the TIMS-machine is working correctly. The Standard used at the University of Oslo is NBS982 Pb standard and U500 U standard.



Figure 15 – turret for the samples to be placed on

A screw inside the machine is turned so that the desired filament is in contact with anode and cathode of the mass spectrometer source. The filament is then gradually heated to around 1150 °C. The machine is normally tuned at 206 (ions with this mass), then the machine is adjusted to find the maximum intensity of the ions. Manual adjustments to electromagnetic lenses are made to optimize transmission of ions.

If the signal is strong enough, the analysis will be made at Faraday-mode. If not, SEM-mode will be used.

Faraday mode is a static measurement, where all the wanted isotopic masses are measured simultaneously. To utilize the Faraday mode, the signal ought to be over 30 mV in each cup throughout the measuring. The transmission of ions follows a bent curve, where the heaviest masses are separated from the lighter masses. In the receiving end, several cups are receiving the ions, and the different masses are measured.

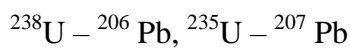
SEM mode is a dynamic measurement where the isotopic masses are measured one by one. The machine varies between the different masses, and an electron multiplier is used to enhance the signal.

The standard deviation (2σ) of the measurements ought to be less than 0.1 %.

3.3.2 Calculating the age

When all ratios have been measured an age can be calculated based on the isotopic ratios. All the numbers must first have been run through the program Tripoli. This is used to reduce the raw data, and to check that the measurements make sense. Finally a sigma test is made by the Tripoli, which gives a mean value with a margin of error.

Isotope ratios that are used to calculate age:



The isotopic ratio $^{232}\text{Th} - ^{208}\text{Pb}$ can also be used, but is not utilized in this thesis.

The measured isotopic ratios are added to the age equation.

Age equation 1:

$$T = \frac{1}{\lambda} * \ln \left(1 + \frac{D}{P} \right)$$

D/P = daughter/parent – ratio. It is the ratio for the parent.

D/P can be calculated by: $\frac{D}{P} = c\lambda^T - 1$.

The common Pb has been subtracted based on the ^{204}Pb measured.

The age equation for the two U-Pb systems gives an equation which can be iteratively solved for T if the $^{207}\text{Pb}^*/^{206}\text{Pb}^*$ is measured. The present day $^{238}\text{U}/^{235}\text{U}$ is 137.88 (Parrish and Noble, 2003). Measurements of ^{207}Pb and ^{206}Pb , Is mostly radiogenic and provides an age estimate based on the equation below:

Age equation 2:

$$T = \left(\frac{^{207}\text{Pb}}{^{206}\text{U}} \right) I \left(\frac{1}{137.88} \right)$$

The decay constant for ^{238}U , ^{235}U and ^{232}Th were determined by Jaffey et al. (1971) og Le Roux and Glendenin (1963) to:

$$1.5512 \text{ e}^{-10}$$

$$9.8485 \text{ e}^{-10}$$

$$4.9475 \text{ e}^{-11}$$

These equations form the basis for all U-Th-Pb- age calculations and all relevant diagrams presented.

Then, the numbers are plotted in a excel document, designed to calculate the age. When all the numbers are plotted, the document calculates the age, and the margin of error. The age of the sample is now measured.

3.3.3 Error analysis

Important aspects of error estimation are compiled by Roddick (1987) and Mattinson (1987).

To measure ^{204}Pb accurately is important in order to make corrections for how much common Pb that is present in the zircon grain, and also interference from organic molecules (Mattinson, 1987).

Every laboratory uses internationally agreed values for decay constants for U and Th (Steiger and Jäger, 1977). Errors in decay constants are only relevant if other schemes are used.

When the data from the geochronological studies are presented, all the relevant factors will be presented. That is, how many grains that have been analyzed, morphologic features, the weight of the grain, uranium concentration and Th/U ratio. In addition, common Pb, relevant isotopic ratios, individual errors and “error correlations” will be accounted for.

4 Results

4.1 Introduction

Field work from the four locations shows two main sections of rock assemblage, with the basement of granite with minor occurrence of gneiss, and the overlying section with felsite, conglomerate and sandstone.

The areas of Yesnaby, Graemsay and Stromness (Figure 10) show the first section. Here mainly granites crop out with additions of gneiss in various amounts. Also, shear zones with mylonite and phyllonite are observed in all the areas, the largest shear zone being at the waterfront at Yesnaby. Above the outcropping basement rocks, conglomerates are observed.

The last location, at Quoyelsh, (Figure 10) shows the second section. This location has outcrops of felsite and highly eroded sandstone. Also outcrops of conglomerate are observed, both in between the felsite layers and in the sandstone.

The observations and measurements of the rocks are presented in the following, starting with the oldest rocks, the granites and the gneisses, and following the stratigraphic record up to the conglomerate and sandstones.

4.2 Granite and gneiss

4.2.1 Exposure of the rocks

Excellent exposures of the local basement are found along the south-eastern shore of Stromness (Figure 10), with small isolated outcrops occurring along road sides and in the foundations of houses in the village. Likewise, small (typically a few square meters) outcrops occur on the hills overlooking Stromness. The basement typically consists of grey and pink granite, and in some instances psammitic gneiss with thin alternating layers of dark and lighter colors. A distinct 4 m wide mylonite zone cutting across the granites, the Stromness mylonite, crops out along the shore. The mylonite is partly overprinted by subparallel cm to dm wide phyllonites, and brittle faults/fractures. The basement is overlain by the Hara Ebb

formation, a basal conglomerate that is locally exposed along the shore, which in its turn is overlain by Devonian sandstones.

The investigated area at Yesnaby is situated ca. 1 km south of the Yesnaby parking by the Yesnaby Castle, a sea stack that has become a local tourist attraction (marked with a blue X in Figure 10). On the grassy hill due south of the sea stack patches of basement granites with some gneissic xenoliths crop out in the grassland. Along the shore below the hill to the north, the granites and gneisses are cut by a 10 m wide mylonite zone, the Yesnaby mylonite, which in its turn is cut by granitic and pegmatitic veins and dykes. The area was chosen because it is one of the three main areas in Mainland Orkney and Graemsay with documented outcrops of basement (Mykura et al., 1976, Strachan, 2003). Also at Yesnaby, two types of granites are observed, one with pink color, and one with more grayish color. The pink and the grey granite observed at Yesnaby are similar to pink and grey granite observed in Stromness in terms of mineralogy, color, grain size. The biotite defined foliation is similar in appearance and intensity. The basal breccia (named Hara Ebb formation) seems to resemble the conglomerate overlying the basement at Stromness.

On the north tip of Graemsay, a small island ca. due 2 km south of Stromness that can be reached by ferry (Figure 10), basement rocks similar to those in the Stromness area are exposed. The outcrops are found approximately in the area from the lighthouse and 200 meters eastwards along the coast. The basement rocks comprise grey and pink granite with subordinate gneiss. The pink granite dominates the outcrop.

The gneiss is isoclinally folded, and is cut by the granite. It is not possible to ascertain whether the gneiss forms xenoliths in the granite or represents the wall rock to the granite intrusions.

4.2.2 The grey granite

This granite has a greyish overall color, in some places slightly pinkish in others with a purple hue. The grain size varies from ca. 1 mm to 4 cm, but it is typically coarse grained.

The granite is made up of typically fine grained grey quartz grains (35%), coarser grains of grey alkali feldspar (40 %) and light grey plagioclase (10-15 %) (Figure 16). The alkali feldspar and quartz grains combined dominate the rock. The sizes of the alkali feldspar grains

are up to 1 cm. Further a small amount of biotite, muscovite and accessory zircon, rutile and opaques (10-15%) occurs in the rock. Biotite, some of it partly altered to chlorite (Figure 16) is the dominating mineral of these. A small grain that is assumed to be amphibole was also observed.

The granite is typically weakly foliated, but the foliation becomes more pronounced towards the Yesnaby Stromness and Graemsay mylonite. Undulose extinction in some of the alkali feldspar and quartz (Figure 31), and alteration of biotite to chlorite (Figure 17) indicates some deformation on the rock after crystallization.

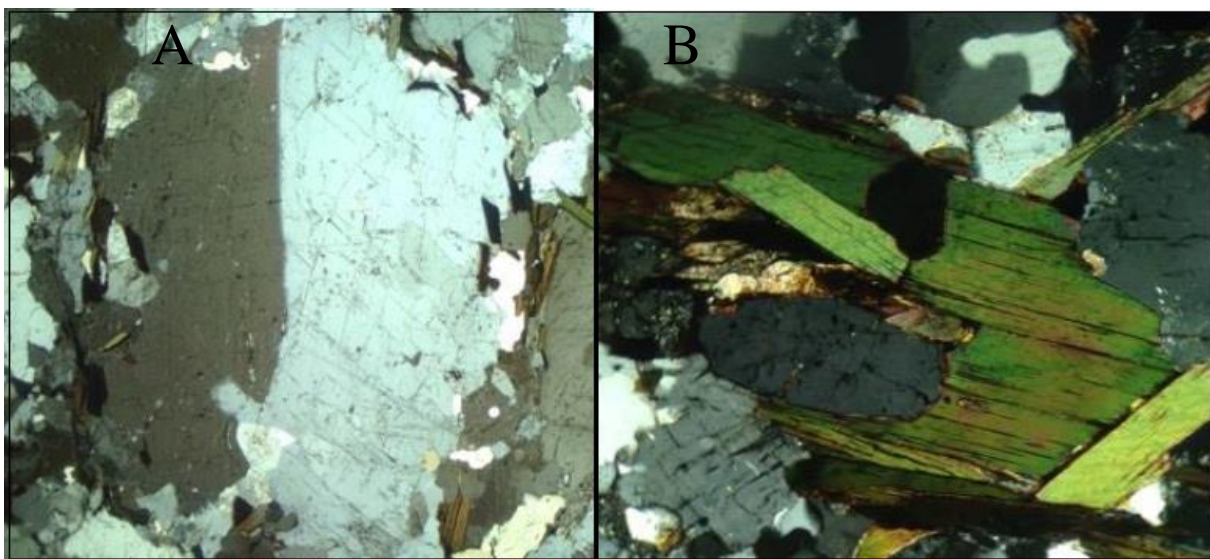


Figure 16 – Photomicrograph in Cross-polarized light (CPL) , of the grey granite (sample A.B.16-05) from Stromness. A) An alkali feldspar grain. These grains are large and dominate the rock. The grain show Carlsbad twinning and is surrounded by smaller clay minerals, mostly biotite. B): picture of biotite surrounding other minerals of feldspar and quartz. Width of view: 5.5 mm.

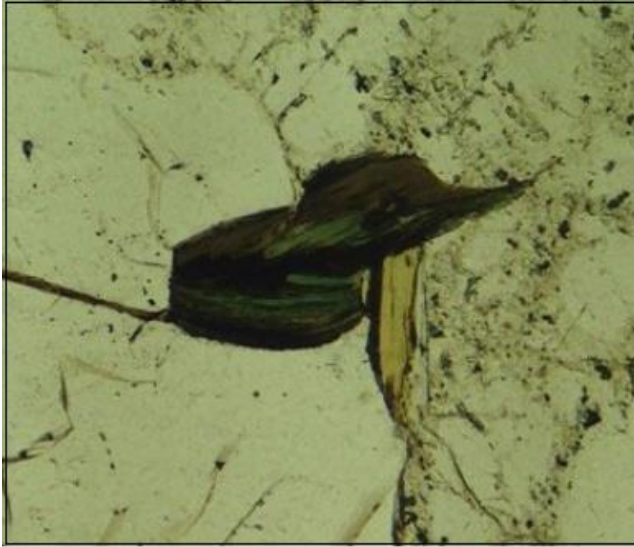


Figure 17 – Photomicrograph in Plane-polarized light (PPL) of the grey granite (sample A.B.16-05) showing chlorite with surrounding biotite. The chlorite seems to be formed by alteration of the biotite. Width of view 5.5 mm.

Thin section of the grey granite within the Yesnaby mylonite, differ from samples collected on the hill away from the shear zone mainly by a slightly larger degree of alteration of biotite to chlorite in the former.

The grey granite sampled at Yesnaby is similar to the grey granite at Stromness, but the amount of biotite is greater at Yesnaby. Furthermore, the foliation in the granite at Yesnaby top has somewhat different orientation.

4.2.3 The pink granite

The mineralogy is the same as the grey granite, but the color of the alkali feldspar is different. The color is reddish, defined by the alkali feldspar. It is porphyric and medium to coarse grained with phenocrysts up to 2 cm of alkali feldspar. Some places it is even fine-grained.

The granite has a weak foliation that increases slightly towards regional shear zones and is similar as in the grey granite.

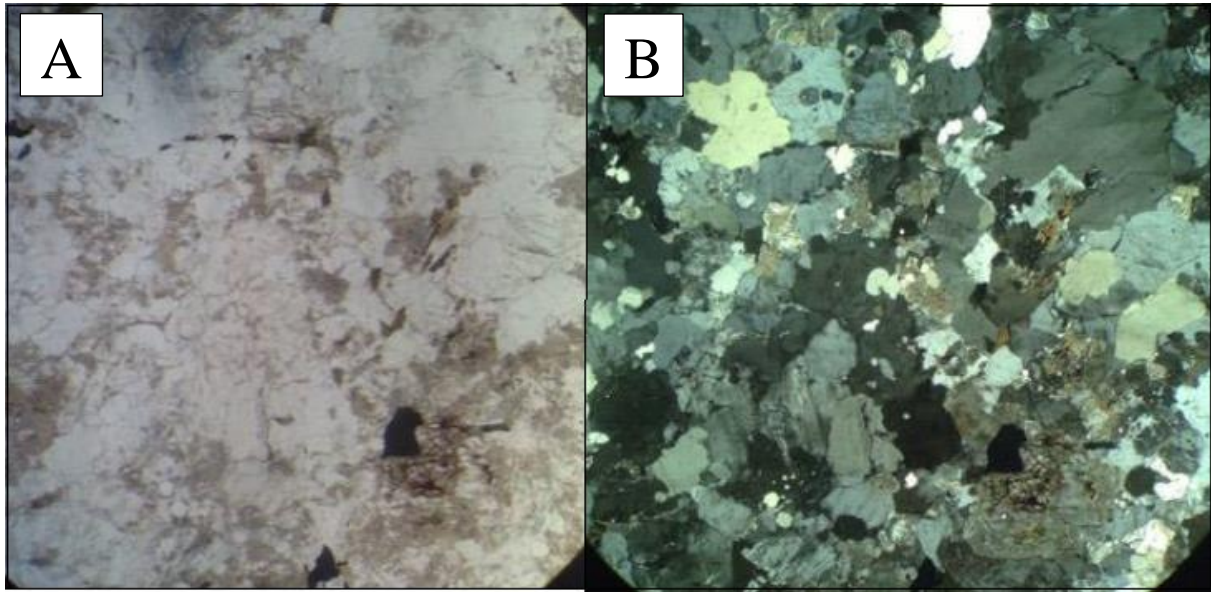


Figure 18 – Photomicrograph of sample A.B.16-04. A) PPL-picture. B) CPL picture. Width of view: 5.5 mm.

The structure in the two samples of the pink granite from Stromness (A.B.16-04) and Yesnaby (A.B.16-11) are, to a large extent, similar (Figure 18 & Figure 19). The sample A.B.16-11 has more areas where grains are deformed into a more matrix like component.

Thin section of the sample from Yesnaby show more destruction of the grains. Around 40 % of the grains are show signs of destruction with inclusions of other minerals (Figure 19).

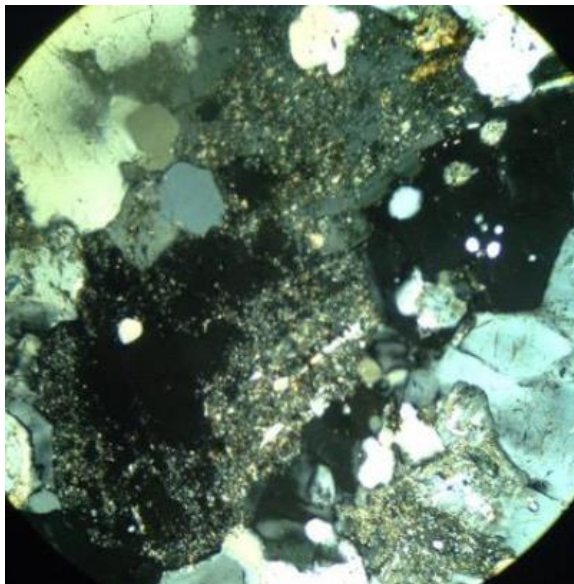


Figure 19 – Photomicrograph in CPL of the pink granite from Yesnaby (sample A.B.16-11) showing reworking of the grains that causes fractures and inclusions inside and between the grains. Width of view: 5.5 mm.

Comparison of the pink granite at Stromness with the pink granite at Yesnaby is given in Figure 20.

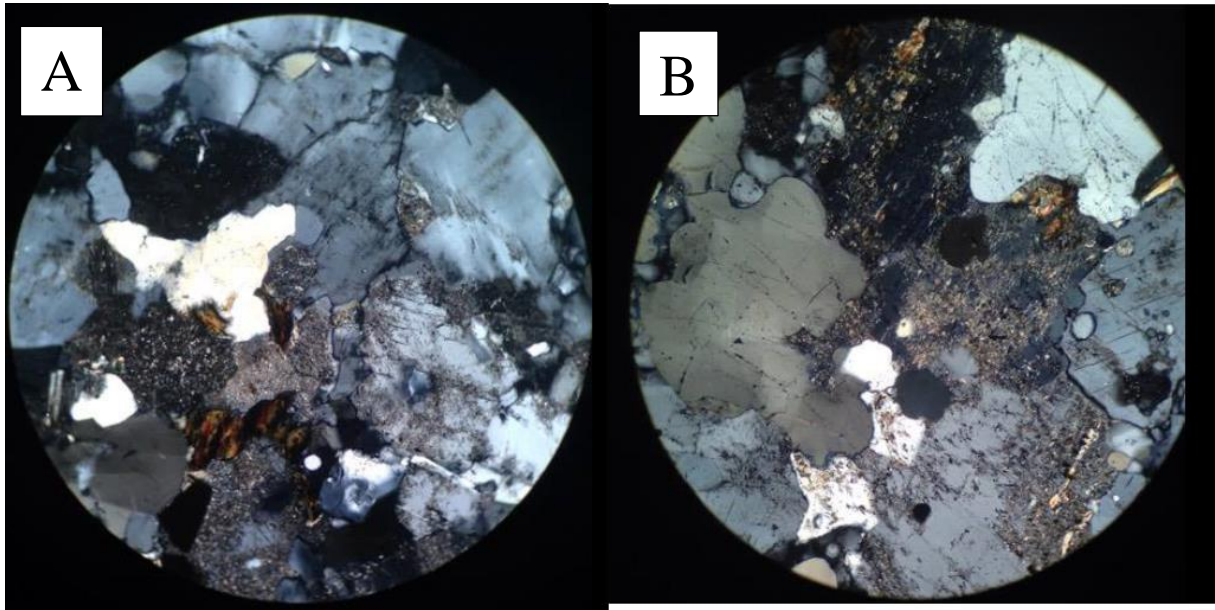


Figure 20 –Photomicrograph of the pink granite. A) Photomicrograph in CPL of the pink granite from Stromness (sample A.B.16-04). B) Photomicrograph in CPL of the pink granite from Yesnaby (sample A.B.16-11). The amount of matrix is slightly higher in A.B.16-11

4.2.4 Relation between the granites

The pink granite intrudes into the grey granite, (Figure 21) and is hence younger. Both granites display a weak foliation defined by biotite. The foliation in the two granites varies concomitantly across the field area (cf. **Feil! Fant ikke referansekilden.**). Similarly, the various deformation structures (mylonites, phyllonites and fractures) affect both lithologies in a similar manner and thus appear to post-date both granites.

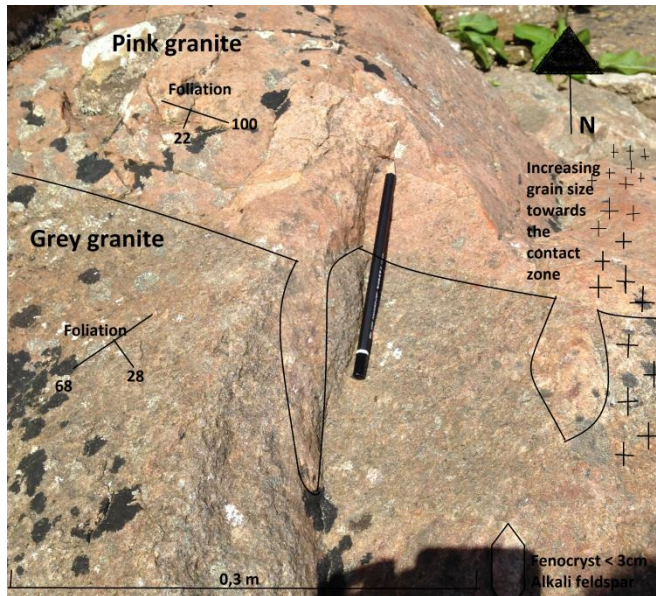


Figure 21 – Picture from Stromness, showing the contact relations between the granites, with apophyses of pink granite *intruding* the grey granite. Grain size is increasing towards the contact zone.

The intrusion shown in Figure 21 is observed at Stromness. The relation between the pink and grey granite is observed at all the locations. The foliation in the granites is typically weak. The foliation in the two granites is similar; the variation is usually no more than 20° strike and 5° dip, and will be treated as one foliation henceforth.

4.2.5 Different phases in the granite

Pink colored and very fine grained aplite vein runs through the granite at Stromness Yesnaby and Graemsay. Similar observations of the granites were made at Stromness. It is feldspar grains in the aplite vein that provides the pink color, and points to this veins occurring as a late phase the pink granite. More coarse grained and greyish pegmatite dikes occur in similar manners.

At Stromness, 100 meters south of the first encountered outcrops at the waterfront, a pink dike, 5 cm wide, cuts with sharp boundaries the granite (Figure 22). One meter beyond the surface of the grey granite shows a gradual transition to a pegmatite. The pegmatite has grains of about 3 cm.

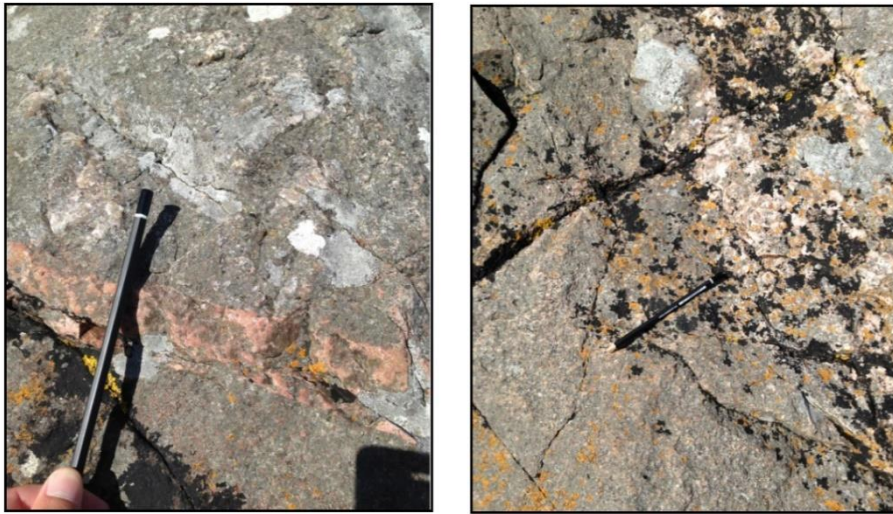


Figure 22 – Picture of the aplite (to the left) and the pegmatite (to the right). The aplite has a distinct pink color, and a sharp contact to the rest of the granite. The contact in the pegmatite however, shows a gradual transition to coarser grains sizes towards the pegmatite.

The veins run through both the granites. Both the aplites and the pegmatites are observed at several areas along the waterfront. The relations between the different facies are illustrated at Figure 23.

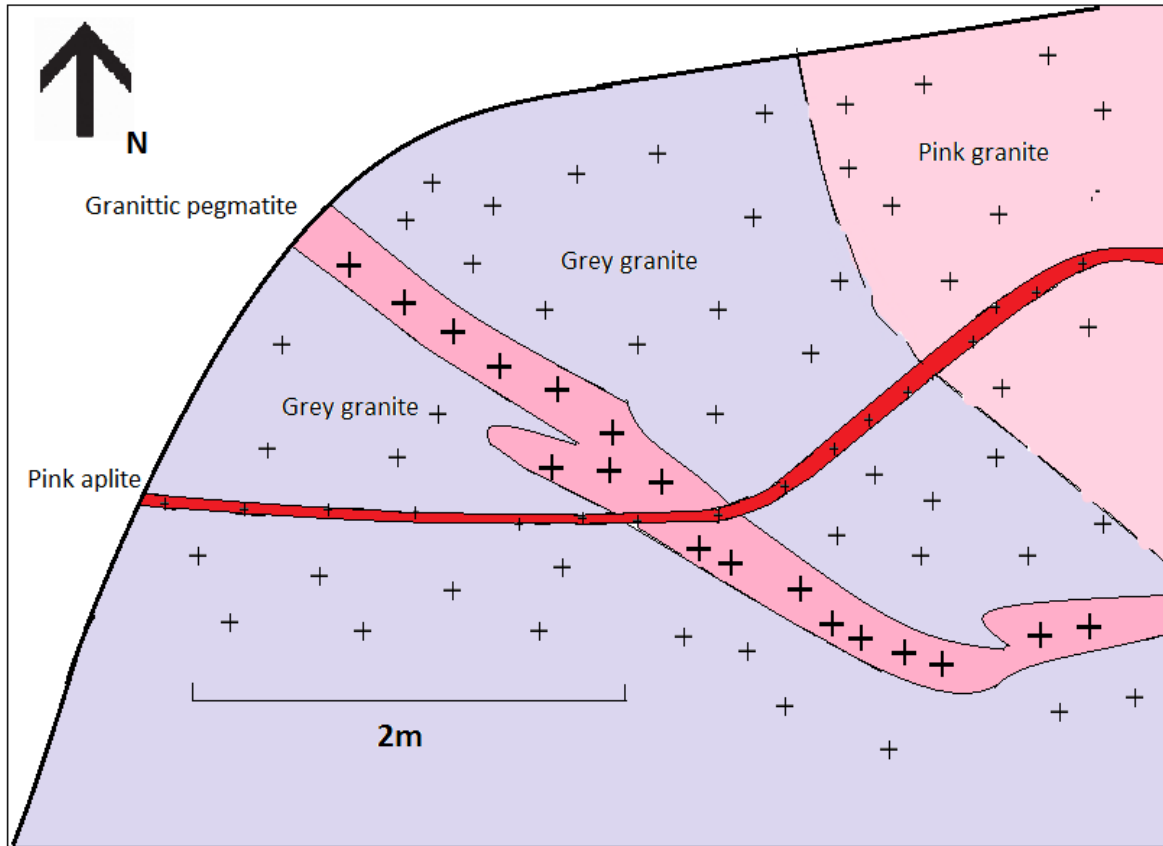


Figure 23 – Contact relation between the granites in the rock, and also the aplite and pegmatite vein. Pink granite is intruding the grey granite. The pegmatite veins is intruding the grey granite and the pink granite. The aplite vein is intruding both the granite types, and also the pegmatite

These phases of aplite and pegmatite are also observed in Yesnaby (Figure 24). Both the location on top of the hill, and at the location approximately 200 meters southeast of «Yesnaby Castle» along the coast, at the promontory down at the water. This is a ca. 10 meters wide, anastomosing mylonite zone. It is associated with many dikes and veins of granite, pegmatite and aplite that seemingly were emplaced syn- and post-deformation based on cross cutting relations.

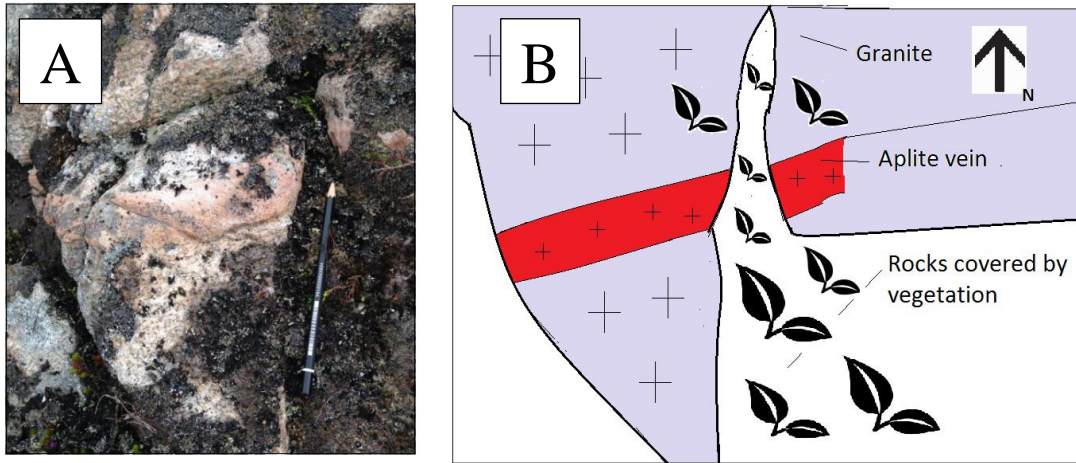


Figure 24 – A) Picture of granite and aplite from Yesnaby. B) Illustration of how the fine grained aplite vein cuts through the granite, and partly covered by vegetation

Figure 25 shows an aplite vein being cut by a pegmatite vein, observed at Yesnaby.

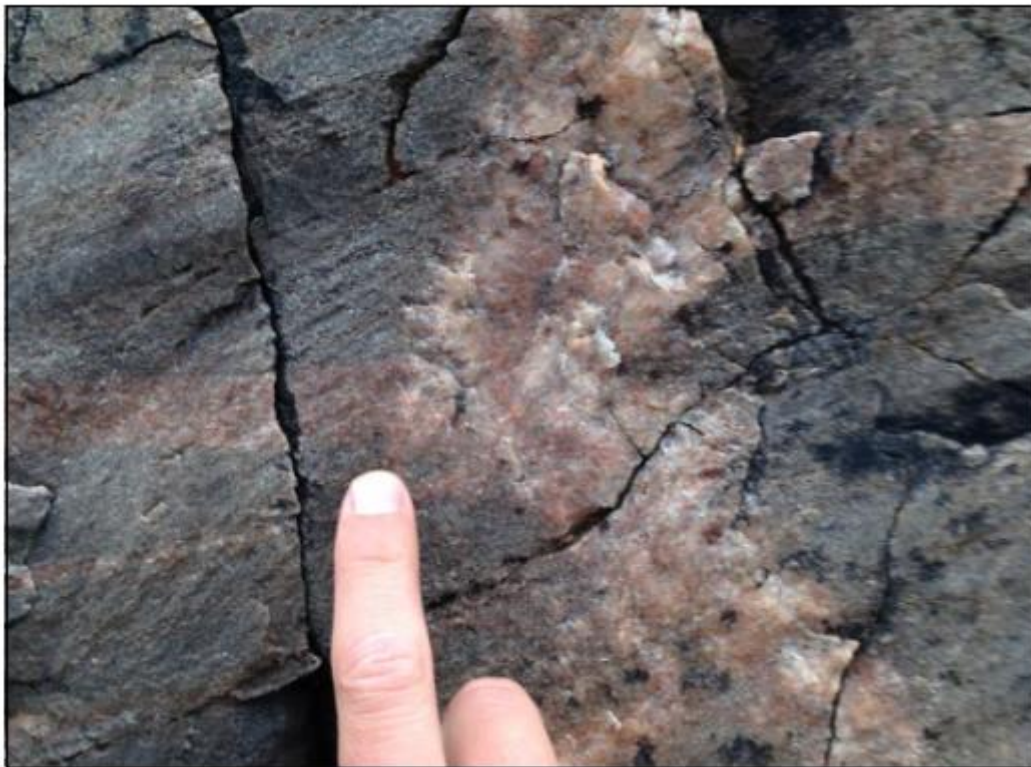


Figure 25 – Aplite vein being cut by a pegmatite vein. Observed at Yesnaby

Also at Graemsay, aplite and pegmatite veins are observed. However, at this location, the pegmatite is cut by the aplite (Figure 26).

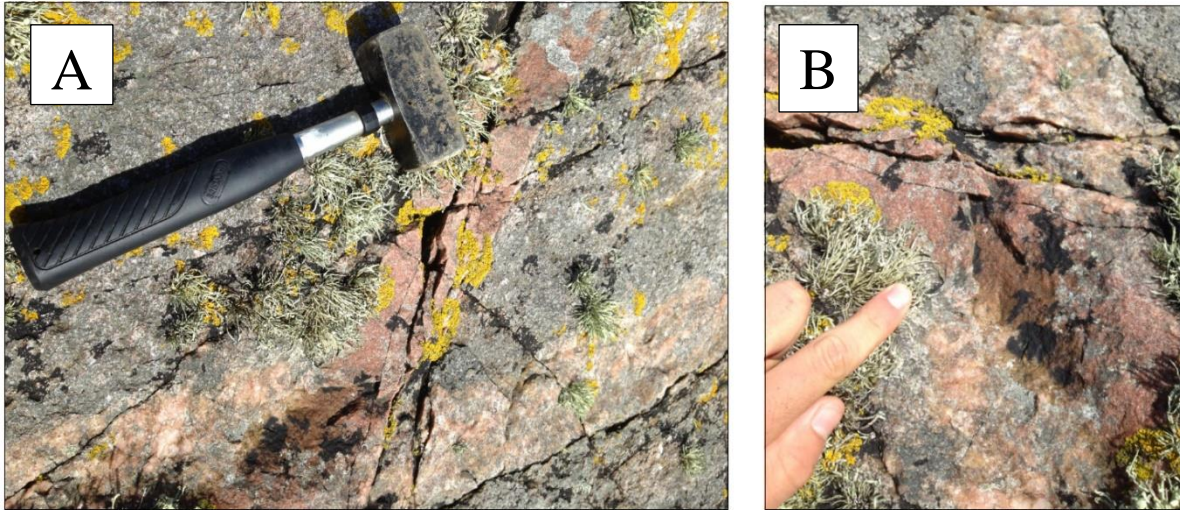


Figure 26 – A & B) Picture of aplites and pegmatite vein in the granite at Graemsay. The pegmatite vein is cut by the aplites.

4.2.6 Contact between the gneiss and the granite

In some areas along the waterfront banded gneiss with alternating dark and light colored layers that varies in thickness from 15 cm to five meters are observed. The banding suggests a sedimentary protolith. The gneiss has sharp contacts to the granite and occurs as xenoliths in the granites. Towards the south-western end of the basement outcrop at Stromness gneisses become increasingly important with a concomitant decrease in the amount of granites. The basement outcrop at Stromness (Figure 10), disappears beneath the Hara Ebb basal conglomerate and associated sandstone. The gneiss is also observed on the top of the hill, behind Stromness. Pictures from this are shown in Figure 27. The granite is associated with gneiss interpreted to represent many small xenoliths (or fewer big ones).

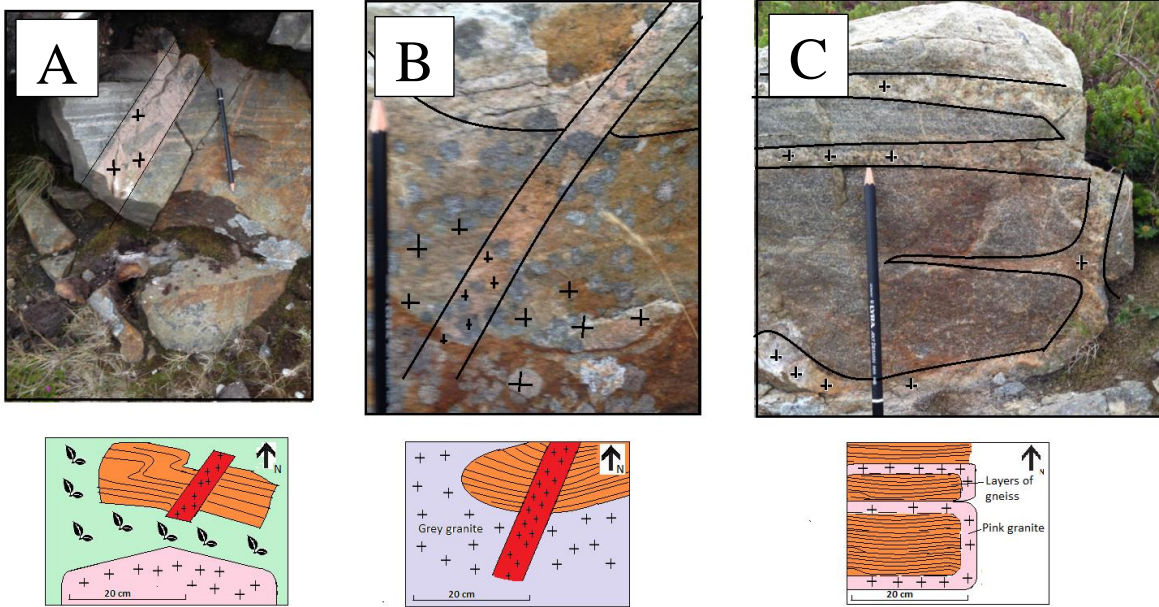


Figure 27 - Pictures and illustrations of the contact between the granite, aplite veins, and the gneiss. Pictures are from top of the hill behind Stromness. A) Aplite vein crosscutting through a gneiss xenolith. B) Picture of an aplite vein, with unclear margins, cutting through both the granite and the gneiss. C) Gneiss xenolith with several layers of granite cutting through the gneiss parallel with the foliation.

At Yesnaby, several gneiss xenoliths are observed in the foliated granite. The gneisses exposed have sizes from 1x1 meter up to 5 x 10 meters. In some instances the gneissosity seems to be parallel with the foliation in the granite, in other the foliation differs at around 40°. The gneiss varies in grain size and has alternating dark biotite rich layers and lighter colored layers of granitic composition, which resembles the banded gneiss observed in Stromness. The contact between the heterogenous gneiss and the granite were not observed on the hill, but xenoliths occur in the granite. However, the contact relations can be studied in the mylonites area along the waterfront, as shown in Figure 28 and Figure 35. In this area the granite was observed to cut through the foliation in the gneiss with high angles.

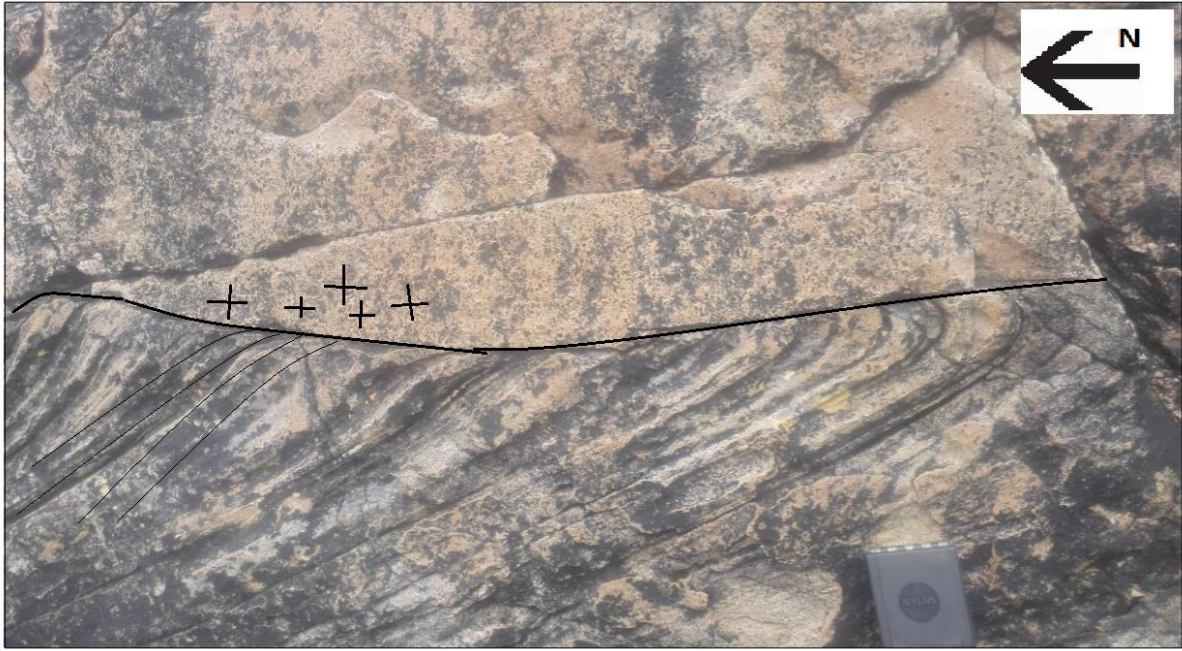


Figure 28 – Picture of the granite and gneiss observed at Yesnaby. The foliation in the gneiss is clearly cut by the granite. Also at Graemsay, the granite was observed to cut through the metasedimentary gneiss. This is shown in Figure 29.



Figure 29 - Picture of contact between granite and gneiss on Graemsay. An apophyses of the granite is cutting through the gneiss

4.3 Mylonites and phyllonites in shear zones

4.3.1 Mylonite zone at Stromness

A shear zone, Figure 30, is observed along the waterfront near Stromness (Figure 10).

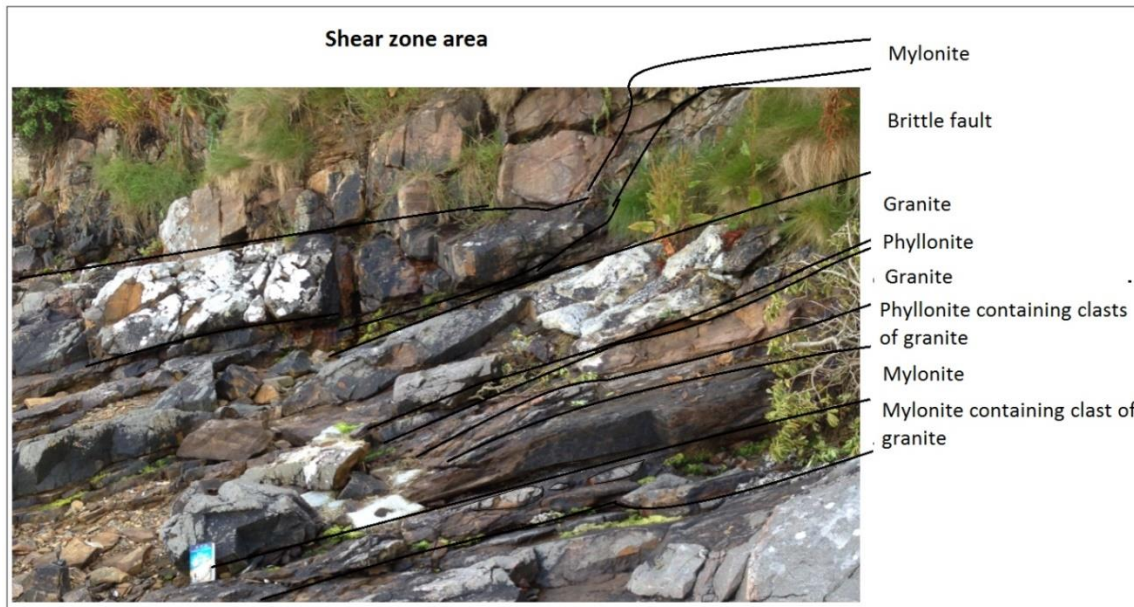


Figure 30 – Overview over the shear zone area. Sketch illustrates the alternating layers between the mylonite layers, granite, phyllonites and a brittle fault in between.

The granite is intensely deformed, displaying a mylonitic fabric. Lenses of the granite occur within the mylonite. The mylonite is layered and contains large amounts of biotite.

In zones within the mylonite there are phyllonites. The phyllonites are defined by silky films of micas that have been smeared out along schistosity surfaces. It has deformed and altered the mylonite, and is further deformed under different conditions. The phyllonite is seen to weather more easily than the mylonite.

There are several layers with mylonite, protomylonite and phyllonite. The most abundant rocks observed in the shear zone are the mylonites. The layers of phyllonite are thinner and are overprinting the mylonite layers. The mylonite-phyllonite shear zone is overprinted by brittle faults, indicating top-so SE movements. In total there are observed 6 phyllonite-layers overprinting the mylonite ranging from 5 cm to 50 cm. The brittle fault area has a width of approximately 50 cm.

Thin section of the mylonite from Stromness shows mostly, quartz and feldspar and some mica minerals. The micas are mostly muscovite and biotite. Grain size is reduced on the quartz and feldspar, and allowed growth of mica.

Subgrain rotation recrystallization is observed in several quartz grains in thin section from the mylonite (Figure 31). These quartz grains also show undulose extinction. The subgrain rotation recrystallization and the undulose extinction point to that this deformation has occurred in the quartz when the setting is somewhat more brittle, thus, this is not the first type of deformation that has occurred in the rock. Figure 31 show example of subgrain rotation recrystallization. It illustrates the manner of one grain, divided into several smaller grains with slightly different extinction angles.

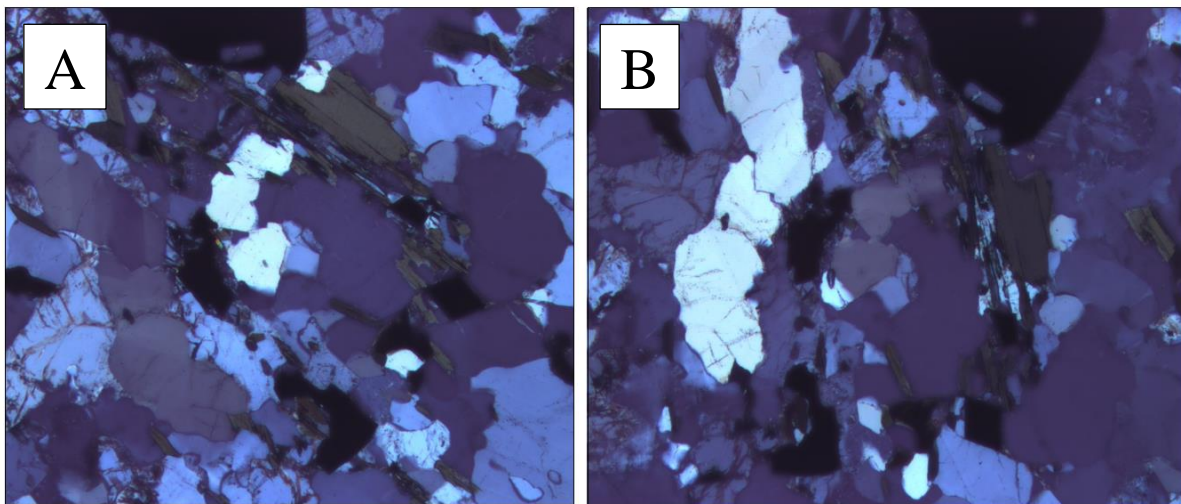


Figure 31 – Pictures showing Subgrain rotation recrystallization (SGR) in quartz grain (in the middle of the picture) with undulose extinction. A & B) Picture of the same grain, only turned 90 ° in B).

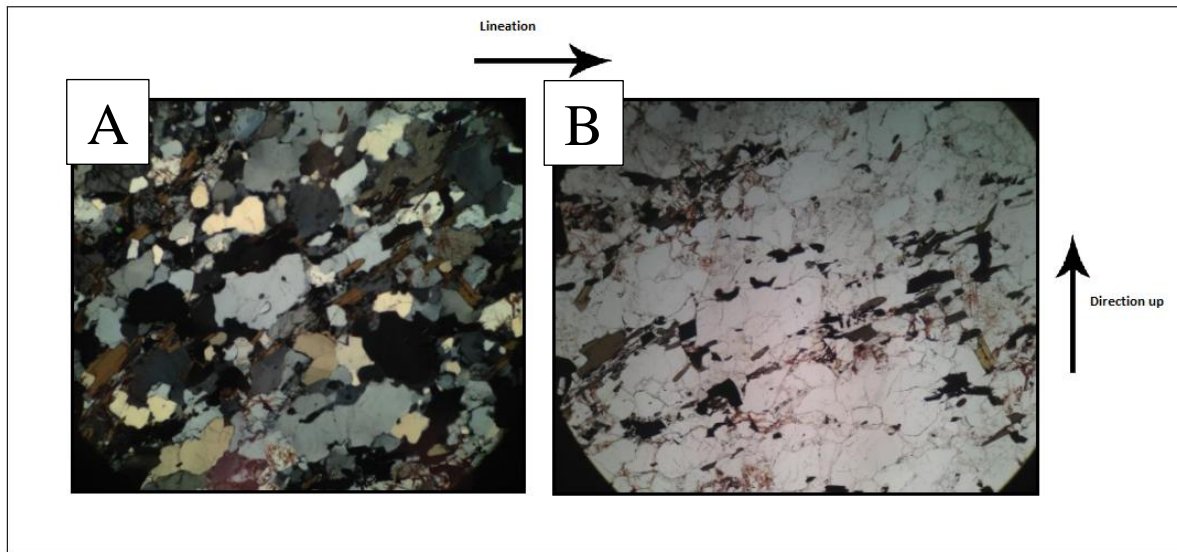


Figure 32 – Thin section of sample A.B.16-01, from the mylonite zone at Stromness. To the right: XPL-picture. To the left: picture of the same area in PPL. Lineation and direction up in the sample is shown with the arrows.

From studying of thin section it is given that it consists mostly of alkali feldspar and quartz. The alkali feldspar grains show zonation in extinction angle, and the alkali feldspar and quartz grains combined dominate the rock. Plagioclase is also present in the rocks, with zonation and polysynthetic twinning, that occurs between albite and pericline. In between there is a number of small to medium grains with elongated shape and brownish to dark color. This is mostly biotite, but some of the biotite is partly altered to chlorite. The rock consists of c. 35 % K-feldspar, c. 25 % quartz, c. 10 % plagioclase, 15 % biotite, 10 % chlorite and 5% muscovite and other accessory minerals.

4.3.2 Mylonite zone at Yesnaby

The mylonite zone encountered in the shear zone are at Yesnaby consist of layers of mylonite and phyllonite, in between granite and metasedimentary gneisses.

Both the pink and the grey granite are observed. Pegmatitic pink intrusions and aplitic pink dikes. The granite has marks of being syn-intrusive. A psammitic type of gneiss also occurs in the mylonite zone. It has a clear folding of the foliated layers. The mylonite is on top of the basement, and the basement is assumed to be gneiss.

Overall, the mylonite is cut by the phyllonite layers, and also the different phases of the granite. The mylonite is cut by both the aplites and the pegmatite.

The pegmatite dikes cut the mylonite, but are cut by the phyllonite layers. The relations between a granitic pegmatite and the mylonites and phyllonites are illustrated in Figure 33.

Granittic pegmatite cutting through the mylonite and being cut by the phyllonite

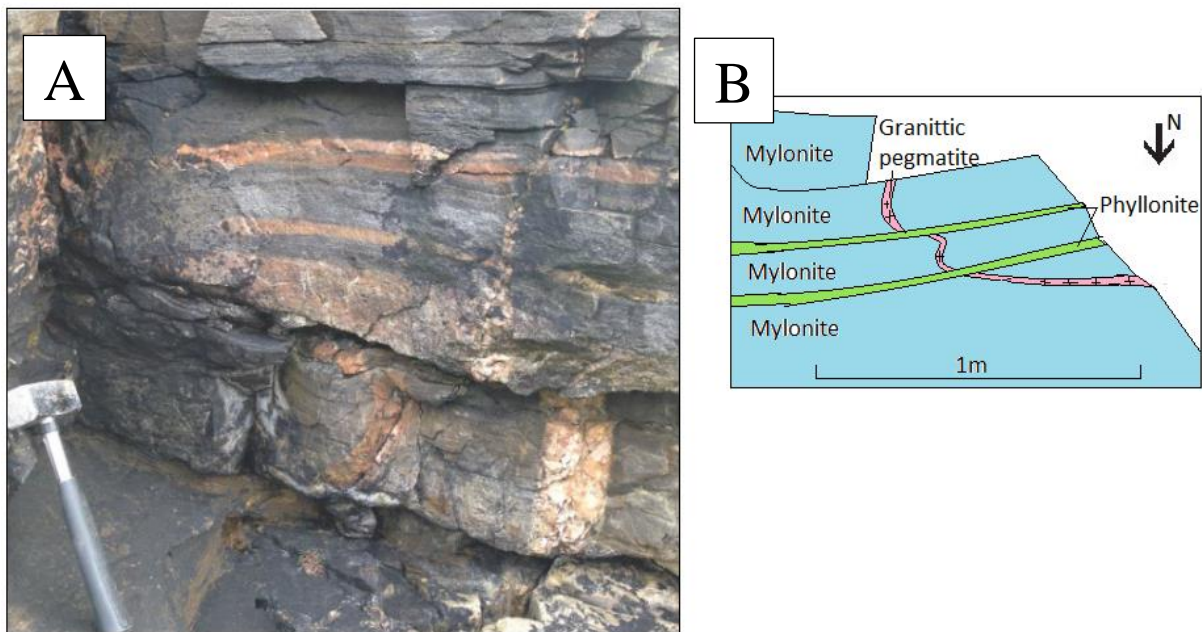


Figure 33 – A; picture of pegmatite vein cutting through the mylonite, then being cut by the phyllonite. Phyllonite layer is visible just below and over the hammer. B: overview over the full cross-section of the mylonite with pegmatite and phyllonite in between (sketch taken from another angle)

The aplite vein is observed cutting through the mylonite and is further cut by a pegmatite dike. This is illustrated in **Feil! Fant ikke referansebildet..**

B



B

Figure 34 – aplite vein cutting through the mylonite, and being cut by a pegmatite dike

Mylonite cutting Moine psammite

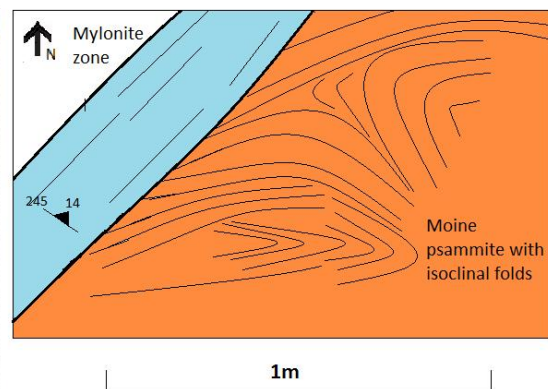


Figure 35 Mylonite cutting Moine (?) psammitic gneiss

Kinematic indicators:

In the mylonite zone at Yesnaby, several kinematic indicators are observed. Most closely studied are sigma clasts in the mylonite and fold vergence in veins cutting through on the rock faces (Figure 36 & Figure 37). These are studied on rock faces parallel to the around 340° lineation in the mylonite.

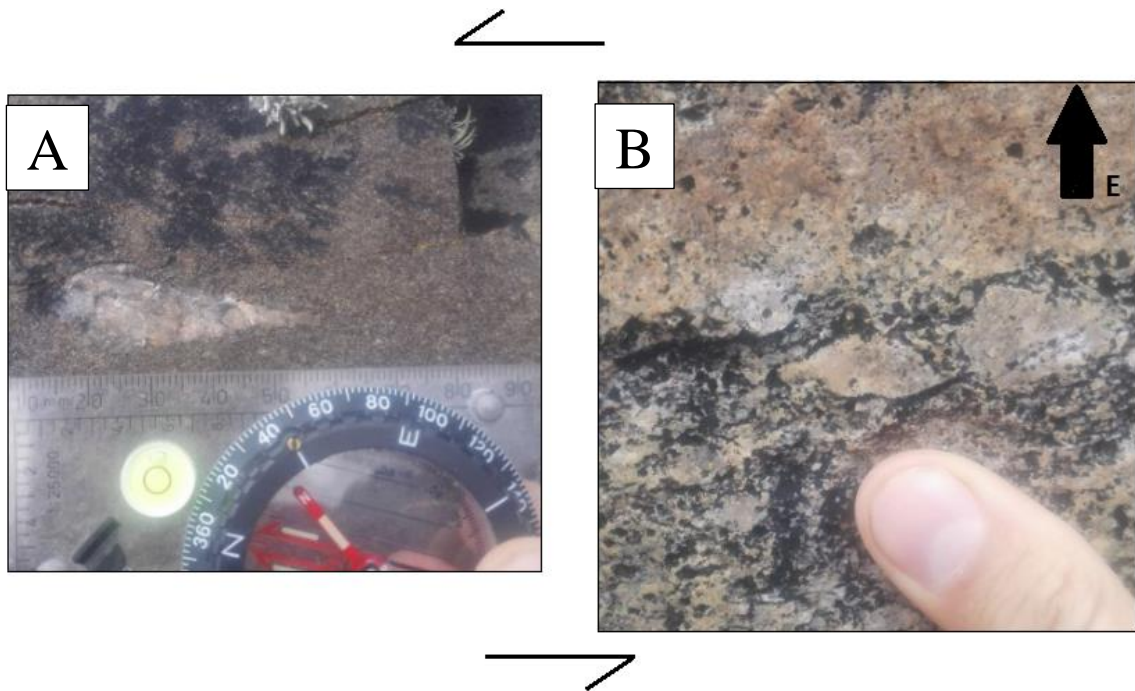


Figure 36 – Sigma clast in the mylonite. The picture is taken towards east. Shear sense indicator is top to north displacement.

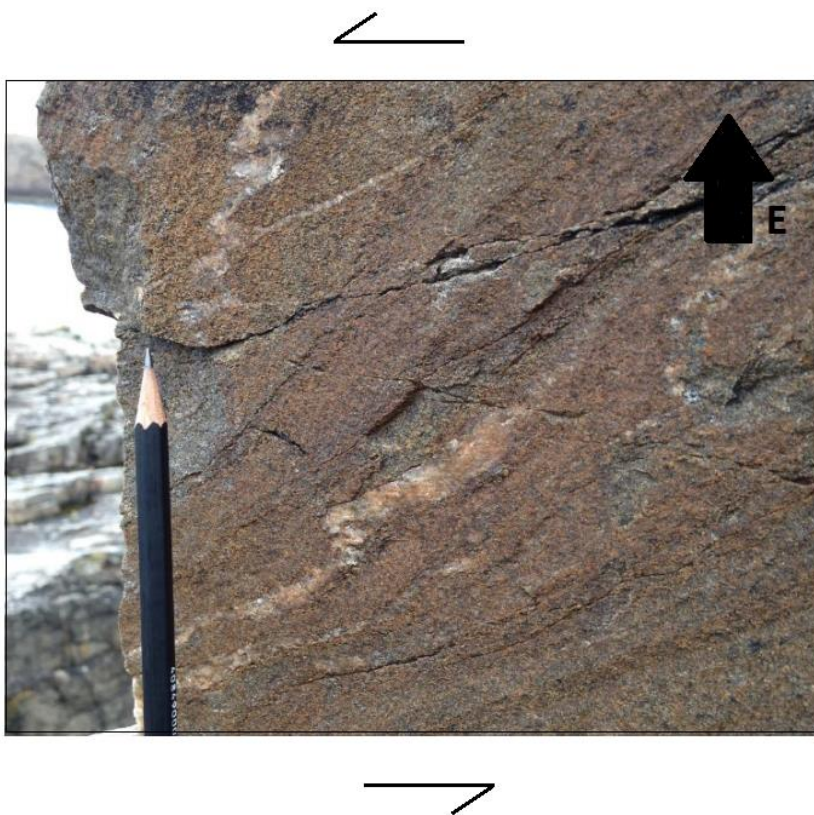


Figure 37 - Picture of two veins of granite in the mylonite. The rock surface is parallel with the lineation in the mylonite. The fold vergence observed in the veins has a northerly direction.

There is observed a syn-kinematic pink granite intrusion in the rock (Figure 37). The vein, parallel with the lineation, shows folding with vergence towards north.

4.3.3 Thin section of granite from the Yesnaby shear zone area

Thin section of the granite from the shear zone area at Yesnaby shows 40 % quartz and 45 % feldspar with around 5-10 % mica mineral.

It is observed mymekite growth in some feldspar grains. This is shown in Figure 38.

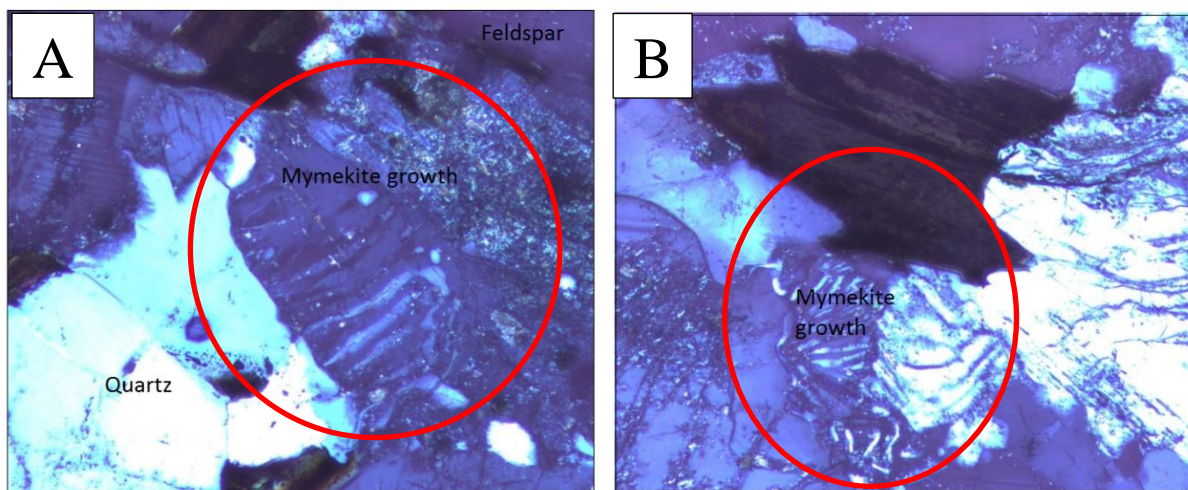


Figure 38 – To examples of mymekite growth in the feldspar grains.

It is observed subgrain rotation recrystallization in the some quartz grains, and in some feldspar grain (Figure 39).

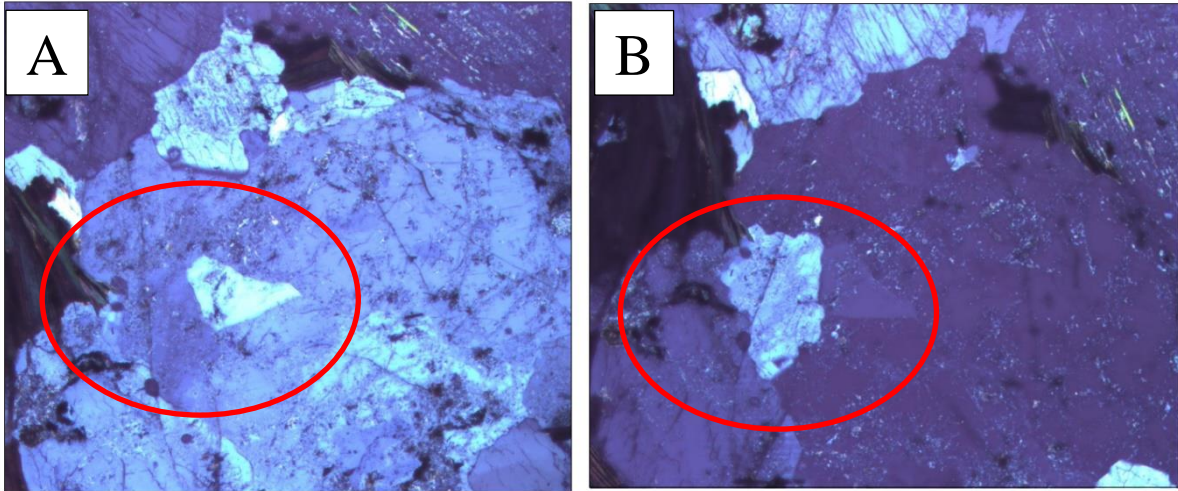


Figure 39 - Picture of a feldspar grain from two angles. The red circle shows the area in which the subgrain rotation is observed.

The beginning of sub grain deformation in the feldspar grain could suggest deformation under amphibolite facies.

The most prominent kinematic indicator observed in the oriented thin section of the granite is a sigma clast object. The section is cut parallel with the lineation, and the clast is indicating top to north sense of shear (Figure 40).

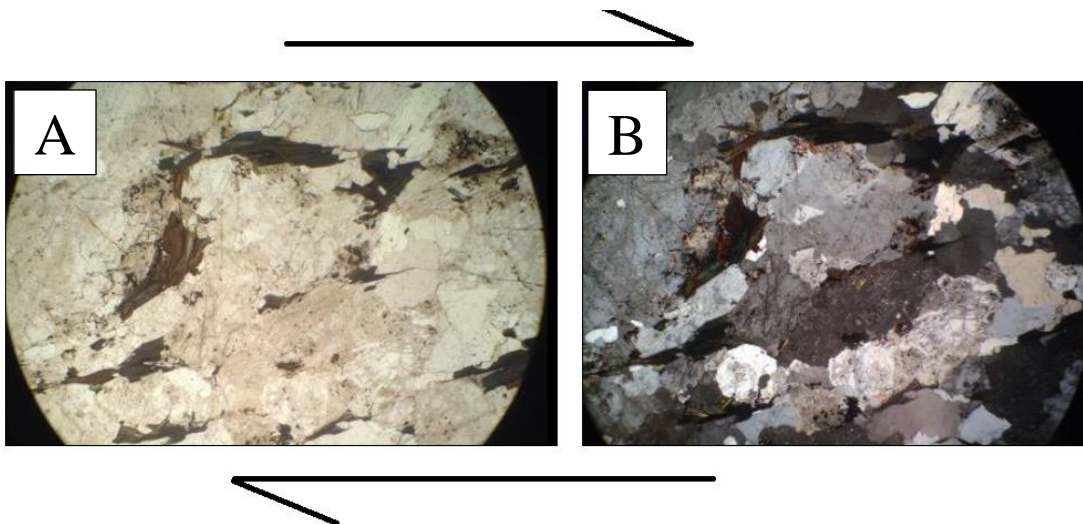


Figure 40 – Photomicrograph in A) PPL and B) CPL, of a sigma clast in the deformed granite from the shear zone area at Yesnaby. The sigma clast is indicating top to north direction.

4.3.4 Shear zone at Graemsay

Also at Graemsay a shear zone area was observed (Figure 41).



Figure 41 - Shear zone area in the basement outcrops at Graemsay

The deformation in this area is not as extensive as the other locations but from thin sections the mylonitic structures are clear in this shear zone area as well (Figure 42).

Phyllonite areas in the shear zone rock from Graemsay

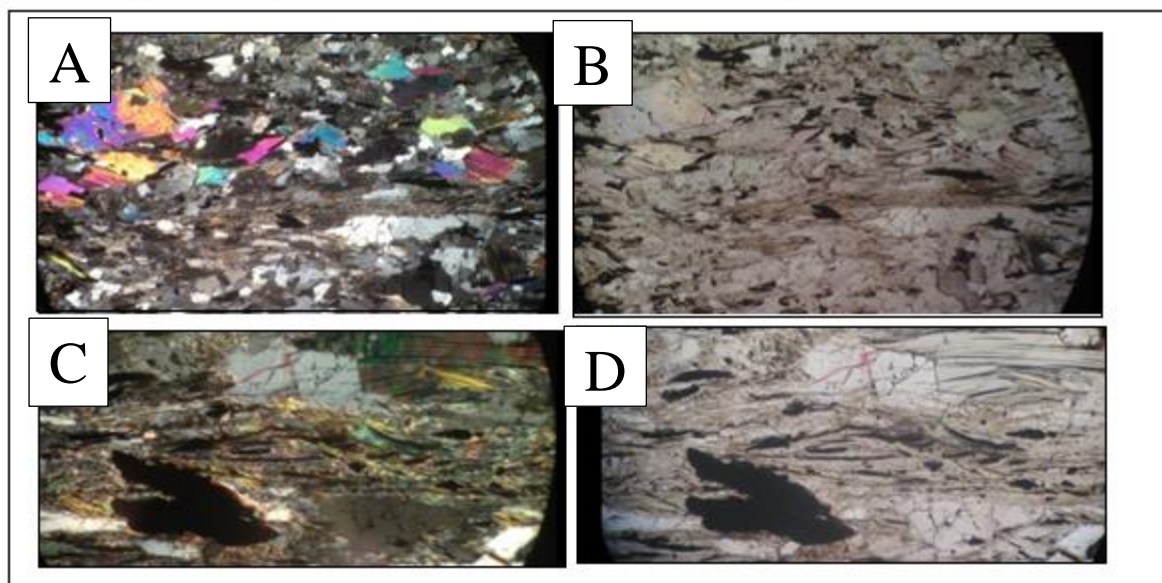


Figure 42 – Photomicrographs of phyllonite areas in the shear zone rock from Graemsay. A & B) Overview over the phyllonitic banding in CPL and PPL C & D) Zoomed in to a single phyllonite area, in CPL and PPL.

There is grain size reduction in the quartz and feldspar grains. Some areas have fine-grained phyllonite areas; this is mainly feldspar grains deformed into light, fine-grained mica.

4.4 Volcanic rocks: felsite layers

4.4.1 Introduction

The following presents the field observation made at Stromness on the other side of the cove, between Copeland dock and the Quoyelsh promontory.

At the easternmost end of the location, felsite is exposed on a ca. 20 m² area on the Quoyelsh promontory (marked with red X on Figure 10). The felsite has an uncertain relation to the surrounding outcrops along the beach of Hara Ebb basal conglomerate and Devonian sandstone. The felsite has previously been interpreted as a small outcrop of volcanic rock that could lie directly on the basement, i.e. pre-date the Hara Ebb formation, or be intercalated and coeval with the Hara Ebb formation, or potentially represent later volcanism, such as the Carboniferous lamprophyres on the Orkney Islands (Lundmark et al., 2011). Alternatively, the felsite could represent a large allocthonous block. In this study, the field relations of the felsite were investigated and the felsite itself was sampled to determine its age and geochemical signature as part of the investigation of the Caledonian tectonomagmatic evolution of the Orkneys.

In search for additional felsite outcrops and contacts, and potentially associated volcanic clastic sediments, a stretch of approximately 200 meter along the beach was investigated west of the promontory. Outcrops of tuff felsite, basal breccia, and sandstones were logged and sampled. Some of these rocks are described below.

4.4.2 Promontory with felsite

At Quoyelsh promontory, felsite rocks are dominating the outcrop. The color is light brown, and very fine grained. Small alteration spots of darker color occur and cover about 5 % of the surface of the rock. Flow banding is visible in most of the felsite and is generally sub-horizontal (Figure 43).



Figure 43 – A) Overview photo of the promontory with felsite. B) Hand piece of the lowest felsite layer (from sample A.B.16-18). Overall a light brown color with flow banding of even lighter brown to white color. Small inclusions of darker colors cover approximately 5 % of the rock surface

The exposed felsite appears to form three separate layers. The lowest felsite layer is only visible during low tide, and is overlain by a second and a third layer that is separated by a layer of conglomerate (Figure 49). These three layers seem intact throughout the outcrop, and would seem to continue below the sandstones that occur on both sides of the promontory. From field observations of the outcrop there is little evidence for this outcrop being a block. On the contrary, the apparent continuity of the subhorizontal felsite layer in the outcrop, the large size of the felsite outcrop relative to any other blocks observed in the Hara Ebb formation, and the generally sub-horizontal flow banding indicates that the felsites represent in situ volcanic rocks.

An overview of the relation between the felsite rocks and the conglomerate in the upper part of the promontory is illustrated in Figure 44. Close up pictures are given in Figure 45 & Figure 46. These show several felsite layers overlying conglomerates with pieces of the felsite inside the intraformational conglomerate.



Figure 44. A) Picture of the upper part of the promontory with two of the felsite layers (felsite layer 3 & 2). Large parts of the rocks are covered by vegetation. The felsite layers display sub horizontal flow banding and are interrupted by layers of conglomerate.

The conglomerate between felsite layer two and three contains mainly felsite clast and boulders. There are observed tiny fragments that could be derived from granitic rock. However, the conglomerate consists mainly of felsite. This view is also supported by field observations by Brown (2017) presented on his website. Both Felsite layer 3 and Felsite layer 2 are sinking into the underlying conglomerate (Figure 45 & Figure 46), and in some spots, pieces of conglomerate clasts seems to be picked up by the felsite layer Figure 47.

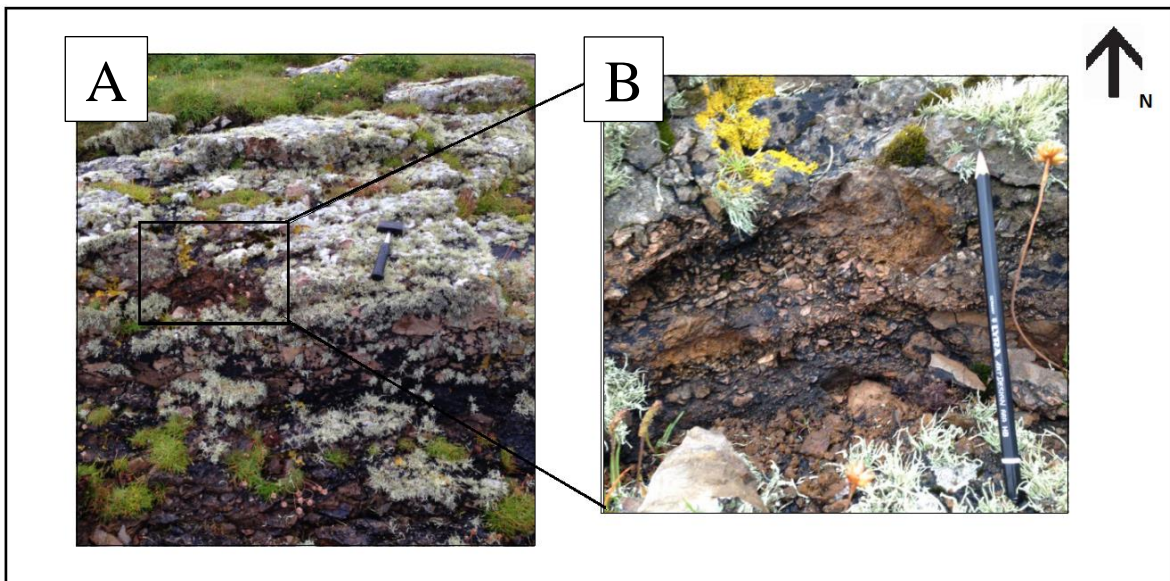


Figure 45 – A) Overview picture of the upper part of the promontory. B) Close up showing a conglomerate layer separating two layers of felsite.



Figure 46 – Picture of contact between Felsite layer 2 and the underlying conglomerate showing that the felsite layer is “sinking” into the conglomerate.

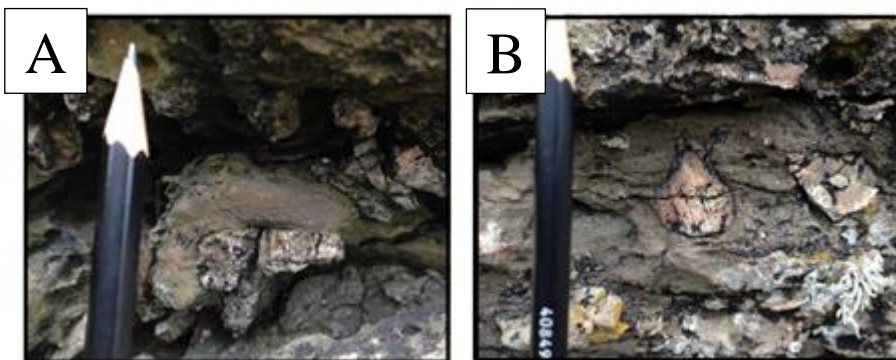


Figure 47 - A & B) Pictures of the relation between the felsite and pieces from the conglomerate (also of felsite). The felsite layer is incorporating fragments of the conglomerate

The three layers of felsite are observed as complete layers from both sides of the promontory, and there are no field evidence that points to that the felsite are blocks that have been derived

from another location Figure 48.

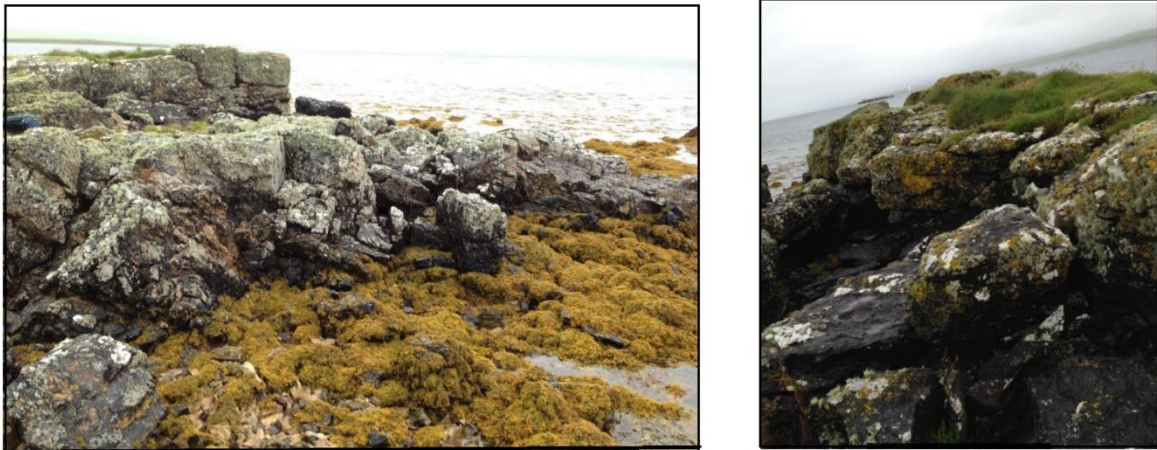


Figure 48 – A) Pictures of the promontory, taken with direction towards east. (B) Picture of the promontory with direction towards west. The pictures show no interruption in the felsite layers.

A simplified model of the stratigraphic sequence is presented in Figure 49.

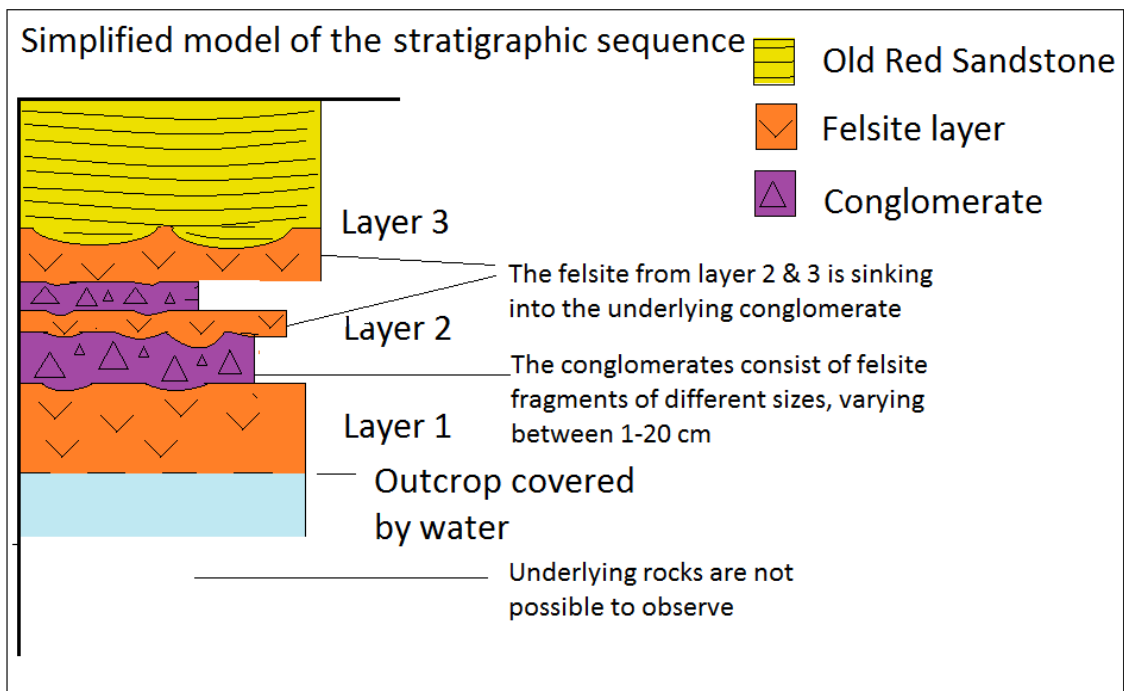


Figure 49 – Simplified model of the stratigraphic sequence of the felsite layers.

4.5 Hara Ebb formation

At the southwestern limit of the basement outcrop at Stromness (Figure 10) the Hara Ebb conglomerate overlies the basement rocks, forming the base of the Devonian sandstone that continues with the Lower Stromness Flags. The conglomerate varies in thickness from 5 to 10 meters. It has small pebbles of sandstone. Further the conglomerate consists of both the two types of granite and the psammitic gneiss of variable size that has already been observed. The granite and gneiss clast have sizes up to half a meter, some are angular, and some partly rounded.

The Hara Ebb conglomerate is also observed at Graemsay at the both sides of the basement exposures (Figure 50). Here as well, the conglomerate is separating the basement area from the Lower Stromness Flags formation. The outcrop of the conglomerate layer west of the basement rocks is approximately of 30 meters stratigraphic thickness. The outcrop of conglomerate layer east of the basement rocks is approximately 10 meters thick, and is followed upwards by sandstone. The conglomerate consists of clasts with high range in sizes, from small rocks of 1 cm up to 50 cm wide big and rounded clasts. Mostly it is the pink granite, but also some of the grey is observed, and also the psammitic gneiss.



Figure 50 – Picture from Graemsay showing the conglomerate, with sandstone formation on top of it. Hammer to the left in the picture is used for scale.

The conglomerate (Figure 50) observed in between the felsite layer at Quoyelsh promontory (Figure 10) contains mainly felsite clast and boulders. This conglomerate differs in appearance to the conglomerate at the other localities.

4.6 Old Red Sandstone east of Stromness bay

4.6.1 Exposures at Stromness beach

Between Copeland dock in the east and the Quoyelsh promontory in the west, a ca. 150-200 meters section of the beach was investigated. The easternmost part of the section exposes light colored sandstones with SE directed faults cutting through. These light colored sandstones are followed by sandstones of darker colors. This lithology has a darker brown color, and it weathers easily (in contrast to other sediments observed). The contact to the

lighter colored sandstones occurs over a gradual transition of 10 cm. The darker colored rock was sampled to determine whether if it is a sandstone or a tuff (sample A.B.16-19).

Throughout the pebbles and the sandstone on the beach, some fine grained beds have a pale color and it is also observed sub horizontal lamination that resembles the flow banding in the felsite from Quoyelsh promontory. Three of these beds were sampled for thin section studies (sample A.B.16-20, A.B.16-22 & A.B.16-24). The relation between the lighter colored sandstones and the more rotten are shown in the pictures in Figure 51. The relation is particularly clear in the site A of Figure 51, were two elevated rocks of light colored sandstone are stratigraphically placed on top of the darker sandstone at the bottom.

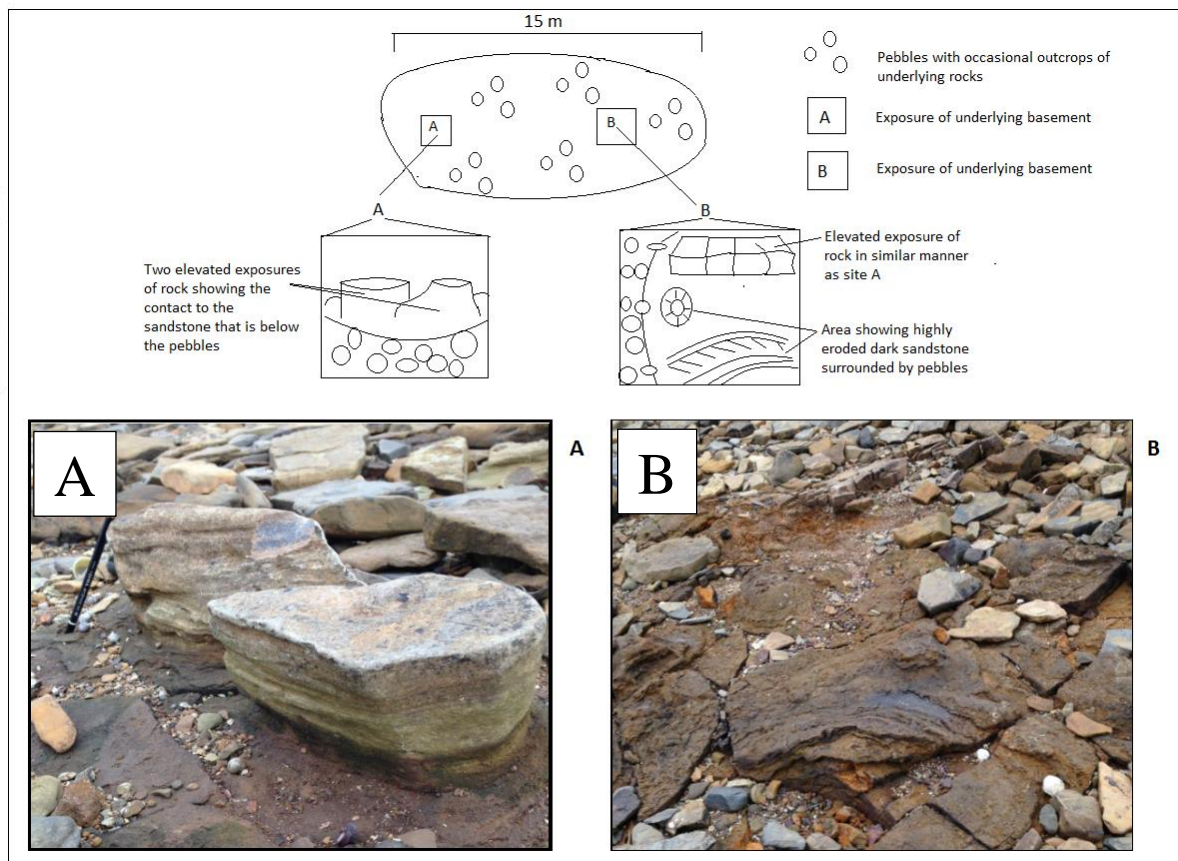


Figure 51 – overview sketch, with two more close up sketches that illustrates eroded sandstone with sandstone of lighter color on top of it. To the left: picture of “site A”. To the right: Picture of “site B”.

Just north of the island with castle and windmill (mark X on Figure 10) there is 30 x 30 m outcrop with basal breccia conglomerates that has a pale white color.

Thin sections were made of some of the lithologies encountered at Stromness beach (Figure 52). The thin section of the rocks did not reveal any volcanic rocks or tuffs. The pale fine grained lithologies are siltstones, and the brown weathering rock is a sandstone. All the encountered layers of sandstone at Quoyelsh are shown in Figure 52. Samples A.B.16-20, A.B.16-22 and A.B.16-24 have high content of silica, indicating long transport time. However, the grains has to a large extent, angular shapes and do not seem to be as highly eroded as the long transport interval should indicate. This contradiction does however make sense as the grain size being so small to obtain high amounts of erosion.

Thus the all the layers observed and sampled at the waterfront are termed “silty sandstones”.

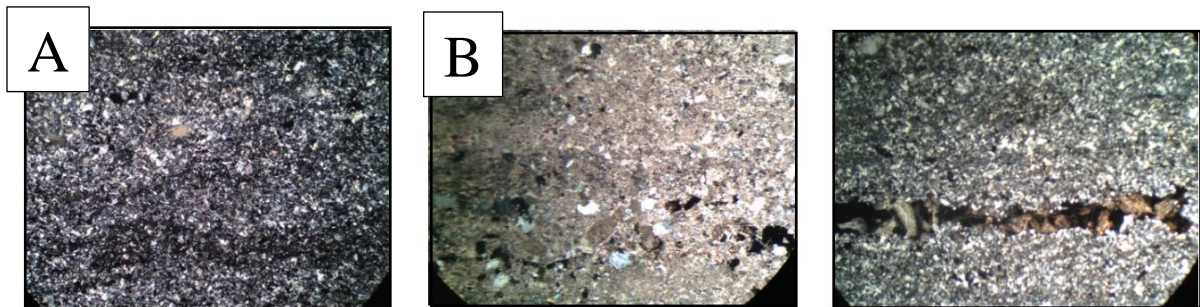


Figure 52 – Cross polarized pictures of sample A.B.16-20, A.B.16-22, A.B.16-24. Grain size is small in all the samples, and the grain shapes varies from angular to partly rounded shapes.

Scans taken of the thin sections of the samples, reveals the lamination in the rocks showing the sedimentary layers that the rocks consists of (Figure 53).

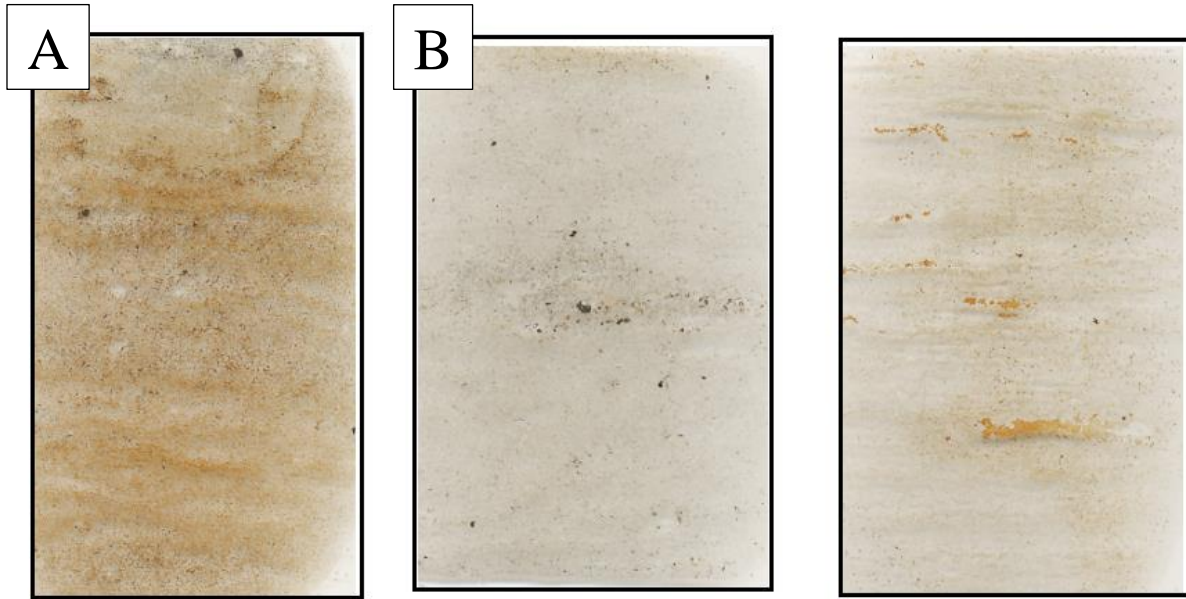


Figure 53 - Scans of thin section A.B.16-20, A.B.16-22, A.B.16-24. The sedimentary lamination is particularly clear in A.B.16-20 and A.B.16-24

4.7 Structural geology

At Yesnaby, the foliation in the granite increased towards the waterfront. Before the area with conglomerates and the mylonites zone started a small regional shear zone in the granite was observed. Around this area, the foliation in the granite was in E-W direction (Figure 54).

Structural measurements - Yesnaby

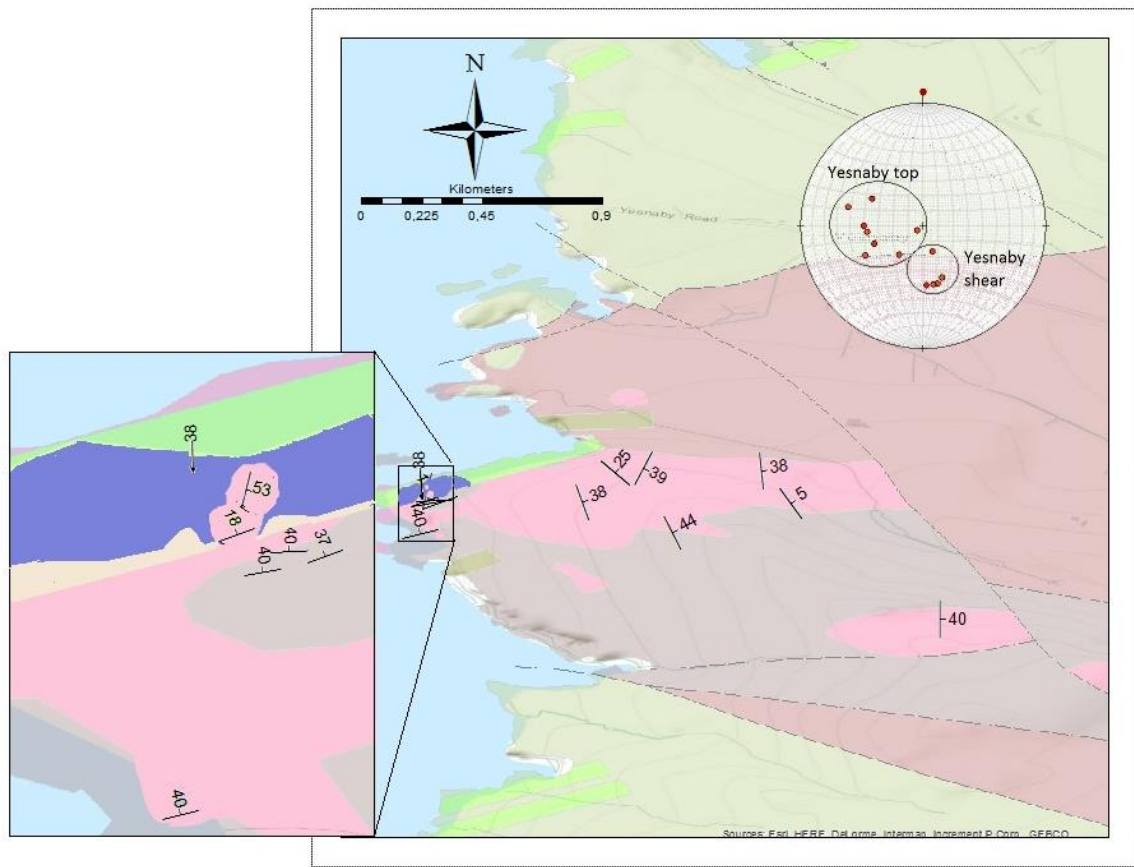


Figure 54 – Structural measurements of the foliation in Yesnaby shear top and Yesnaby shear zone

A similar behavior in the granites was found along the waterfront at Stromness, above the shear zone. Summary of the structural measurements are given in Figure 55.

Structural measurements – Stromness & Graemsay

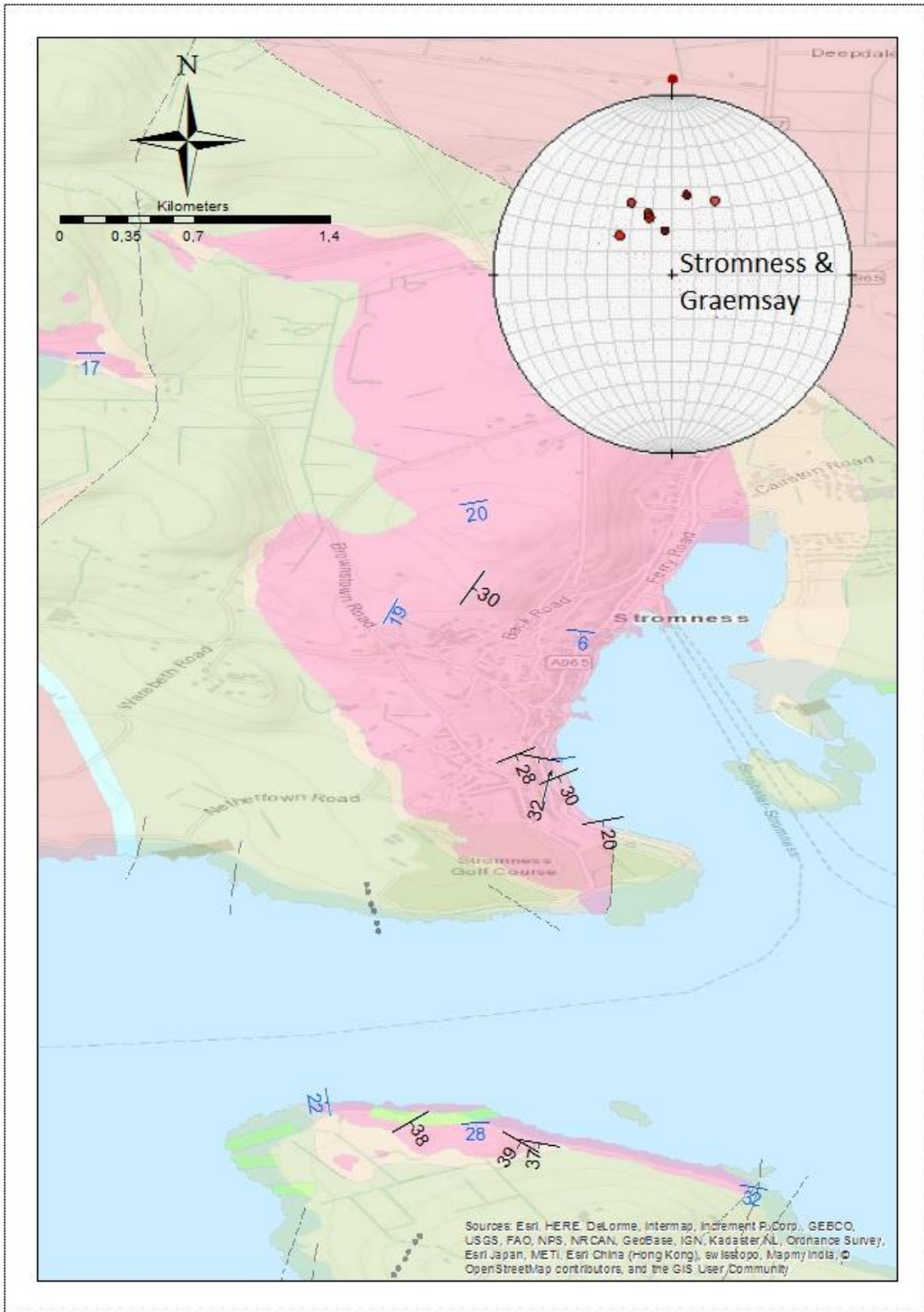


Figure 55 – structural measurements of the granites from Stromness and Graemsay. Measurements marked with blue are measurements from Strachan (2003).

The grey and the pink granites are typically weakly foliated in all the three investigated areas Yesnaby, Stromness and Graemsay. However, the general foliation direction varies from

mainly NW direction at Stromness, Graemsay and Yesnaby, in the area near the shear zone, to the more NS directed foliation at the rest of the Yesnaby area. In all three areas, previously undescribed mylonite zones, partly overprinted by phyllonites were found. These deformation zones are roughly east trending, but are dipping to the north at Yesnaby, accompanied by north-dipping lineations, and to the south at Stromness and Graemsay, accompanied by south-dipping lineations (Figure 56). The foliations in the granites become more pronounced towards the shear zones, and rotates to parallel to the shear zones. At Stromness, the mylonite and phyllonites are overprinted by brittle, top-to-south brittle faults (Figure 56)

Mylonite, phyllonite and fault plane from shear zone areas

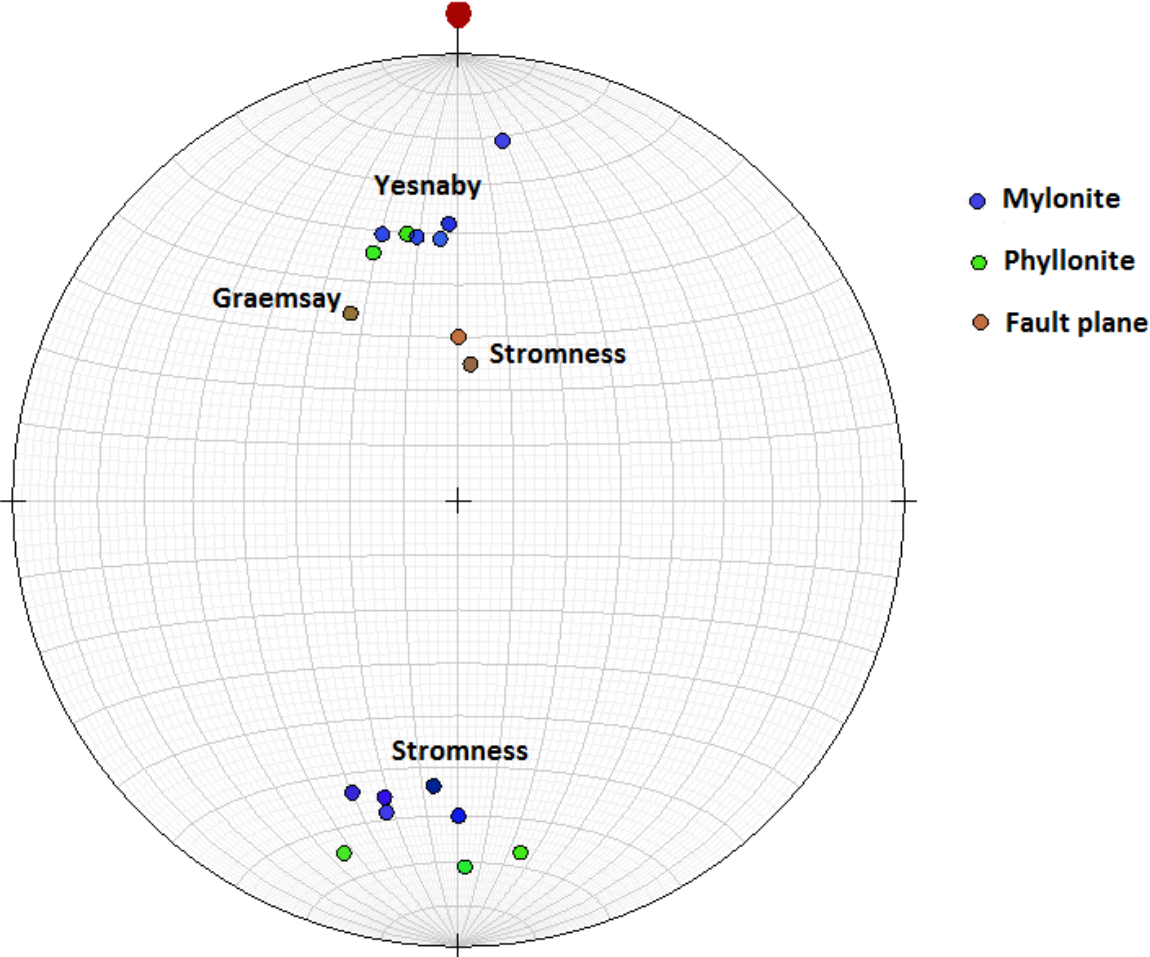


Figure 56 – Measurements of the lineation measurements in the mylonites and phyllonites found at Yesnaby and Stromness. Both are directed in a NS-direction. The plunge however is opposite of each other in Yesnaby and Stromness. The fault planes encountered at Stromness and Graemsay also plot in the same NS-direction.

5 Geochronology and geochemistry

5.1 U/Pb geochronology; results and interpretations of data

5.1.1 Introduction

Geochronological age determinations were made on five samples (Table 1).

Table 1 - Overview of samples for geochronology and sampling coordinates.

Sample	Description	Locality	Latitude	Longitude
A.B.16-04	Pink granite	1.4	58°57'20.49'' N	3°18'01.43'' W
A.B.16-05	Grey granite	1.4	58°57'20.49'' N	3°18'01.43'' W
A.B.16-11	Grey granite	2.3	59°0'54.80'' N	3°21'56.01'' W
A.B.16-12	Pegmatite cutting mylonite	2.3	59°0'54.80'' N	3°21'56.01'' W
A.B.16-18	Felsite layer 1	6.1	59°57'39.52'' N	3°16'46.57'' W

A total of 11 grains were analyzed from A.B.16-04. Four zircon grains were analyzed from A.B.16-05. Five zircon grains were analyzed from A.B.16-11. Six zircon grains were analyzed from A.B.16-12. Six zircon grains were analyzed from A.B.16-18. The results are presented in Table 2.

5.1.2 Grey granite

Zircons from the grey granite at Stromness

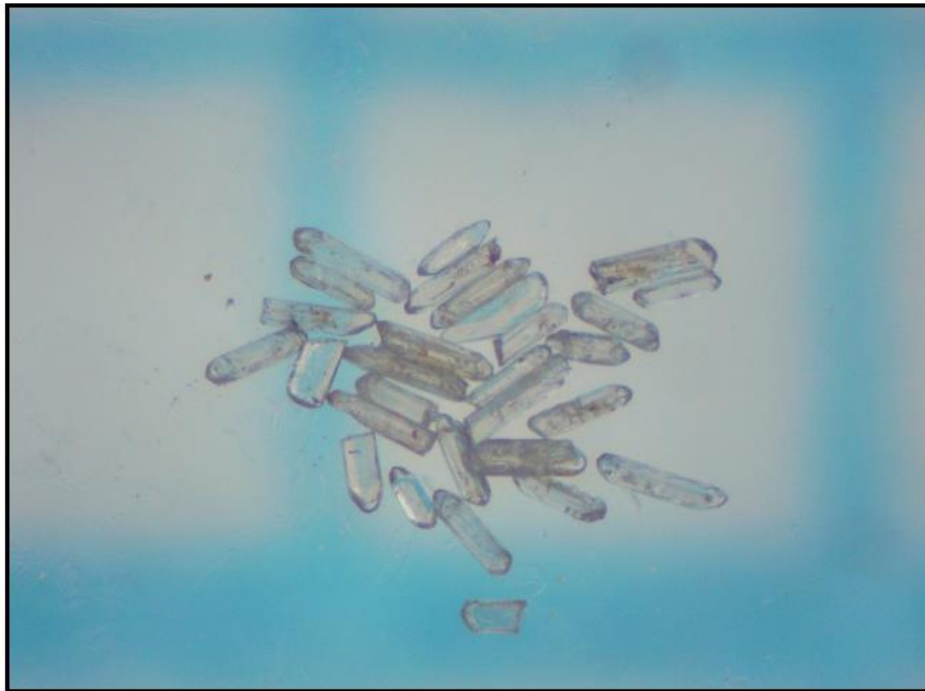


Figure 57 - Assemblage of zircon grains from A.B.16-05. The zircons were chemical abraded, and four grains were analyzed

All the zircons from the population from A.B.16-05, the grey granite sampled at Stromness are elongated prisms (Figure 57). The elongation ratios are ranging from 3 to 5. The grains have clear, glassy color and seldom contain visible cores or inclusions. No grains of older ages were encountered during the analysis of this sample. This makes sample A.B.16-05 a reliable source for dating of the granites.

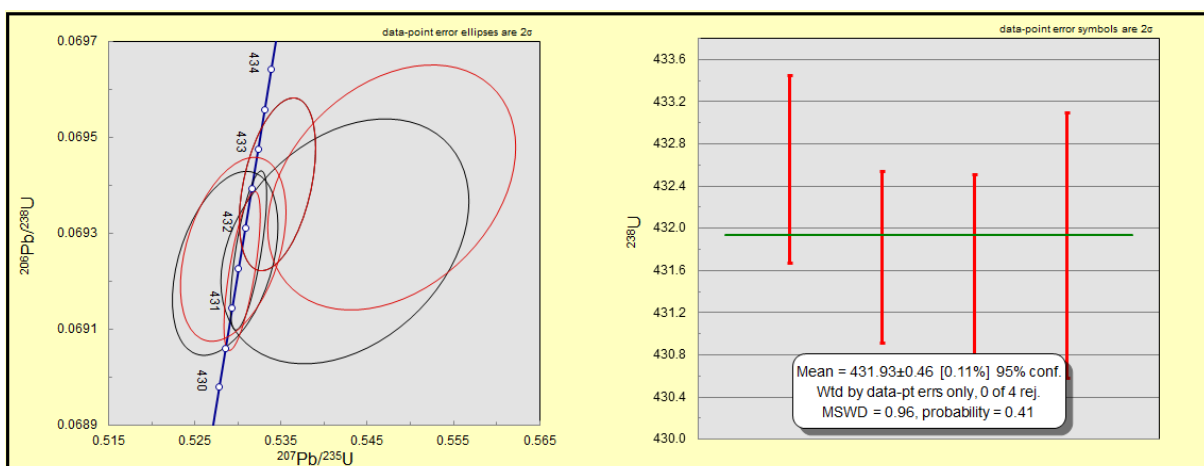


Figure 58 - To the left: Concordia plot. To the right: weighted $^{238}\text{U}/^{206}\text{Pb}$ average plots of grey granite (sample A.B.16-05)

A concordant age estimate of the analyzed points are shown in Figure 58. The two grains that plot on top are interpreted to yield some inheritance from older age rocks. In the weighted

average plot (Figure 58), utilized to estimate the age, only the other four of the analyzed points are selected, yielding an age estimate of 431.93 ± 0.46 Ma with 95 % confidence.

5.1.3 Pink granite

Zircons from the pink granite at Stromness

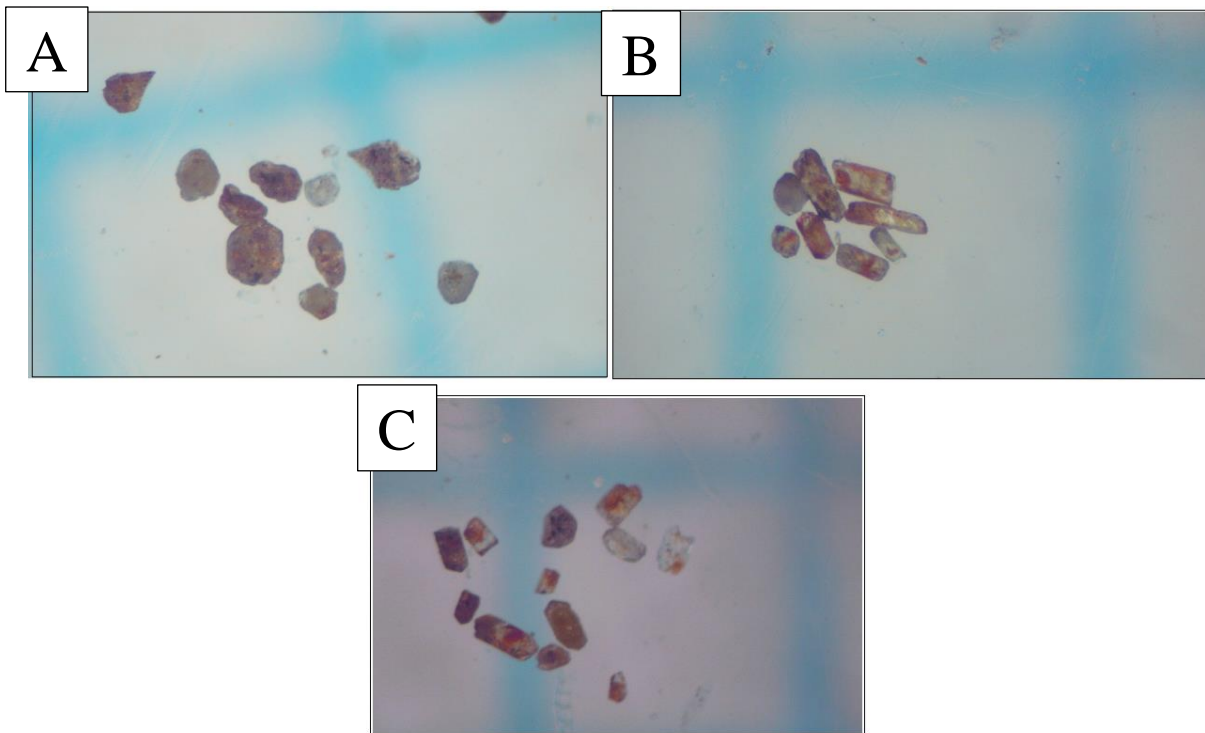


Figure 59 – Three assemblages of zircon grains from A.B.16-04. The two populations in the upper pictures were chemical abraded. The population on the lower picture was air abraded.

The zircon populations of A.B.16-04 (Figure 59) are reddish to brown grains all show highly metamict grains. The elongation ratios are ranging from 2 to 5. The grains are generally rich in inclusions and seldom contain visible cores. Due to all grains being severely metamict, several grains were dissolved during chemical abration. Further, most of the remaining grains that were possible to analyze gave age estimates between 1200-1500 Ma. These grains are thought to be extracted from surrounding material in which the granite intruded (age estimates correlates with Moine schist). However, one grain that was intact and possible to analyze after chemical abration, gave an age estimate around 430 Ma.

For the last round of analyses, some tips at the end of zircon prisms were broken off and used. These grains were thought to be too metamict for chemical abration and were therefore processed through air abration.

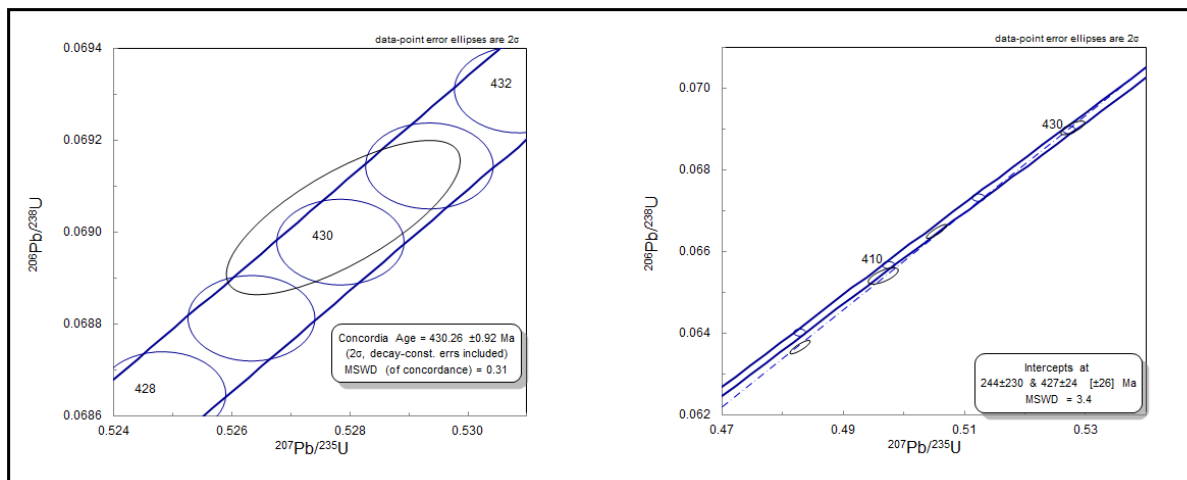


Figure 60 – Concordia plot for sample A.B.16-04. To the left: concordant point for analyzed zircon grains from chemical abrasion process. To the right: intersection between concordant analyzed points from air abrasion.

A concordant age estimate based on the chemically abraded zircon is shown in Figure 60 and gives an age estimate of 430.26 ± 0.92 Ma. Furthermore, there are 3 analyzed air abraded zircon grains that show Pb-loss but that are collinear. These intersect at 244 ± 230 & 427 ± 24 Ma. The results from the air abraded zircon have large margins of error, but the overlap with the concordant age estimate from the chemically abraded zircon is good.

Therefore, the concordant age estimate from the air abraded zircon is interpreted to be the age of the pink granite. This give an age estimate of 430.26 ± 0.92 Ma for the pink granite.

In total 6 grains were analyzed that gave estimation of zircon grains from older rocks, that has contaminated the granite. The $^{206}\text{Pb}/^{238}\text{U}$ ages were 1150.2 943.8, 769.4 808.5, 975.5, 530.9 Ma.

Zircons from Yesnaby shear zone area

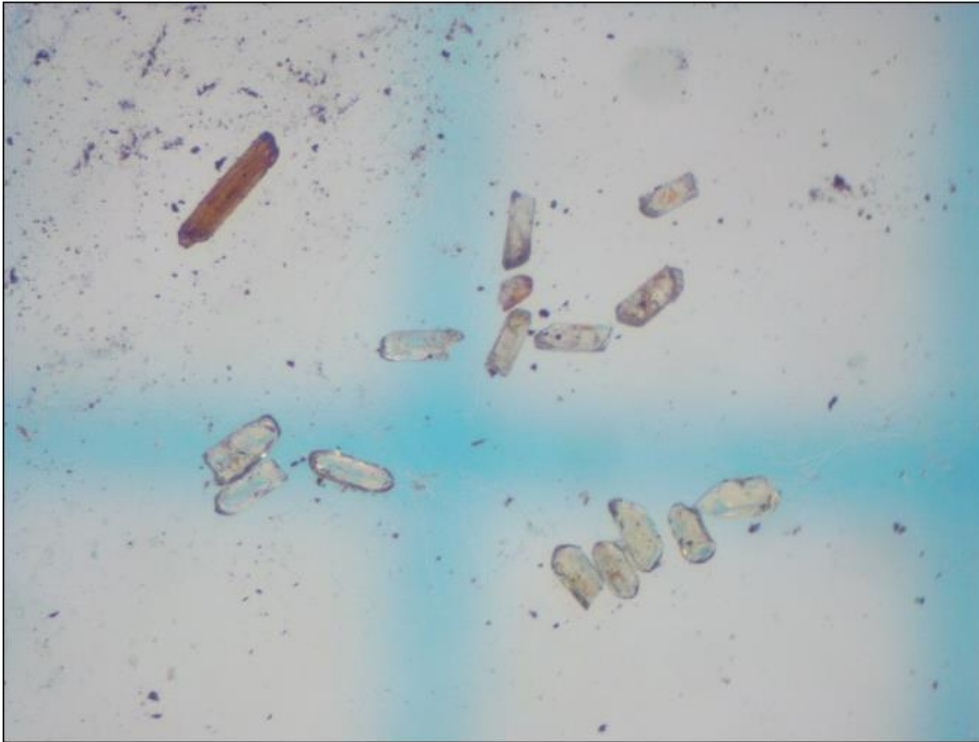


Figure 61 - Assemblage of zircon grains from A.B.16-11. The zircon grains were chemical abraded.

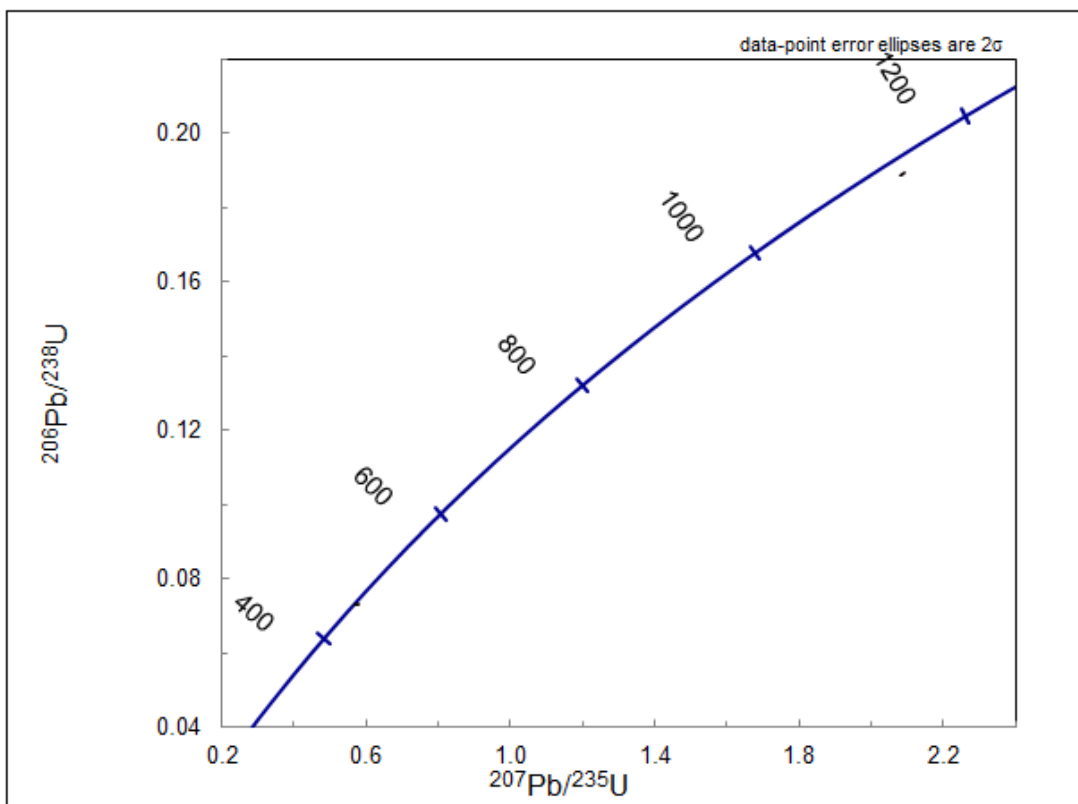


Figure 62 - Concordia plot of the two analyzed grains of the pink granite from Yesnaby shear zone area (sample A.B.16-11).

Only two zircon grains were possible to analyze after chemical abrasion. Concordant Age estimate of one of the analyzed zircon (Figure 62) gave an age estimate of 457.88 ± 0.94 Ma. The other zircon was dated to 1119 ± 2.22 Ma. Based on field, and geochemical data, the sample is interpreted to be of same age as sample A.B.16-04 of the pink granite. Thus both zircon analyzes of this sample are interpreted to be of inherited zircons in the granite. Therefore, analyze of the pink granite from Yesnaby shear zone area (sample A.B.16-11) could not be used to make interpretation of the age of rock formation.

Another round of air abraded zircon grains was prepared to get more analysis and hopefully link the granite with the other granite samples. However, time for this analysis run out due to troubles with the TIMS machine at University of Oslo.

5.1.4 Pegmatite

Zircons from the pegmatite from Yesnaby shear zone

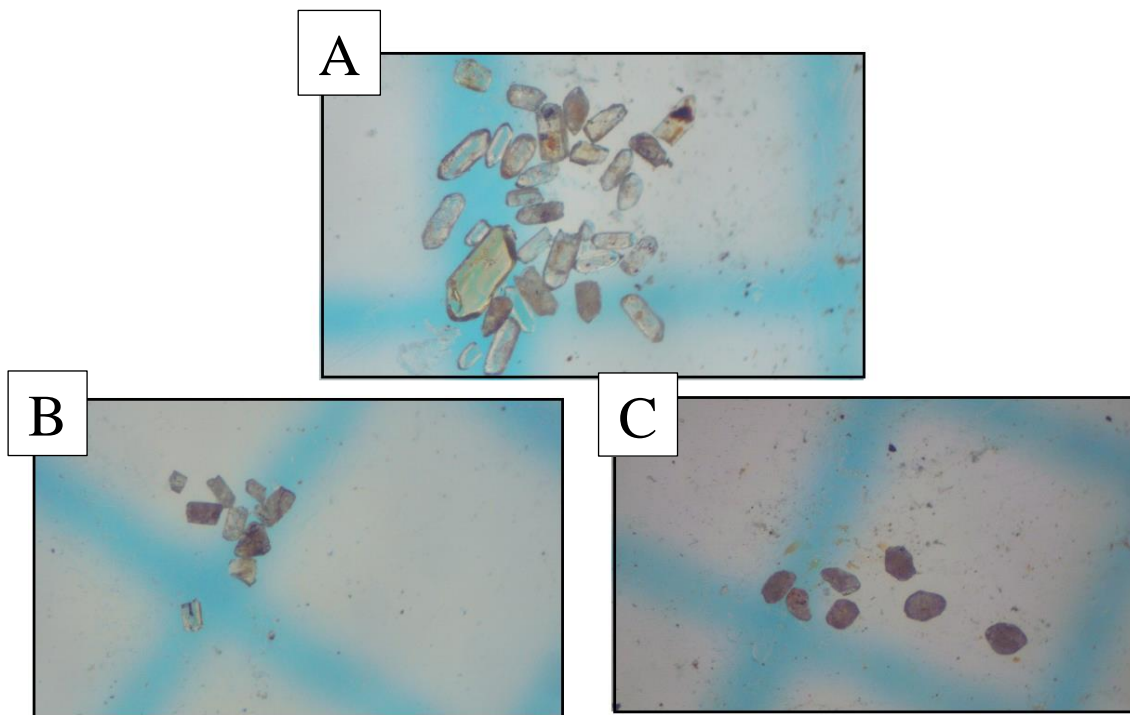


Figure 63 – A, B & C) Three assemblages of zircon grains from A.B.16-12

The zircon populations of A.B.16-12 (Figure 63) are reddish to brown, highly metamict grains. The elongation ratios are ranging from 2 to 5. The grains are generally rich in inclusions and seldom contain visible cores. Due to all grains being severely metamict, several grains were dissolved during chemical abrasion. Further, most of the remaining grains

that were possible to analyze gave age estimates between 1200-1500 Ma. These grains are thought to be extracted from surrounding material in which the granite intruded (age estimates correlates with Moine schist).

5.1.5 Felsite

Zircons

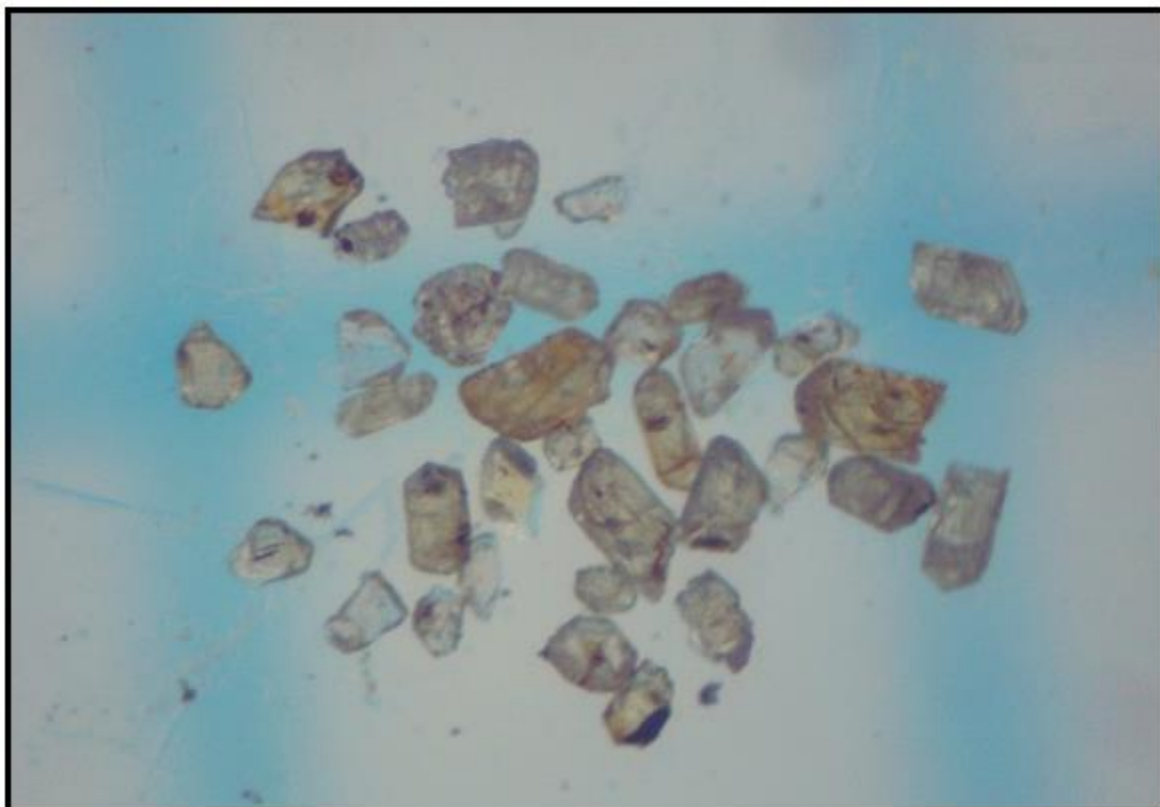


Figure 64 – Picture of the zircon population from sample A.B.16-18. These zircons were chemical abraded before analysis. The zircon population of A.B.16-18 (Figure 64) has clear white to yellow grains. Some of the grains are moderate metamict grains, others only weakly metamict. The elongation ratios are ranging from 1 to 3. The grains are generally rich in inclusions and seldom contain visible cores.

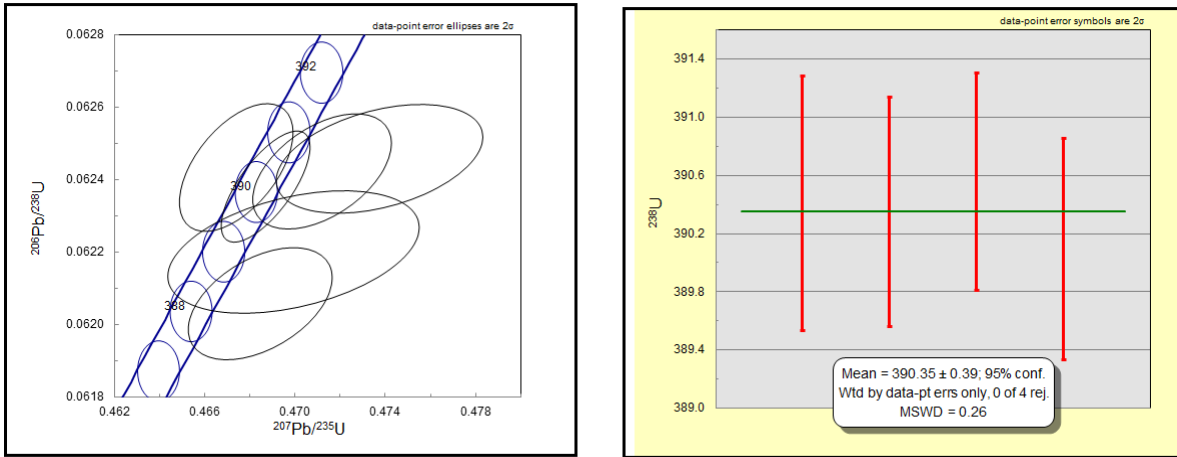


Figure 65 – To the left: Concordia plot of all six analyzed zircon grains. To the right, average plot made of four of the six analyzed grains from sample A.B.16-18

A concordant age estimate of the analyzed points are shown in Figure 65. The two zircons with lowest $^{206}\text{Pb}/^{238}\text{U}$ are thought to occur from lead loss. Therefore, these are excluded from the average plot utilized to estimate the age. The remaining four zircon grains give an age estimate of 431.93 ± 0.46 Ma with 95 % confidence.

Table 2 – U-Th-Pb isotopic data

Sample	Compositional parameters						Radiogenic isotope ratios							Isotopic ages					
	Wt. mg	U ppm	Th U	Pb ppm	Pb* Pb _c	Pb _c (pg)	$\frac{^{207}\text{Pb}}{^{206}\text{Pb}}$	% err	$\frac{^{207}\text{Pb}}{^{235}\text{U}}$	% err	$\frac{^{206}\text{Pb}}{^{238}\text{U}}$	% err	corr. coef.	$\frac{^{207}\text{Pb}}{^{206}\text{Pb}}$	±	$\frac{^{207}\text{Pb}}{^{235}\text{U}}$	±	$\frac{^{206}\text{Pb}}{^{238}\text{U}}$	±
(a)	(b)	(c)	(d)	(c)	(e)	(e)	(g)	(h)	(g)	(h)	(g)	(h)		(i)	(h)	(i)	(h)	(i)	(h)
A.B.16-05																			
493/1_zr	0.001	219.835	0.2061	15.612	16.0878	0.913614	0.055865	0.61845	0.534584	0.67657	0.0694	0.21203	0.4190193	447	13.74275	433.2	2.393128	432.6	0.8868732
493/3_zr	0.002	200.777	0.219	13.739	45.5914	0.589751	0.055625	0.23375	0.531227	0.32369	0.06926	0.19581	0.6979728	437.419	5.202883	432.6	1.1402467	431.7	0.8174845
497/8_zr	0.001	202.304	0.9606	19.08	6.01256	2.720999	0.055362	0.88036	0.528517	0.94681	0.06924	0.22632	0.4028391	426.887	19.63159	430.8	3.3241538	431.6	0.9445855
501/7_zr	0.001	74.4963	0.1813	7.1541	2.23976	2.20837	0.056779	2.08748	0.542405	2.1666	0.06928	0.30115	0.3274225	482.977	46.09918	440	7.7363153	431.8	1.257597
A.B.16-04																			
493/4_zr	0.001	302.179	0.3693	63.133	70.0149	0.889014	0.098364	0.12331	2.649199	0.25315	0.19533	0.19862	0.8783727	1593.34	2.302791	1309	1.8660781	1150	2.092226
493/5_zr	0.001	503.878	0.0774	32.944	48.2561	0.668829	0.055461	0.20887	0.527891	0.30644	0.06903	0.19876	0.7370339	430.871	4.654403	430.4	1.0750361	430.3	0.8271982
493/7_zr	0.001	68.5833	0.0438	10.963	13.9055	0.735501	0.085352	0.44861	1.855474	0.52694	0.15767	0.23186	0.5327248	1323.55	8.689055	1065	3.4766941	943.8	2.035489
497/11_zr	0.001	1647.49	12.628	744.92	80.9742	9.088156	0.055357	0.29538	0.84831	0.39141	0.11114	0.24296	0.657121	426.686	6.588657	623.7	1.824063	679.4	1.5672255
501/9	0.001	658.284	0.2907	93.937	19.4198	4.60069	0.079422	0.8852	1.46327	0.91307	0.13362	0.32747	0.263128	1182.68	17.4938	915.4	5.5073841	808.5	2.4880553
501/10	0.001	141.965	0.4766	25.245	26.6224	0.913937	0.072697	0.84129	1.637581	0.89014	0.16337	0.30978	0.3273713	1005.52	17.0705	984.8	5.6116101	975.5	2.8041983
501/11	0.001	853.879	0.3418	75.326	82.9574	0.897199	0.064589	0.13947	0.76449	0.26576	0.08584	0.20613	0.854898	760.983	2.940608	576.6	1.1691452	530.9	1.0503345
A.B.16-11																			
497/1_zr	0.001	509.121	0.23	96.694	79.0773	1.207509	0.079686	0.12078	2.082986	0.26439	0.18958	0.21563	0.8929198	1189.22	2.384587	1139	1.813802	1119	2.2152097
497/6_zr	0.001	213.239	0.2709	16.678	12.0772	1.275324	0.056226	0.81408	0.570669	0.86668	0.07361	0.21344	0.3621051	461.287	18.04535	458.4	3.1973445	457.9	0.9432176
A.B.16-12																			
497/5_zr	0.001	185.229	0.3339	41.1	38.4668	1.041369	0.094321	0.17706	2.716577	0.28794	0.20889	0.20241	0.7938172	1514.55	3.341052	1328	2.1370433	1223	2.2545331
501/3	0.001	192.454	0.274	42.785	26.6713	1.546215	0.089035	1.97883	2.601848	1.94111	0.21194	0.63577	0.1038669	1404.92	37.89787	1301	14.237627	1239	7.1668097
501/4	0.001	91.9001	0.4696	22.071	27.4375	0.776109	0.087307	1.52773	2.631318	1.51119	0.21859	0.51277	0.1372308	1367.29	29.41083	1309	11.118792	1274	5.9290646
501/5	0.001	197.954	0.6125	60.818	39.1359	1.515322	0.102192	0.90348	3.803076	0.9117	0.26991	0.38316	0.2314874	1664.32	16.71881	1593	7.3298516	1540	5.2495298
501/6	0.001	668.521	0.3415	165.28	214.954	0.765325	0.096097	0.26554	3.150251	0.34754	0.23776	0.22102	0.645225	1549.68	4.987441	1445	2.678599	1375	2.7366291
A.B.16-18																			

493/10_Zr	0.001	312.522	0.7836	22.676	22.8255	0.951774	0.0548	0.56669	0.468703	0.6188	0.06203	0.21258	0.4065491	404.066	12.68734	388.8	2.0051276	388	0.8002607
493/11_Zr	0.001	183.231	1.8044	17.683	9.40822	1.699073	0.054781	0.95842	0.470181	1.02071	0.06225	0.22969	0.3754289	403.312	21.46108	391.3	3.3145709	389.3	0.8676184
493/12	0.001	1217.99	0.72	86.696	29.4702	2.845506	0.054408	1.00711	0.468554	1.02046	0.06246	0.3154	0.1966118	387.991	22.61101	390.2	3.3059554	390.6	1.1950115
497/10	0.001	307.046	0.716	21.992	24.5176	0.86185	0.054746	0.46794	0.471196	0.53296	0.06242	0.20811	0.4885829	401.871	10.48048	392	1.7332156	390.3	0.7881062
501/8	0.001	216.952	0.7737	16.307	13.3595	1.135651	0.055043	0.78191	0.474081	0.83236	0.06247	0.20824	0.359996	413.98	17.47538	394	2.7181338	390.6	0.7890945
501/12	0.001	1174.54	0.6222	83.688	16.073	4.902193	0.054344	0.24023	0.467388	0.33725	0.06238	0.20369	0.7097848	385.337	5.395952	389.4	1.0907109	390.1	0.7708127

(a) 493/1, 493/2 etc. are labels for fractions composed of single zircon grains or fragments; all fractions annealed and chemically abraded after Mattinson (2005) or air abraded after Krogh (1982).

The latter are marked with an asterix

(b) Fraction weights measured on a micro balance.

(c) U and total Pb concentrations subject to uncertainty in weight.

(d) Model Th/U ratio calculated from radiogenic $^{208}\text{Pb}/^{206}\text{Pb}$ ratio and $^{207}\text{Pb}/^{235}\text{U}$ age.

(e) Pb^* and Pbc represent radiogenic and common Pb, respectively.

(f) Measured ratio corrected for spike and fractionation only.

(g) Corrected for fractionation, spike, and common Pb; up to 1 pg of common Pb was assumed to be procedural blank: $^{206}\text{Pb}/^{204}\text{Pb} = 18.59 \pm 0.77\%$; $^{207}\text{Pb}/^{204}\text{Pb} = 15.24 \pm 0.38\%$;

$^{208}\text{Pb}/^{204}\text{Pb} = 35.8 \pm 1.2\%$ (all uncertainties 1-sigma). Excess over blank was assigned to initial common Pb.

(i) Calculations are based on the decay constants of Jaffey et al. (1971). $^{206}\text{Pb}/^{238}\text{U}$ and $^{207}\text{Pb}/^{206}\text{Pb}$ ages corrected for initial disequilibrium in $^{230}\text{Th}/^{238}\text{U}$ using $\text{Th}/\text{U} [\text{magma}] = 3$.

5.2 Geochemistry

5.2.1 Classification diagrams

TAS diagram

The total-alkali diagram classification is based on major element rock analyses, is non-genetic, and is as nearly consistent as possible with the Quartz-Alkali feldspar-Plagioclase-Feldspathoid modal classification (Le Bas et al., 1986). Several attempts have been made in the past to calculate modal contents from chemical analyses (Le Bas et al., 1986).

The fields are distinguished and defined by straight lines to get a simple and easily applicable diagram. Thus, the choice of chemical parameters was on silica and total alkalis, which led to the total alkali-silica (or TAS) classification (Le Bas et al., 1986).

Geochemistry data from the rocks encountered at Mainland Orkney and Graemsay (classified as granites in the field) are plotted in TAS-diagram from Cox et al. (1979) (Figure 66).

Samples used are A.b.16.04, A.B.16-05, A.B.16-07, A.B.16-09, A.B.16-11, and A.B.16-29.

TAS diagram for the granites from Orkney

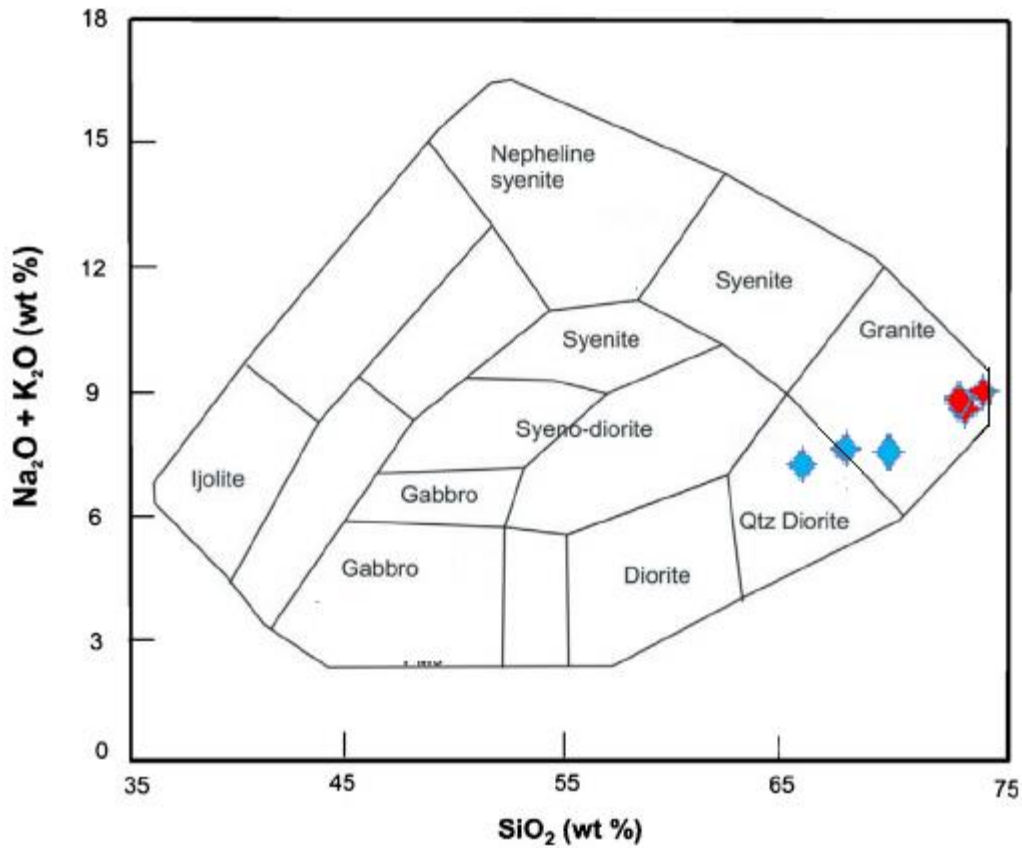


Figure 66 – Total-Alkali-Silica diagram from Cox et al. (1979). Sample A.B.16-04, A.B.16-05, A.B.16-07 A.B.16-09, A.B.16-11, A.B.16-29. Five of six samples plot as granites, with one analysis from the grey granite plotting in the quartz diorite field.

The Total-Alkali-Silica-diagrams are also utilized on the felsites encountered at Quoyelsh promontory (Figure 10). The resulting plot is shown in Figure 67.

TAS diagram with plots from the Felsite layers

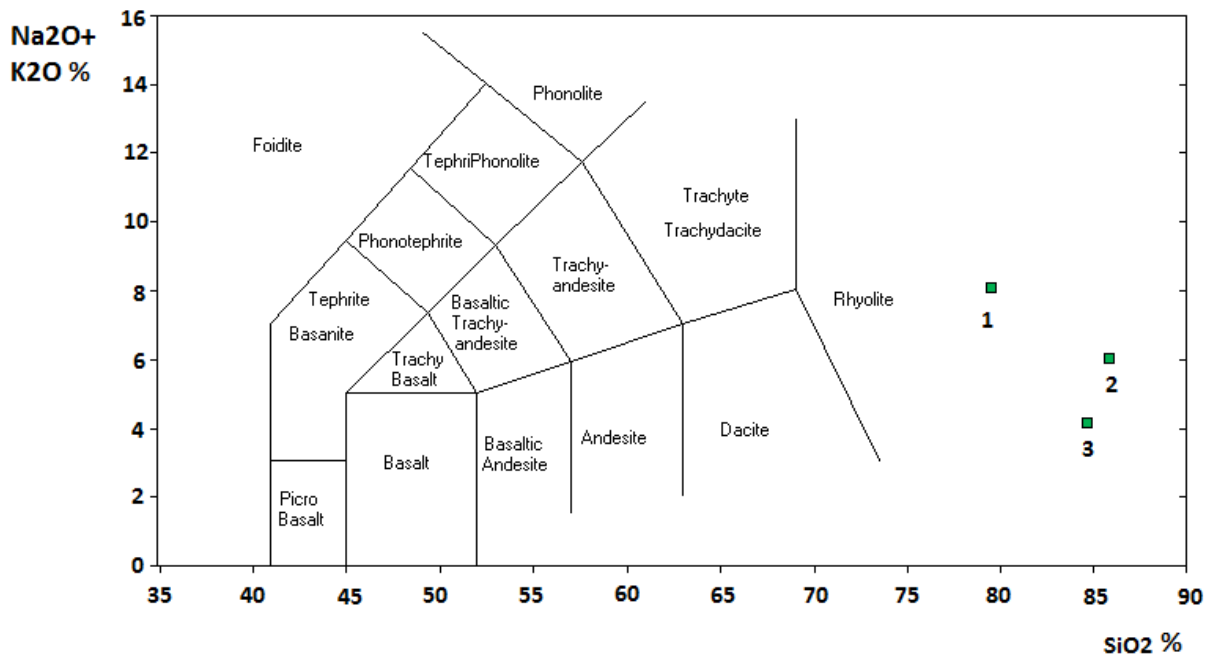


Figure 67 – Total Alkali Silica diagram from Le Bas et al. (1986). Sample A.B.16-16, A.B.16-17 and A.B.16-18. All plot within the range of rhyolites.

The Total-Alkali-Silica diagram plots (Le Bas et al., 1986) confirms that the field classification of the grey and the pink granite at the three investigated localities, Stromness, Yesnaby and Graemsay (Figure 10) are granites. Further, the felsites at the outcrop on the promontory at Quoyelsh promontory (Figure 10) are confirmed to be rhyolites, and they will be referred to as rhyolites henceforth.

5.2.2 Tectonic discrimination diagrams

Rb-Y+Nb plots

Geochemical data from the grey and the pink granite are plotted in the binary Rb-Y+Nb discrimination (Pearce et al., 1984). The grey granite, and the pink granite found at Stromness and Yesnaby are represented in respectively sample A.B.16-05, A.B.16-07, A.B.16-29 and A.B.16-04, A.B.16-09, A.B.16-11 and. The resulting plot is shown in Figure 68. Further the rhyolite layers are plotted in a similar diagram, shown in Figure 69.

Rb, Y+Nb plot of the granites from Yesnaby and Stromness

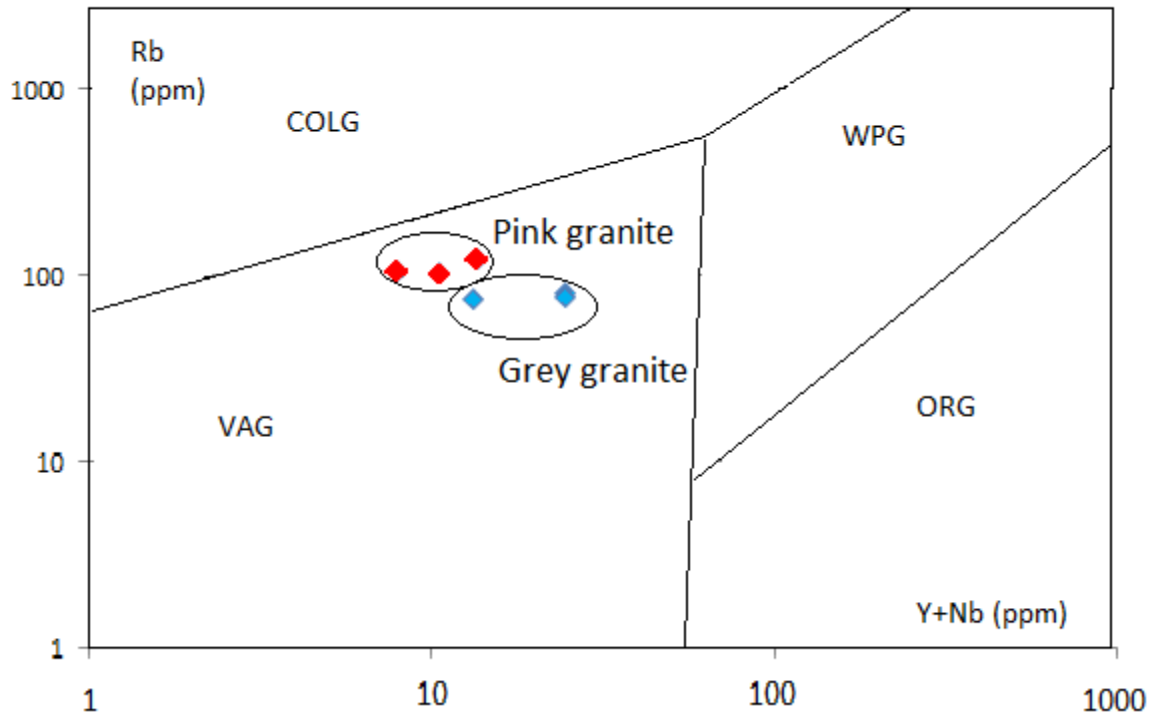


Figure 68 – Discrimination diagram for granites by Pearce et al. 1984. All six samples plots within the range for Volcanic Arc Granites (VAG). Note: two of the grey granite plot, overlap and is seen as one plot in the diagram.

Rb, Y+Na plot of the felsite from Stromness beach

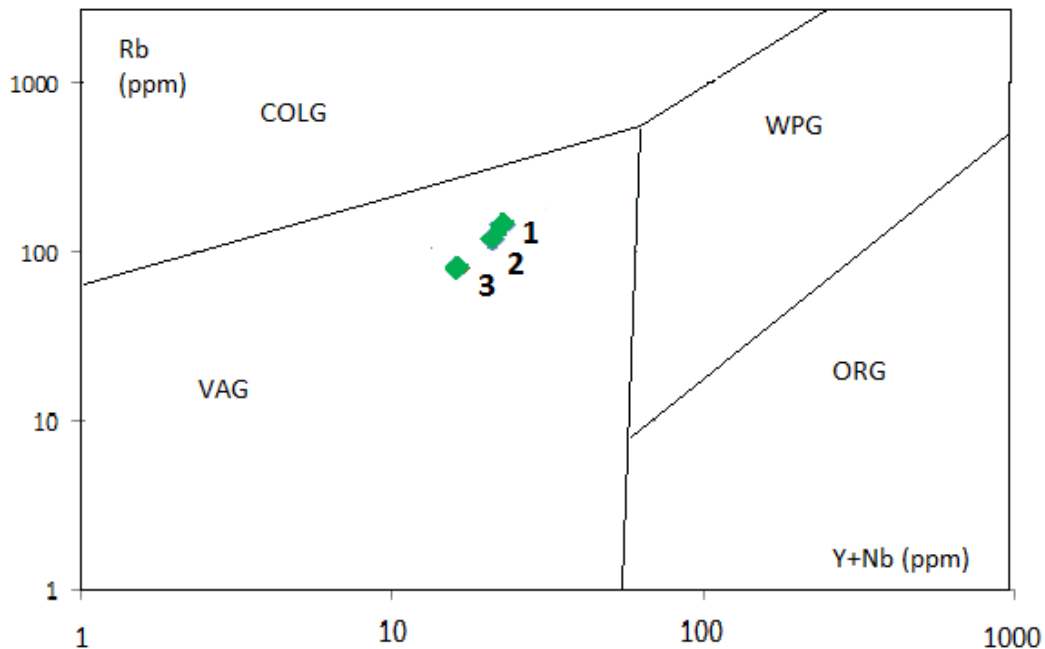


Figure 69 – Discrimination diagram for the rhyolite layers at Quoyelsh promontory. All plot within the range of VAG, with a trend towards the field of Within-Plate Granitoids (WPG). The three layers are shown as layer 1 (A.B.16-18), layer 2 (A.B.16-17) & layer 3 (A.B.16-16).

All six analyzed granite samples and the three analyses of the felsite layers plot within the range of Volcanic Arc Granites. Volcanic arcs may be oceanic or continental and the granites usually form by melting of mantle asthenosphere (Pearce et al., 1984). However, there are some aspects to this interpretation that requires consideration.

Pearce et al. (1984) stated that granite composition is fundamentally controlled by source rock composition and not by tectonic setting, and also demonstrated empirically that granites from different tectonic settings have distinct trace element characteristics. Opponent to the view that is possible to discriminate the tectonic setting of the granite is presented in for example (Brown et al., 1984).

According to LeBas and Streckeisen, (1991), a workable classification should be based on measurable properties and should be free of interpretation. This is the case for the IUGS classification of igneous rocks. Inferred properties, however, such as depth of emplacement, source characteristics and tectonic setting, are potentially more useful because they contain more information and may have direct geological consequences. But they are also more dangerous because the inferred properties on which they are based are open to dispute. Classification based on incorrect inferences may do more harm than good (Förster et al., 1997).

A consideration of the discrimination diagrams of Pearce et al. (1984) was made by Förster et al. (1997).

Förster et al. (1997) argue against the term 'syn-collisional granite' from Pearce et al. (1984) chose (syn-COLG). The prefix 'syn-' introduces an interpretative problem of deciding whether any given granite formed during collisional orogeny or later. Because of this, Foster et al (2010) choose not to separate syn- and post-collisional types and use the overall term 'collisional' (COLG) for granites that are related to a collisional event. COLG is the most complex tectonic setting and in order to correctly interpret granites from collisional orogens, one must have a lot more information than just their geochemical composition. Granites from a COLG setting may plot in the VAG, WPG or COLG field. One must, for example, know at what stage of collision the granite formed, whether arc-related source rocks are involved, and what sort of regime developed after collision.

Sr-Rb-Ba plot

The Sr-Rb-Ba discrimination diagram is of particular interest in the context of Caledonian granites in Scotland, since these include a distinct high Ba-Sr suite (Fowler et al., 2008). From the multi-element variation diagrams of Tarney and Jones (1994), contrasting the High Barium-Strontium (Ba-Sr) granitoids with “normal (i.e. low Ba-Sr) granitoids, a number of discrimination diagrams could be produced. The simplest one is a triangular Sr-Rb-Ba (Figure 4) which shows the normal type trending, with increasing SiO₂, toward the Rb corner and the *HiBaSr* type trending toward the Ba corner. These areas are marked on Figure 70, and the data from grey and pink granites analyzed in this study are plotted. The rhyolites from the Quoyelsh promontory is plotted in a similar diagram shown in Figure 71.

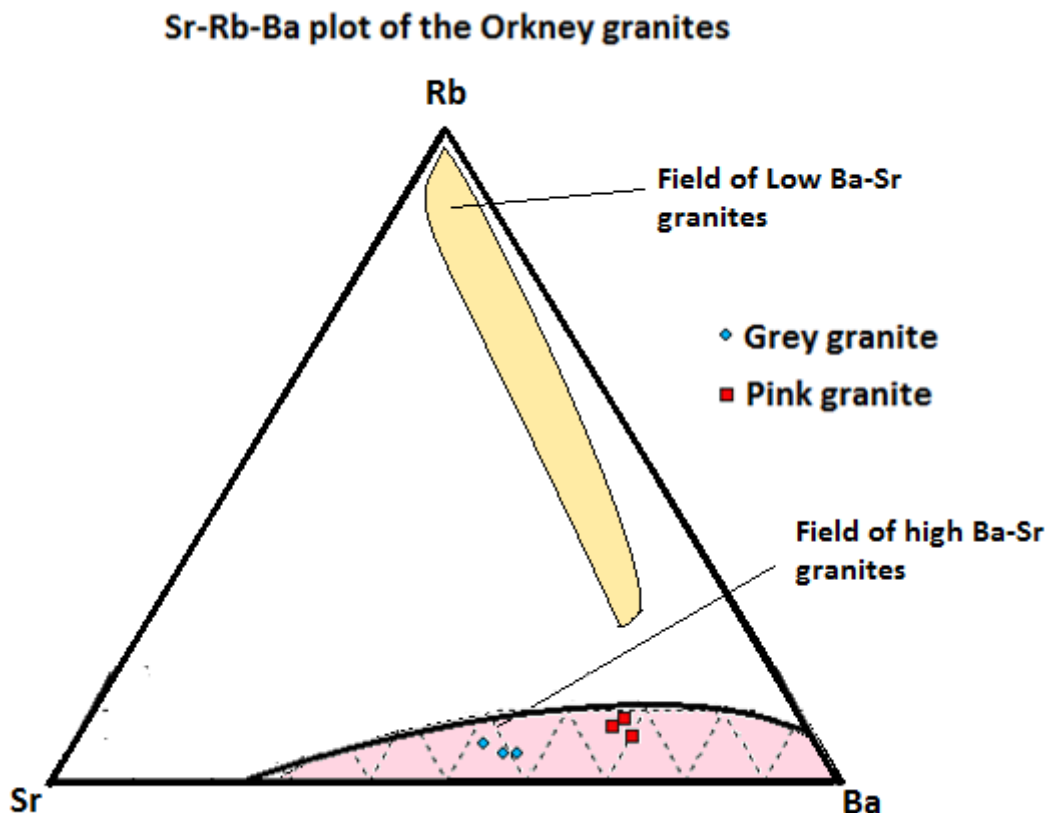


Figure 70- Triangular Sr-Rb-Ba plots. To the left: plot of granites from Scottish granitoids. West Scotland granitoids evolve towards high Ba, but East Scotland granitoids evolve towards high Rb. Source of data O'Brien (1985). To the right: plot of the granites from Orkney Islands. Pink granite: A.B.16-04, A.B.1-09, A.B.16-11. Grey granite: A.B.16-05, AB.16-07, A.B.16-29. All granites from Orkney Islands plot in the area of the high Ba-Sr granites.

The pink granite, and the grey granite found at Stromness and Yesnaby plots within the field of High Ba-Sr granites (Tarney and Jones, 1994).

Sr-Rb-Ba plot of the Felsite layers

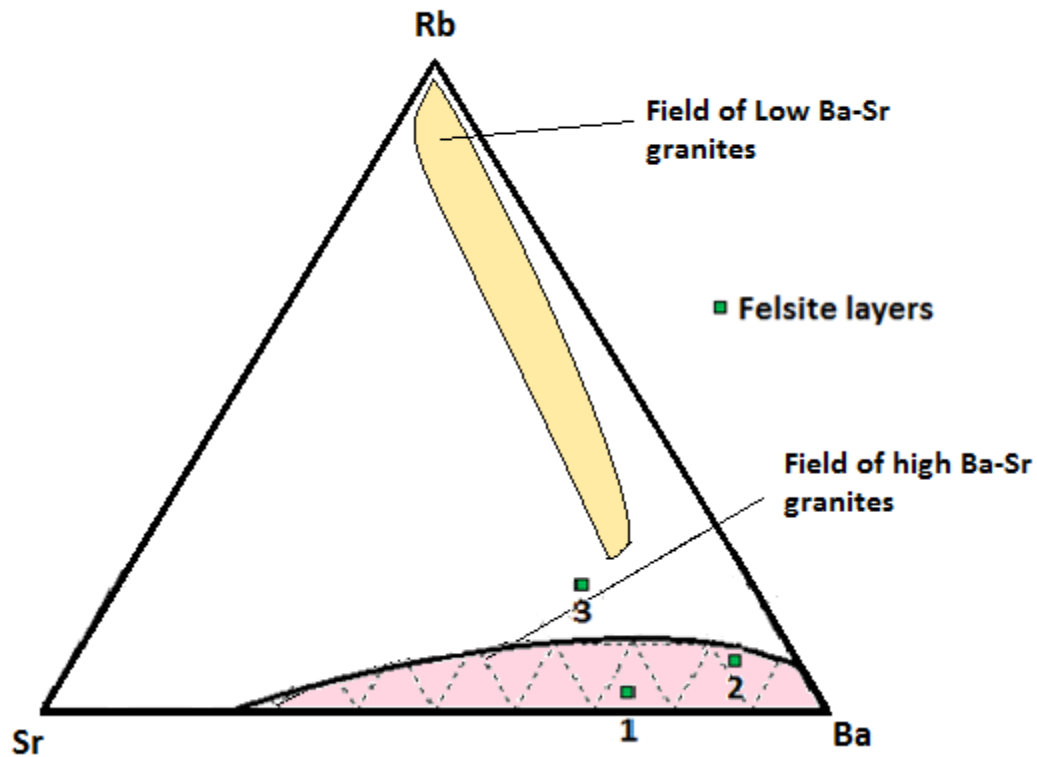


Figure 71 – Sr-Rb-Ba plot for the Rhyolite layers on Orkney.

5.2.3 Multi-element diagrams

Multielement diagram for the granites from Stromness and rhyolites from Quoyelsh are presented in Figure 72 and Figure 74. The data are normalized after Thompson (1982). In Figure 73 data from the Orkney granites is plotted against data from average High Ba-Sr granites from Fowler et al. (2008) to compare the results.

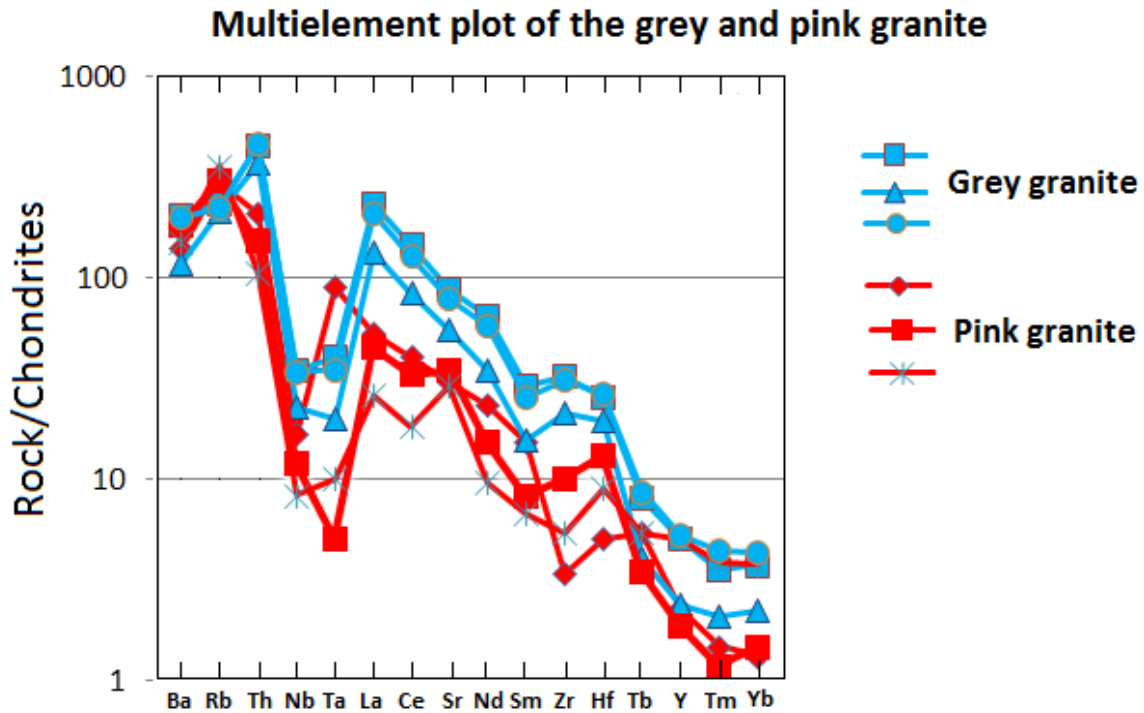


Figure 72 – Multielement diagram for all the sampled granites. The data are normalized for chondrite values by Thompson (1982). All the granites have high amounts of Ba, Rb and Th, a negative Nb anomaly and a steep decreasing slope towards the lighter REE's

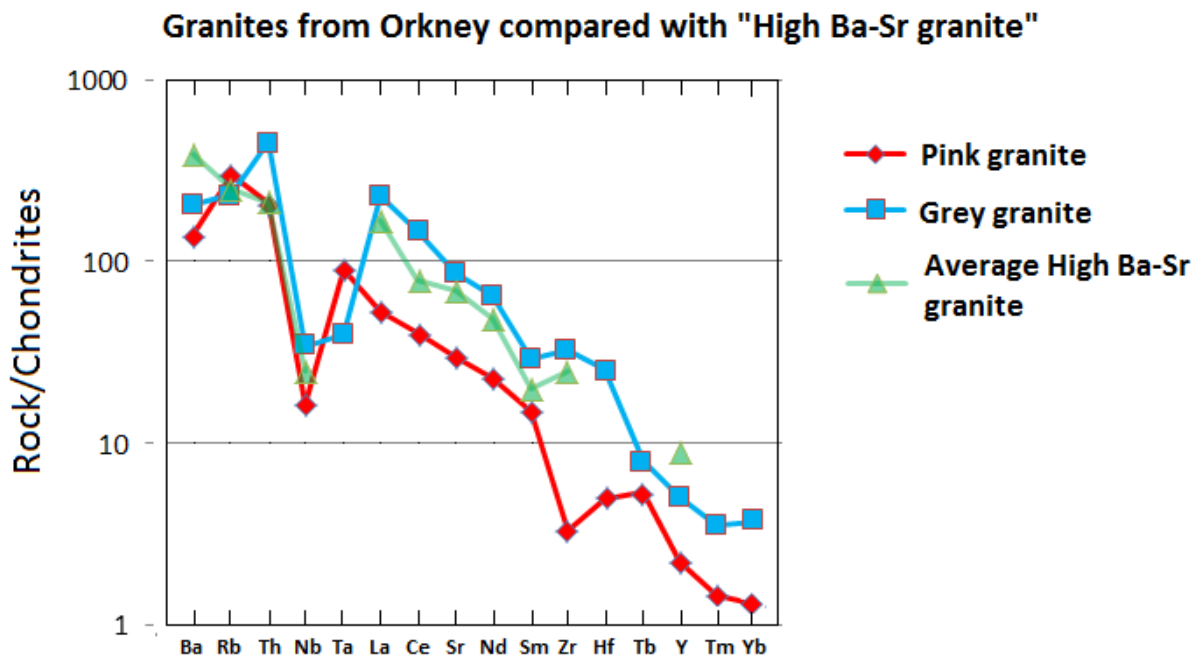


Figure 73 – Multielement diagram for the pink granite (sample A.B.16-04) and the grey granite (sample A.B.16-05) plotted against an average plot from studied High Ba-Sr granites for comparison. The High Ba-Sr granite data are from Fowler et al (2008)

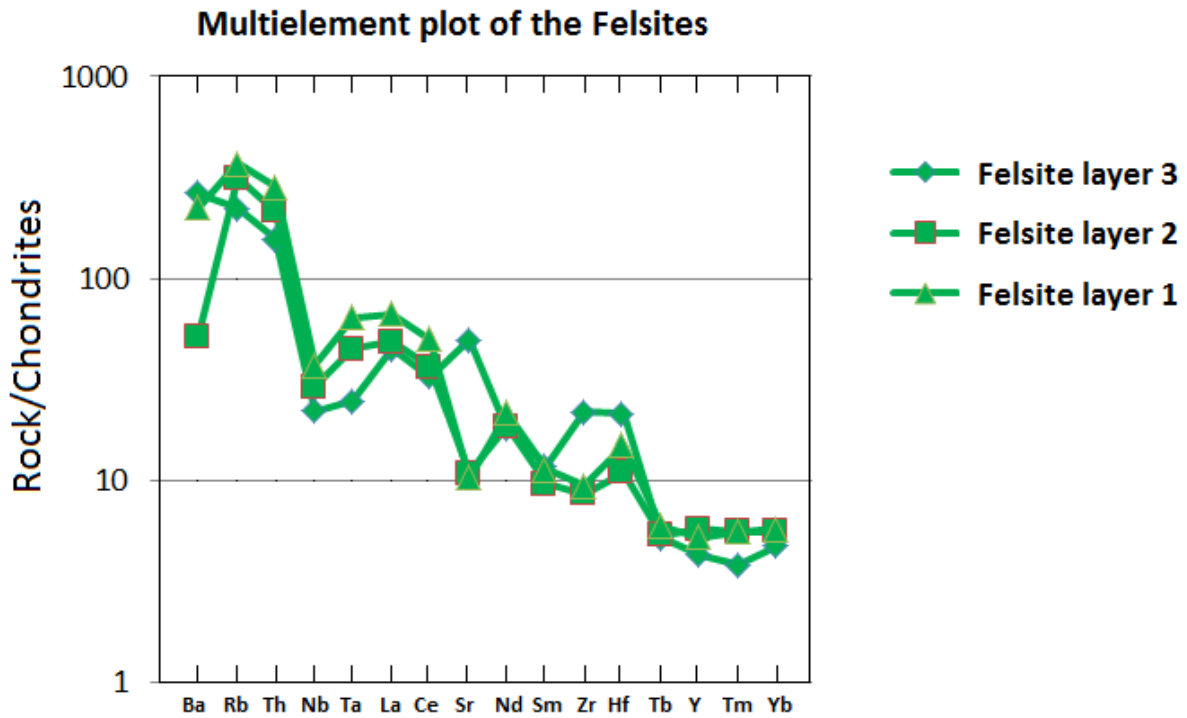


Figure 54 - Multi-element diagram for all the sampled rhyolite layers. The data are normalized for chondrite values by Thompson (1982). The rhyolites have high amounts of Ba, Rb and Th, and negative Nb anomaly and a steep decreasing slope towards the lighter REE's, but not as markedly as the granites from the basement complex.

5.2.4 REE-patterns

REE patterns of the granites and rhyolites are plotted in Figure 75 & Figure 76. Values are chondrite normalized after Sun and McDonough (1989)

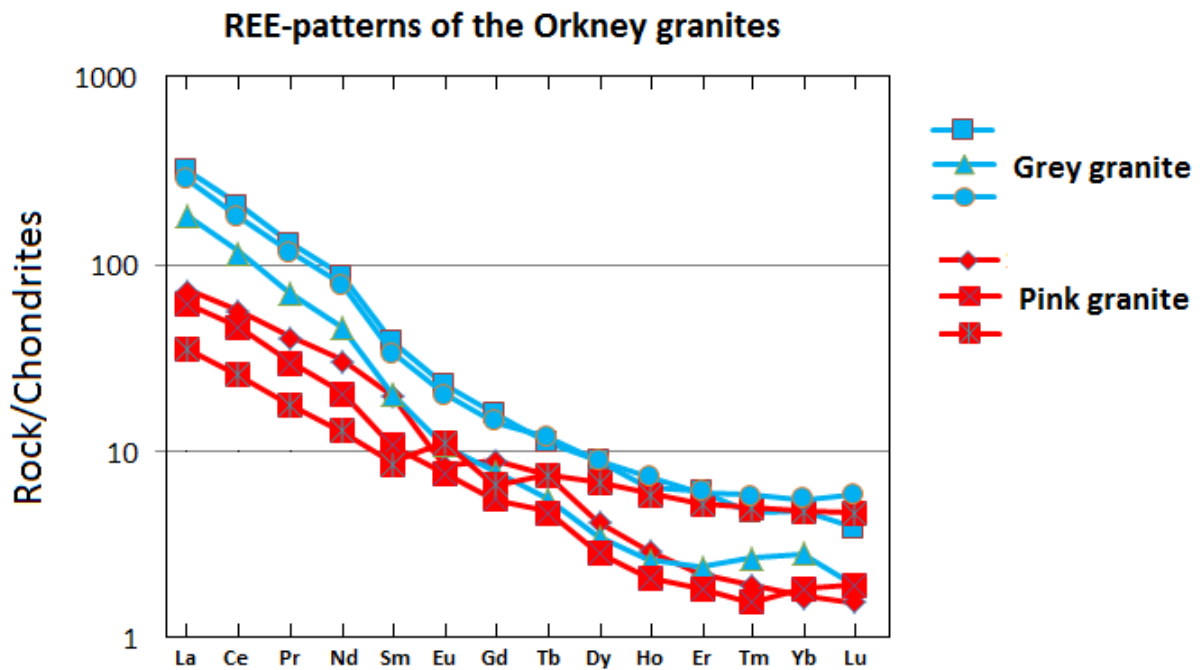


Figure 75 – REE plot of the granites from Orkney, chondrite normalized after Sun and McDonough (1989). The grey granite is represented in A.B.16-05, A.B.16-07 and A.B.16-29. The pink granite is represented in A.B.16-04, A.B.16-09 and A.B.16-29. It is a clear trend that all the samples from the grey granite generally plot above the samples from the pink granite.

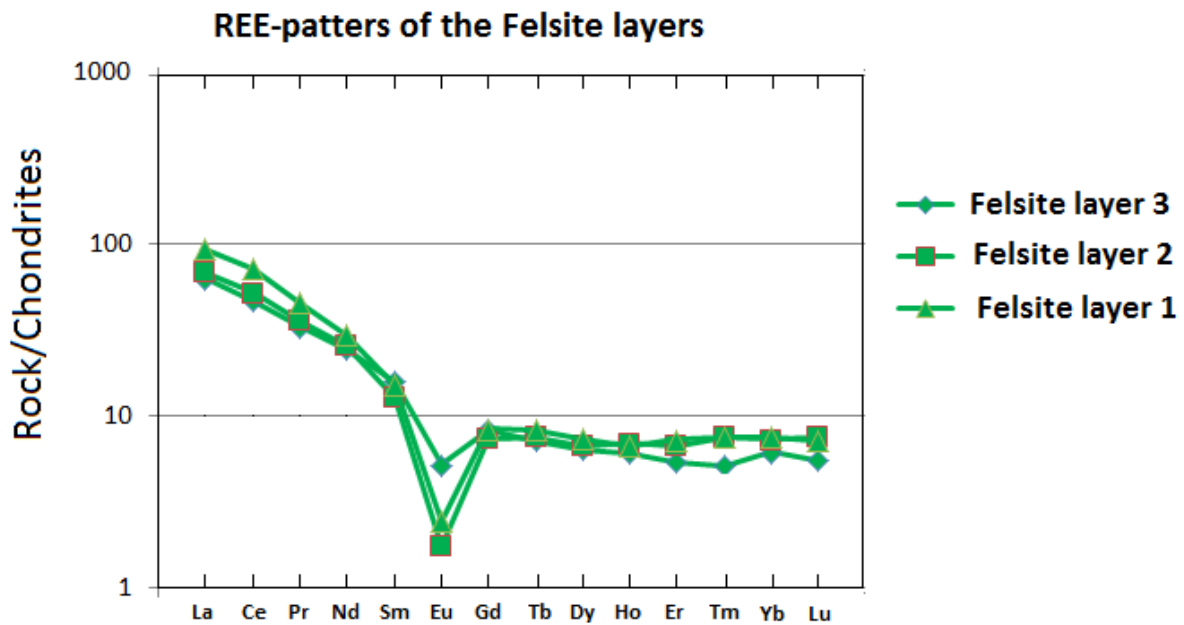


Figure 76 - REE plot of the granites from rhyolites, chondrite normalized after Sun and McDonough (1989). All the rhyolite layers have a negative Eu anomaly, in contrast to the granite, in the upper plot.

The REE patterns for the granites are fractionated with light REE up to several hundred times chondrites and heavy REE only about ten times chondrites. This gives La/Yb ratios of 50 or more. Eu anomalies do *not* occur (or are negligible small) in all of the samples. It is a clear trend that all the samples from the grey granite generally plot above the samples from the pink granite.

In the REE-plot for the Rhyolite-layers however, La/Yb-ratio is not as steep as for the granites. Further, an Eu anomaly is present in all the three samples.

6 Discussion

6.1 Introduction

Studies of the basement on Mainland Orkney and Graemsay indicate several stages of rock formation. The oldest rocks are the metasedimentary gneisses, with appearance and mineralogy resembling Moine schists. These metasedimentary gneisses have been intruded by granites, and the gneisses are found as xenoliths in them. Inherited zircon grains in the granite dated in this study, most likely derived from the host rock, gives age that are typical of Moine schist. The granites intruded at ca 430 Ma, during the Scandian phase of the Caledonian orogeny. At the northwestern (Yesnaby) and southwestern (Stromness) margins of the granite outcrop, the xenoliths of gneiss seem to occur more frequently, suggesting that the contact to the country rock is nearby. Resting unconformably on the basement rocks (granites and gneisses) lies the Hara Ebb formation conglomerate, followed by Old Red Sandstone.

At Quoyelsh promontory (Figure 10) the rhyolite, previously referred to as gives an age of 390 Ma. The only outcrop found in this study is at the Quoyelsh promontory. The rhyolite seems to occur as three beds, with rhyolite conglomerate in between. This shows that the rhyolites were extrusive. It is proposed that the rhyolite beds marks the beginning of the Old Red Sandstone basin.

6.2 Orkney granite complex

6.2.1 Age relation between the grey and the pink granite

The intrusive relationship in the field demonstrates that the pink granite is relatively younger than the grey granite. The age of the grey granite is 431.93 ± 0.46 Ma age and the age of the pink granite is 430.26 ± 0.92 Ma. The geochemical signatures of the granites are similar (e.g. Figure 72), particularly with respect to the enrichment in e.g. Ba and Sr, further supporting a relation between the two granites. The shared fabric in the two granites indicates that both of them predates or are coeval with fabric formation.

6.2.2 Deformation

All the basement outcrops, at Stromness, Yesnaby and Graemsay, have the two types of granites, the grey granite and the pink granite. In each location, xenoliths of gneiss are observed. In Yesnaby, the foliation measurements in the gneiss differ from the foliation in the surrounding granite. In the Yesnaby shear zone area, the foliation in the gneiss is cut with relatively high angle by the granite. These observations are not in line with previous work made by Strachan (2003), that states that the foliation in the granite and the gneiss is highly similar, and that the foliation in the gneiss is only seen to be cut *obliquely* in some areas.

Between the different locations, the structural data has clear similarities. The degree of how strongly foliate the granites are, are similar between the localities. However, the foliation in the granites at Graemsay and Stromness has a main dip direction in southerly direction, and at the upper area at Yesnaby, the dip direction is more easterly directed. The dip varies between 25-40°.

Shear zone are observed at all three locations. In the shear zone areas at Stromness there are top-to-south extensional mylonite, phyllonite and brittle faulting. The mylonites are overprinted by phyllonites, and brittle faults overprint both. At Yesnaby, top-to-north extensional mylonites are overprinted by similarly oriented phyllonites. Further, both grey and pink granite is observed cutting through the mylonite, and being sheared in the mylonite. This indicates that the formation of the granite was syn-tectonic. Similar to all localities is that the foliation in the granite near a shear zone is intensified and reoriented to parallel with the shear zone, which shows that it has been clearly affected by the shear deformation. This is implying that the extension observed in the shear zones have occurred around the same time interval as the granites intruded.

The similar features and structural properties of the granites indicates that all the observed granites belongs to one plutonic system, with syn-kinematic emplacement in an extensional setting of the grey granite at ca. 432 and of the pink granite at ca. 430 Ma.

6.3 Geochemical signature

6.3.1 Tectonic discrimination diagram

Y+Nb vs Rb – diagram

Interpretation of the tectonic environment is based on the discrimination diagram of Pearce et al. (1984). A plot of Y+Nb vs Rb content in the Orkney granites show that all plot in the field of volcanic arc granites (VAG). Thus, the simplest interpretation is that the Orkney granite complex was formed in a volcanic arc setting (for more considerations with regards to this interpretation; see result section).

However, the most common dispersion of syn-collisional granites is into the VAG field, for example as a function of less mature source rocks (arc-inheritance) or of a low level of fractionation. Thus, a collisional setting for the Orkney granites could not be entirely ruled out. The age of the granites could be considered to correlate well with both a volcanic arc setting and a collision zone setting.

6.3.2 REE patterns

Based on Fowler et al. (2008) rocks with the petrogenesis of ‘normal’ I and S-type granites” will have gently-fractionated patterns (La/Yb ratios commonly 10–15) with substantial negative Eu anomalies. The REE-plot of the Orkney granites (Figure) show steeply inclined patterns (highly fractionated La/Yb ratios), and lacks Eu anomalies. This suggests a different petrogenesis of the Orkney granites from typical I and S-type granites. Further, the REE-patterns are to a large extent similar to the granites of the high Ba-Sr granites presented in Fowler et al. (2008). These similarities are further discussed in the next section.

6.3.3 High Ba-Sr granite

The occurrences of High Ba Sr granites north of the Great Glen fault are shown in Figure 4 and provides a line of outcrop areas that runs NE parallel with the Great Glen Fault. The occurrence of similar granites in Orkney is compatible with the alignment in the NE direction along the Great Glen Fault.

In any one region, the High Ba-Sr type or the low Ba-Sr (i.e. “normal” granites) tends to be exclusively developed. The High Ba-Sr granitoids dominate in the Archaean and the Low Ba-Sr type is equally dominant in the mid-Proterozoic, and much of the Palaeozoic (Tarney and Jones, 1994). An important exception to this is the High Ba-Sr granites found in West

Scotland (Tarney and Jones, 1994). Studies of the petrogenesis of high Ba-Sr plutons from the Northern Highlands of the British Caledonian Province have been done by Fowler et al. (2008). The geochemistry and age estimates of the plutons of the High Ba-Sr granites studied by Fowler et al. (2008) are presented below.

The geochemical data from the granites on Orkney are compared with the criteria's for high Ba-Sr granite from Tarney and Jones (1994).

Table 3 - Comparison of the Orkney granites with the High Ba-Sr granite criteria's given by Tarney and Jones (1994)

Characteristic, data from Tarney and Jones (1994)	Geochemical data from granites of Orkney	Check box for criteria
High Ba-Sr	Granites plot within Ba-Sr area	✓
Low Rb	Rb values between 74.8-125.5 ppm	✓
High K/Rb ratio	K/Rb ratios between 2.79×10^2 - 4.28×10^2	✓
Low Th and U	Values of Th between 4.4-19.4 ppm, values of U between 1.17-2.41 ppm	X
Negative Nb anomaly	Negative Nb in Multielement diagram	✓
Low Y	Y value between 3.7-10.5 ppm	✓
Low HREE	HREE data are low and matches data from Tarney and Jones	✓

Five of the six criteria are met based on geochemistry of the Orkney granites. Tarney and Jones (1994) stated that some geochemical variation will occur. Based on the geochemical signature the granites are thus classified as *High Ba-Sr granites* (sensu Tarney and Jones, 1994).

The age estimates of the plutons of the High Ba-Sr granites studied by Fowler et al. (2008) are presented in Table 4.

Table 4 - Age of the high Ba-Sr plutons from Fowler et al (2008).

Northern Highland plutons	Age estimate & and method
Strath Halladale	423±2 U-Pb monazite
Helmsdale	c. 420 K-Ar whole rock
Rogart	c. 420 K-Ar whole rock
Loch Borralan	430 ±4 U-Pb bulk zircon
Ratagain	425±3 U-Pb bulk zircon
Cluanie	425±4 Rb-Sr whole rock
Clunes	427.9±1.8 U-Pb single grain zircon TIMS
Strontian	425±3 U-Pb bulk zircon

Fowler et al. (2008) also studied three syenite plutons. However, on Orkney, only the calc-alkaline granites have been observed and thus, only the granites are mentioned for comparison here.

These age estimates varies in quality and reliability. The most precise and accurate method is the U-Pb- single grain zircon TIMS. This is utilized on the Clunes pluton providing an age of formation that overlap within error with the age estimates at the Orkney granite complex. The Rb-Sr whole rock, used at the Cluanie pluton, gives more unprecise age estimates that hold less reliability.

Thus, by considering of age, the granites from Orkney *could fit with being part of the High-Ba-Sr granites* although extending the age estimate of the High Ba-Sr magmatism slightly towards 431 Ma.

6.3.4 Fractionation mechanisms

Datasets from the plutons studied by Fowler et al. (2008) have been used to investigate the magma sources and place constraints on the fractionation mechanisms. Nd-Sr isotope covariations form well-defined clusters that could fit with rock formation occurring within a

host rock from the Moine group. This also indicates that Moine rocks could be incorporated during melt evolution in mid-upper crustal magma chambers (Fowler et al., 2008).

The plutons studied by Fowler et al. (2008) are thought to represent complex pluton assembly that could involve several pulses of magma, with different degree and rate of contamination. This is thought to explain the low degree of correlation of the radiogenic isotope to silica relationship between the plutons.

An alternative hypothesis for granite petrogenesis is melting of basaltic crust. Tarney and Jones (1994) presented the explanation that mafic magma undergoes hydrous melting and that the crust is underplated by these mafic magmas. High Ba-Sr signature would be consistent with this model, but several other aspects of the chemistry would not.

With the Orkney granites being placed within the High Ba Sr group of rocks, these mechanisms can likely be applied here as well. Thus, analogous to Fowler et al.'s (2008) interpretation, the elemental signatures of the Orkney granites are proposed to reflect evolution from mafic magmas derived from a mantle source contamination with pelagic sediment, which underwent fractional crystallization of a feldspathic assemblage in mid-crustal magma chambers. Here, crustal assimilation of Moine type rocks took place. Different degrees of contamination could potentially be the cause of the more enriched geochemical signature in the grey compared to the pink granite on Orkney,

6.4 Regional comparisons

6.4.1 Tectonic movements – Scandian phase

The granite is dated to the Scandian phase of the Caledonian orogeny. Thus, the large scale tectonic setting during the granite formation is the Scandian oblique collision between Laurentia and Baltica. Direction of thrusting during this period is NW-SE.

Older weaker structures in the lithosphere could be reactivated during a collisional event. In NW Scotland, crustal thickening is considered to have been partly overlapping in time with, and partly followed by major sinistral displacements along orogen-parallel strike-slip faults such as the Great Glen Fault Zone (Stewart et al., 1999). This have led to a transition from a

regime of sinistral transpression to a regime of transtension ((Dewey and Strachan, 2003) and resulted in the juxtaposition of the Scottish segment of Laurentia with Avalonia (Coward, 1990). Stewart et al. (1999) propose that sinistral displacements along the Great Glen Fault Zone occurred more or less continuously during oblique convergence and uplift from about 428 Ma until 400-390 Ma.

The granites on Orkney are contemporaneous with the alkaline magmatism in Assynt, which dates the last movements along the Moine thrust (Goodenough et al. 2011). This last push along the Moine thrust is dated from deformed granitoids at 430 ± 0.5 Ma, and from post-kinematic magmatism at 429 ± 0.5 .

6.4.2 Magma emplacement during the Scandian phase

The granite formation during a thrusting phase would need some channel for magmas to intrude through. During an oblique collision there can be zones with extension. The zones of extension can provide space for the magmas to intrude. According to Holdsworth et al. (2015) igneous activity and associated mineralization in the Northern and Grampian highlands related to slab breakoff were associated with this transition from sinistral transpression to transtension, so that earlier granites were syntectonically emplaced along Scandian thrusts (e.g. Naver Thrust) and later volumetrically larger volumes of melt were emplaced along steeply dipping strike-slip or normal faults (e.g. Great Glen Fault Zone).

The extensional (NNW-SSE directed) setting during the formation of the Orkney granite complex is difficult to understand in terms of the NW-SE directed Scandian compression, or as a pull-apart directly related to movements on the Great Glen fault (which should result in roughly NE-SW extension), but could be compatible with pull-aparts associated with antithetic shear zones associated with the sinistral Great Glen fault movement. Other granite plutons with similar structures (i.e. syn-kinematic), petrology (i.e. High Ba Sr signatures) and ages (i.e. Scandian) as the Orkney granite complex north of the Great Glen Fault have been interpreted in this way, by for example Holdsworth et al. (2015).

6.4.3 Other plutons emplaced during the Scandian phase

Strike slip and extension north of the great Glen Fault has been interpreted by Holdsworth et al. (2015). Inferred buried structures (based on geological, geophysical or geochemical

alignments) are seen as shear that define regional-scale transverse lineaments that run generally at high angles to orogenic strike. Such a line is the *Loch Shin Line* that follows a strong NW-SE gravity gradient (Holdsworth et al., 2015). The Loch Shin Line is associated with an anomalous zone of mantle derived appinites granites and brittle faulting, SE of the Moine Thrust on the north side of the Assynt Culmination.

Field observations, microstructural studies, U-Pb zircon and Re-Os molybdenite geochronology and fluid inclusion analyses from Holdsworth et al. (2015), have shown that a suite of granite plutons (most important the Grudie, Loch Shin and Rogart pluton) have intruded in the mid-Silurian (c.430-425 Ma). The associated faulting is interpreted to be antithetic to regional sinistral strike-slip movements along the NE-SW trending Great Glen Fault Zone.

Watson (1984) suggested the “Loch Shin Line” to be a shear zone that controlled the siting and ascent of magmas and associated mineralization during the Silurian. Zircon U-Pb dating of various synkinematic igneous intrusions constrains thrust movements to c. 435-425 Ma (Kinny et al., 2003, Goodenough et al., 2011).

Samples of Loch Shin Granite from the SW shore of Loch Shin have been selected for La-ICP-MS geochronology. The majority of the analyzed grains yield Silurian ages (as the Orkney granite complex). Although there is some age ranging from 1725-1771Ma inferred as older grains from host rock.

A concordia age from a younger group of prismatic zircons is taken as the best estimate of intrusion age of the Loch Shin granite. This intrusion is dated to 427 ± 3.7 Ma.

The findings in Holdsworth et al. (2015) support the existence of the *NW-SE trending Loch shin Line* and the hypothesis of Watson (1984) that it has acted as deep crustal channelway controlling the ascent and emplacement of Silurian granitic and appinitic magmas into the overlying Moine Nappe.

6.4.4 Tectonic model for magma emplacement of the Orkney granite complex

Analogous with the Loch shin line, an antithetic fault to the Great Glen Fault is proposed to explain the extensional setting at Orkney Islands.

Strike slip and extension in the NS direction occurs throughout exhumation of the granites, as shown by the overprinting of the extensional mylonite zones by phyllonite and brittle faults, all with matching orientations and shear sense directions.

A combined model with the delamination model from Miles et al. (2016) as the trigger mechanism and source for mantle products creating the High Ba-Sr signature, combined with Anti-Riedel strike slip faulting as the channeling and space creating mechanism reason for the Orkney Granite complex is presented in Figure 77.

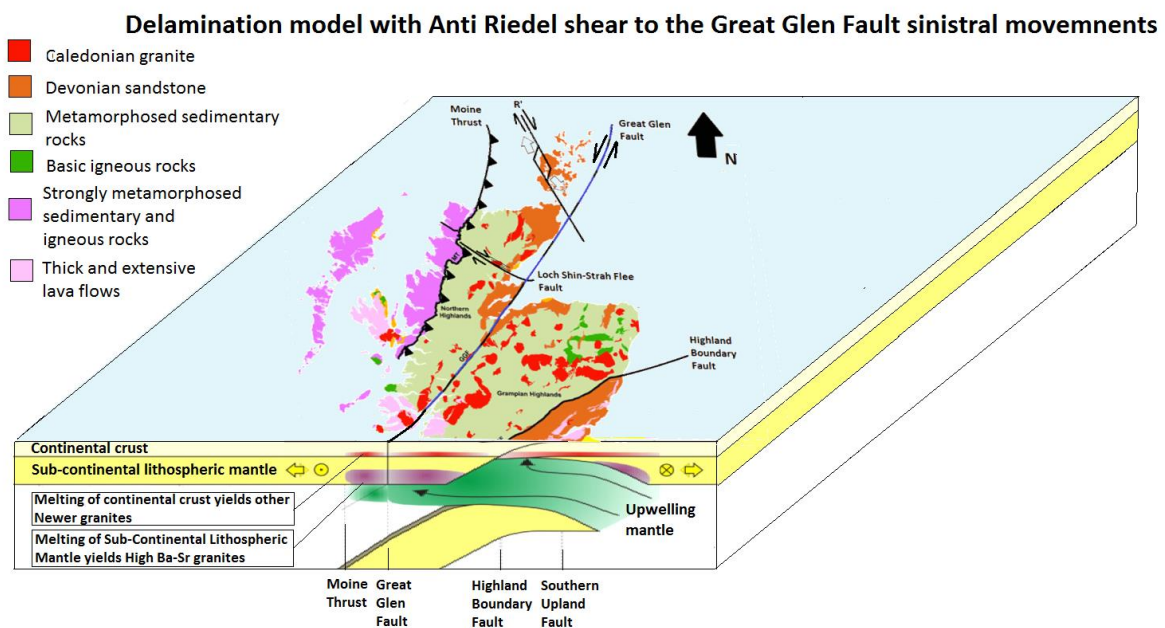


Figure 77 – Delamination model with Anti Riedel shear to the Great Glen Fault sinistral movements. Tectonic model is modified from Miles et al. (2016), and the simplified geological map of Scotland is modified from Bridge (2016)

6.4.5 Exhumation history

Figure provides a tectonic setting allowing intrusion and exhumation of the Orkney granite complex. The dating of the oldest granite (the grey granite) constrains the beginning of the formation to 431.93 ± 0.46 Ma, with continued magmatism and extensional shear on the mylonite zones dated by pink granite to ca. 430 Ma .

The field observations of the extensional mylonite zones, overprinted by phyllonite, and finally by brittle faults, reveals exhumation of the rock complex over time (phyllonites being formed at shallower depths than mylonites). Late phases of the granite magmatism (pegmatite and aplite) are cutting through the mylonite, but are cut by the phyllonite (e.g. Figure 33).

The exhumation from mid-crustal mylonites via phyllonites to brittle faulting at shallow crustal depth could have been fast and continuous, causing the mylonite, phyllonite and brittle faulting over a short time interval. This would imply that between the exhumation of the granites, and the formation of the felsite there is a large time gap.

Alternatively, the deformation occurred in short pulses over a long time interval (potentially the entire Scandian phase), as the strike slip faults were repeatedly reactivated during the orogeny. In this scenario the granite complex could have been partly exhumed as part of the stacking of thrust sheets, uplift caused by delamination, and orogenic collapse, with the extensional shear zones contributing to the extension. This explanation would seem more easily compatible with the limited amount of deformation observed relating to the Orkney shear zones (which are after all only some meters or 10's of meters thick), and the large amount of exhumation required to raise the granite complex from mid-crustal levels to the surface by the time of rhyolite magmatism at 390 Ma. Thus, this is the explanation held as the most likely.

This exhumation story is summarized in Figure 78. In the figure, the fifth stage shows the formation of the Hara Ebb formation. The Hara Ebb formation, unconformably overlying the granite and containing numerous granite clasts attributable to the grey and pink granites, varies in thickness between the localities investigated on the island. The thickest deposits are measured at Graemsay, with a stratigraphical thickness of the conglomerate layer of 30 meters, and the thinnest is measured at Stromness of around 3-10 meters. This is compatible with derivation Hara Ebb formation from elevated and exposed areas of the granite (pers. comm. John Brown, 2016) in the center of the investigated field area. The setting of the rhyolite magmatism is discussed in the next chapter.

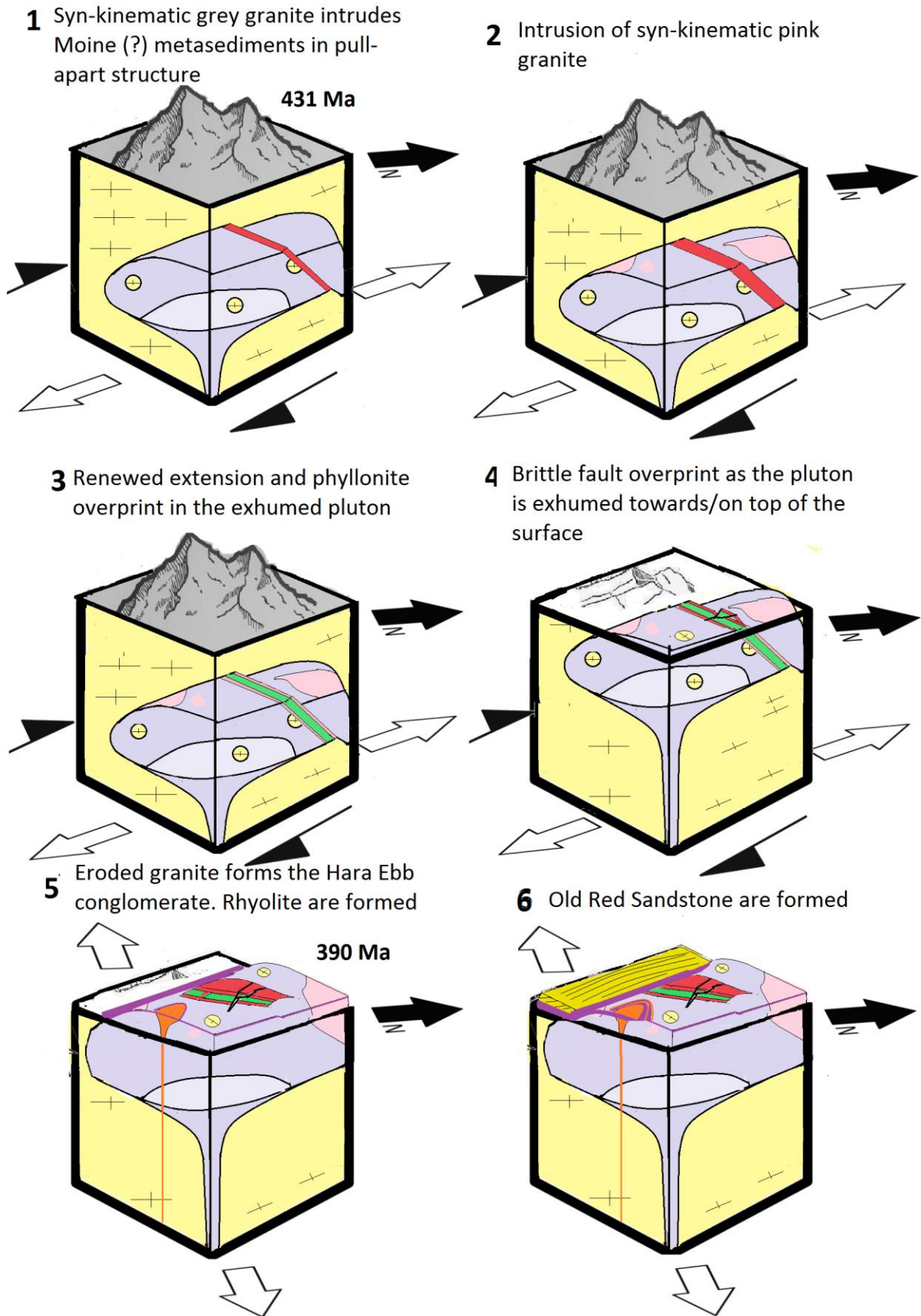


Figure 78 – Interpreted history of the Orkney Granite complex

6.5 Tectonic setting during Rhyolite formation

The rhyolite magmatism could have occurred as a result of yet another pulse of movement on the Great Glen Fault and its subsidiary faults at around 390 Ma, which could have triggered magmatism, local subsidence and the initiation of deposition of the Old Red Sandstone on the Orkney Islands. However, at this time regional extension was taking place in the central Caledonides Fossen (2010) suggesting that there is little need to invoke strike slip movements to explain extension on the Orkneys. Furthermore, strike slip movements such as those proposed for the granite formation and exhumation are not able to explain the creation of the large extensional basin in which the Old Red sandstone was deposited in the Devonian. This basin, the Orcadian basin, forms part of a basin system that extends from Scotland to East Greenland, Svalbard and the Norwegian Devonian basins (Fossen, 2010). The basin system is therefore not to scale with the much smaller basins envisaged for the proposed anti Riedel movements. According to Fossen (2010) the main Devonian extension in the southern part of the North Atlantic was postcontractional, while strike slip movements was occurring further north.

Throughout the outcrops at the promontory, the rhyolite seems to occur as three layers. Separating the layers is conglomerate in between.

Within one of the rhyolite layers it is observed rounded clasts. These clasts are interpreted to originate from rhyolite from a previous layer. The flowbanding in these clasts differ from the flowbanding in the rhyolite layer itself. The layer of rhyolite on top of the conglomerate sank into the conglomerate (Figure 46). Thus, the conglomerate was formed before the overlying rhyolite, implying several stages of rhyolitic eruptions. Illustration of a hypothesized stratigraphic record is presented in Figure 49.

The erosion of the beds of rhyolite to form the coarse conglomerate between eruptions indicates lava eruption *above sea-level*. This suggests that the rhyolites formed before the Old Red Sandstone basins covered the Orkney Islands. Thus, the rhyolite layers are suggested to pre-date the Old Red sandstone formation, but were likely contemporary with the Hara Ebb deposits since most of the rhyolites appear to have been removed by erosion, but some still remain. Thus, the rhyolites constrain the basins subsidence to occur after 390.35 ± 0.39 Ma.

7 Conclusions

Studies of the basement on Mainland Orkney and Graemsay give clues for several stages of rock formation, with the oldest rocks being metasedimentary gneisses. Their appearance and mineralogy, in addition to inherited zircons with ages between 900-1300Ma that are interpreted to derive from the para gneisses, all point to the metasedimentary gneisses belonging to Moine schists.

These rocks have later been intruded by High Ba Sr granitic rocks during the Caledonian Orogeny. This led to formation of two main phases of granite, each cut by later phases of aplite and pegmatite. The metasedimentary gneisses occur as xenoliths in the granites. The number of xenoliths increases towards the margins of the granite outcrops, suggesting that the margins of the plutons are nearby. Geochronology by U-Pb single grain zircon TIMS method, yield estimates at 431.93 ± 0.46 & 430.26 ± 0.92 Ma of granite formation. This places the magmatism in the Scandian phase of the Caledonian orogeny.

Field work revealing extensional shear zones and faults points to an extensional setting during the granite formation. However, the tectonic regime on a large scale point to formation during the collisional setting of the Scandian phase. Strike-slip displacement along a subsidiary fault to the Great Glen Fault is suggested as an explanation of the apparent contradiction (Figure 66). Thus, the slab breakoff proposed by Atherton and Ghani explains the geochemical signature of the granites and acts as the trigger mechanism for the magmatic activity, whereas the strike-slip deformation provides the pathway for the granites and aid their exhumation.

The Felsite layers observed at Stromness beach are proposed to occur as three beds with conglomerate in between, predating the Old Red Sandstone, but possibly contemporary with the Hara Ebb formation. If so, the age of the felsite layers, dated by U-Pb single grain zircon TIMS method to 390.35 ± 0.39 Ma, constrains the age of the basin formation and the deposition of the Old Red Sandstone on Orkney. However, the presence of underlying sandstone cannot be conclusively ruled out.

Reference list

- ASTIN, T. 1990. The Devonian lacustrine sediments of Orkney, Scotland; implications for climate cyclicity, basin structure and maturation history. *Journal of the Geological Society*, 147, 141-151.
- ATHERTON, M. & GHANI, A. 2002. Slab breakoff: a model for Caledonian, Late Granite syn-collisional magmatism in the orthotectonic (metamorphic) zone of Scotland and Donegal, Ireland. *Lithos*, 62, 65-85.
- BARBARIN, B. 1990. Granitoids: main petrogenetic classifications in relation to origin and tectonic setting. *Geological Journal*, 25, 227-238.
- BLUCK, B. 1983. Role of the Midland Valley of Scotland in the Caledonian orogeny. *Transactions of the Royal Society of Edinburgh: Earth Sciences*, 74, 119-136.
- BLUCK, B., COPE, J. & SCRUTTON, C. 1992. Devonian. *Geological Society, London, Memoirs*, 13, 57-66.
- BONSOR, H. & PRAVE, A. 2008. The Upper Morar Psammite of the Moine Supergroup, Ardnamurchan Peninsula, Scotland: depositional setting, tectonic implications. *Scottish Journal of Geology*, 44, 111-122.
- BRIDEN, J., TURNELL, H. & WATTS, D. 1984. British paleomagnetism, Iapetus Ocean, and the Great Glen fault. *Geology*, 12, 428-431.
- BRIDGE, L. 2016. *Geologia d'Escòcia* [Online]. Myotragus' Weblog: Bridge, L. . Available: <https://myotragus.wordpress.com/2016/08/12/geologia-descocia/#more-1189> [Accessed 10.05 2017].
- BROWN, G., THORPE, R. & WEBB, P. 1984. The geochemical characteristics of granitoids in contrasting arcs and comments on magma sources. *Journal of the Geological Society*, 141, 413-426.
- BROWN, J. F. 2017. Basement of Quoyelsh Felsite.
- BROWN, P., RYAN, P., SOPER, N. & WOODCOCK, N. 2008. The Newer Granite problem revisited: a transtensional origin for the Early Devonian trans-suture suite. *Geological Magazine*, 145, 235-256.
- CHAPPELL, B. & WHITE, A. 1974. Two contrasting granite types. *Pacific geology*, 8, 173-174.
- COWARD, M. 1990. The Precambrian, Caledonian and Variscan framework to NW Europe. *Geological Society, London, Special Publications*, 55, 1-34.
- COX, K., BELL, J. & PANKHURST, R. 1979. Phase diagrams—introduction. *The Interpretation of Igneous Rocks*. Springer.
- DALLMEYER, R., STRACHAN, R., ROGERS, G., WATT, G. & FRIEND, C. 2001. Dating deformation and cooling in the Caledonian thrust nappes of north Sutherland, Scotland: insights from $^{40}\text{Ar}/^{39}\text{Ar}$ and Rb–Sr chronology. *Journal of the Geological Society*, 158, 501-512.
- DEMPSTER, T., ROGERS, G., TANNER, P., BLUCK, B., MUIR, R., REDWOOD, S., IRELAND, T. & PATERSON, B. 2002. Timing of deposition, orogenesis and glaciation within the Dalradian rocks of Scotland: constraints from U–Pb zircon ages. *Journal of the Geological Society*, 159, 83-94.
- DEWEY, J. & MANGE, M. 1999. Petrography of Ordovician and Silurian sediments in the western Irish Caledonides: tracers of a short-lived Ordovician continent-arc collision orogeny and the evolution of the Laurentian Appalachian-Caledonian margin. *Geological Society, London, Special Publications*, 164, 55-107.

- DEWEY, J. & STRACHAN, R. 2003. Changing Silurian–Devonian relative plate motion in the Caledonides: sinistral transpression to sinistral transtension. *Journal of the Geological Society*, 160, 219-229.
- DEWEY, J. F., DALZIEL, I. W., REAVY, R. J. & STRACHAN, R. A. 2015. The Neoproterozoic to Mid-Devonian evolution of Scotland: a review and unresolved issues. *Scottish Journal of Geology*, 51, 5-30.
- DEWEY, J. F. & SHACKLETON, R. M. 1984. A model for the evolution of the Grampian tract in the early Caledonides and Appalachians. *Nature*, 312, 115-121.
- EARTHTIME Earthtime
- FOSSON, H. 2010. Extensional tectonics in the North Atlantic Caledonides: a regional view. *Geological Society, London, Special Publications*, 335, 767-793.
- FOWLER, M., HENNEY, P., DARBYSHIRE, D. & GREENWOOD, P. 2001. Petrogenesis of high Ba–Sr granites: the Rogart pluton, Sutherland. *Journal of the Geological Society*, 158, 521-534.
- FOWLER, M., KOCKS, H., DARBYSHIRE, D. & GREENWOOD, P. 2008. Petrogenesis of high Ba–Sr plutons from the northern highlands Terrane of the British Caledonian Province. *Lithos*, 105, 129-148.
- FRIEND, P. F., WILLIAMS, B., FORD, M. & WILLIAMS, E. 2000. Kinematics and dynamics of Old Red Sandstone basins. *Geological Society, London, Special Publications*, 180, 29-60.
- FÖRSTER, H.-J., TISCHENDORF, G. & TRUMBULL, R. 1997. An evaluation of the Rb vs.(Y+ Nb) discrimination diagram to infer tectonic setting of silicic igneous rocks. *Lithos*, 40, 261-293.
- GALLAGHER, M., MICHIE, U. M., SMITH, R. & HAYNES, L. 1971. NEW EVIDENCE OF URANIUM AND OTHER MINERALIZATION IN SCOTLAND. Inst. of Geological Sciences, London.
- GILLEN, C. 2003. *Geology and landscapes of Scotland*, Terra Publishing (UK).
- GOODENOUGH, K., MILLAR, I., STRACHAN, R., KRABBENDAM, M. & EVANS, J. 2011. Timing of regional deformation and development of the Moine Thrust Zone in the Scottish Caledonides: constraints from the U–Pb geochronology of alkaline intrusions. *Journal of the Geological Society*, 168, 99-114.
- HALLIDAY, A., STEPHENS, W., HUNTER, R., MENZIES, M., DICKIN, A. & HAMILTON, P. 1985. Isotopic and chemical constraints on the building of the deep Scottish lithosphere. *Scottish Journal of Geology*, 21, 465-491.
- HOLDSWORTH, R., DEMPSEY, E., SELBY, D., DARLING, J. R., FEELY, M., COSTANZO, A., STRACHAN, R. A., WATERS, P., FINLAY, A. & PORTER, S. 2015. Silurian–Devonian magmatism, mineralization, regional exhumation and brittle strike-slip deformation along the Loch Shin Line, NW Scotland. *Journal of the Geological Society*, 172, 748-762.
- HUTTON, D. H. 1987. Strike-slip terranes and a model for the evolution of the British and Irish Caledonides. *Geological Magazine*, 124, 405-425.
- JACQUES, J. & REAVY, R. 1994. Caledonian plutonism and major lineaments in the SW Scottish Highlands. *Journal of the Geological Society*, 151, 955-969.
- JAFFEY, A., FLYNN, K., GLENDENIN, L., BENTLEY, W. T. & ESSLING, A. 1971. Precision measurement of half-lives and specific activities of U 235 and U 238. *Physical Review C*, 4, 1889.
- KINNY, P., FRIEND, C., STRACHAN, R., WATT, G. & BURNS, I. 1999. U–Pb geochronology of regional migmatites in East Sutherland, Scotland: evidence for crustal melting during the Caledonian orogeny. *Journal of the Geological Society*, 156, 1143-1152.

- KINNY, P., STRACHAN, R., FRIEND, C., KOCKS, H., ROGERS, G. & PATERSON, B. 2003. U–Pb geochronology of deformed metagranites in central Sutherland, Scotland: evidence for widespread late Silurian metamorphism and ductile deformation of the Moine Supergroup during the Caledonian orogeny. *Journal of the Geological Society*, 160, 259-269.
- KOCKS, H. 2002. *Structural setting and petrogenesis of Silurian granites in the Caledonides of northern Scotland*. Oxford Brookes University.
- KRABBENDAM, M., PRAVE, T. & CHEER, D. 2008. A fluvial origin for the Neoproterozoic Morar Group, NW Scotland; implications for Torridon–Morar Group correlation and the Grenville Orogen foreland basin. *Journal of the Geological Society*, 165, 379-394.
- KROGH, T. 1982. Improved accuracy of U-Pb zircon ages by the creation of more concordant systems using an air abrasion technique. *Geochimica et Cosmochimica Acta*, 46, 637-649.
- LE BAS, M. J., LE MAITRE, R., STRECKEISEN, A. & ZANETTIN, B. 1986. A chemical classification of volcanic rocks based on the total alkali-silica diagram. *Journal of petrology*, 27, 745-750.
- LE ROUX, L. & GLENDENIN, L. Half-life of ^{232}Th . Proceedings of the National Meeting on Nuclear Energy, Pretoria, South Africa, 1963. 83-94.
- LEGGETT, J., MCKERROW, W. T. & EALES, M. 1979. The Southern Uplands of Scotland: a lower Palaeozoic accretionary prism. *Journal of the Geological Society*, 136, 755-770.
- LESLIE, A. G., ROBERTSON, S., SMITH, M., BANKS, C. J., MENDUM, J. R. & STEPHENSON, D. 2013. The Dalradian rocks of the northern Grampian Highlands of Scotland. *Proceedings of the Geologists' Association*, 124, 263-317.
- LI, Z.-X., BOGDANOVA, S., COLLINS, A., DAVIDSON, A., DE WAELE, B., ERNST, R., FITZSIMONS, I., FUCK, R., GLADKOCHUB, D. & JACOBS, J. 2008. Assembly, configuration, and break-up history of Rodinia: a synthesis. *Precambrian research*, 160, 179-210.
- LUNDMARK, A. M., GABRIELSEN, R. H. & BROWN, J. F. 2011. Zircon U–Pb age for the Orkney lamprophyre dyke swarm, Scotland, and relations to Permo-Carboniferous magmatism in northwestern Europe. *Journal of the Geological Society*, 168, 1233-1236.
- MACDONALD, F., RYAN-DAVIS, J., COISH, R., CROWLEY, J. & KARABINOS, P. 2014. A newly identified Gondwanan terrane in the northern Appalachian Mountains: Implications for the Taconic orogeny and closure of the Iapetus Ocean. *Geology*, 42, 539-542.
- MATTINSON, J. M. 1987. U · Pb ages of zircons: A basic examination of error propagation. *Chemical Geology: Isotope Geoscience section*, 66, 151-162.
- MATTINSON, J. M. 2005. Zircon U–Pb chemical abrasion (“CA-TIMS”) method: combined annealing and multi-step partial dissolution analysis for improved precision and accuracy of zircon ages. *Chemical Geology*, 220, 47-66.
- MCKERROW, W., MAC NIOCAILL, C. & DEWEY, J. 2000. The Caledonian orogeny redefined. *Journal of the Geological Society*, 157, 1149-1154.
- MILES, A., WOODCOCK, N. & HAWKESWORTH, C. 2016. Tectonic controls on post-subduction granite genesis and emplacement: The late Caledonian suite of Britain and Ireland. *Gondwana Research*, 39, 250-260.
- MYKURA, W., FLINN, D. & MAY, F. 1976. *British regional geology: Orkney and Shetland*, Stationery Office Books (TSO).

- NANCE, R. D., MURPHY, J. B. & KEPPIE, J. D. 2002. A Cordilleran model for the evolution of Avalonia. *Tectonophysics*, 352, 11-31.
- NEILSON, J., KOKELAAR, B. & CROWLEY, Q. 2009. Timing, relations and cause of plutonic and volcanic activity of the Siluro-Devonian post-collision magmatic episode in the Grampian Terrane, Scotland. *Journal of the Geological Society*, 166, 545-561.
- O'BRIEN, C. 1985. *The petrogenesis and geochemistry of the British Caledonian granites, with special reference to mineralized intrusions*. University of Leicester.
- PARRISH, R. R. & NOBLE, S. R. 2003. Zircon U-Th-Pb geochronology by isotope dilution—thermal ionization mass spectrometry (ID-TIMS). *Reviews in Mineralogy and Geochemistry*, 53, 183-213.
- PEARCE, J. A., HARRIS, N. B. & TINDLE, A. G. 1984. Trace element discrimination diagrams for the tectonic interpretation of granitic rocks. *Journal of petrology*, 25, 956-983.
- PRAVE, A., FALLICK, A., THOMAS, C. & GRAHAM, C. 2009. A composite C-isotope profile for the Neoproterozoic Dalradian Supergroup of Scotland and Ireland. *Journal of the Geological Society*, 166, 845-857.
- READ, H. H. 1961. Aspects of Caledonian magmatism in Britain. *Geological Journal*, 2, 653-683.
- RODDICK, J. 1987. Generalized numerical error analysis with applications to geochronology and thermodynamics. *Geochimica et Cosmochimica Acta*, 51, 2129-2135.
- ROGERS, D., MARSHALL, J. & ASTIN, T. 1989. Short Paper: Devonian and later movements on the Great Glen fault system, Scotland. *Journal of the Geological Society*, 146, 369-372.
- ROGERS, G. & SAUNDERS, A. 1989. Magnesian andesites from Mexico, Chile and the Aleutian Islands: implications for magmatism associated with ridge-trench collision. *Boninites and Related Rocks*. Unwin Hyman, London, 416-445.
- SCOTLAND, N. 1987. Tectonic evolution of Devonian basins in northern Scotland and southern Norway. *Norsk Geologisk Tidsskrift*, 67, 323.
- SILVER, L. T. & DEUTSCH, S. 1963. Uranium-lead isotopic variations in zircons: a case study. *The Journal of Geology*, 71, 721-758.
- SMITH, D. & WATSON, J. 1983. Scale and timing of movements on the Great Glen fault, Scotland. *Geology*, 11, 523-526.
- SOPER, N. 1986. The Newer Granite problem: a geotectonic view. *Geological Magazine*, 123, 227-236.
- SOPER, N., HARRIS, A. & STRACHAN, R. 1998. Tectonostratigraphy of the Moine Supergroup: a synthesis. *Journal of the Geological Society*, 155, 13-24.
- SOPER, N. & HUTTON, D. 1984. Late Caledonian sinistral displacements in Britain: implications for a three-plate collision model. *Tectonics*, 3, 781-794.
- STEIGER, R. H. & JÄGER, E. 1977. Subcommittee on geochronology: convention on the use of decay constants in geo- and cosmochronology. *Earth and planetary science letters*, 36, 359-362.
- STEPHENS, M. B. & GEE, D. G. 1989. Terranes and polyphase accretionary history in the Scandinavian Caledonides. *Geological Society of America Special Papers*, 230, 17-30.
- STEPHENS, W. & HALLIDAY, A. 1984. Geochemical contrasts between late Caledonian granitoid plutons of northern, central and southern Scotland. *Transactions of the Royal Society of Edinburgh: Earth Sciences*, 75, 259-273.
- STEWART, M., STRACHAN, R. & HOLDSWORTH, R. 1999. Structure and early kinematic history of the Great Glen Fault Zone, Scotland. *Tectonics*, 18, 326-342.
- STORETVEDT, K. 1974. A possible large-scale sinistral displacement along the Great Glen Fault in Scotland. *Geological Magazine*, 111, 23-30.

- STRACHAN, R. 2003. The metamorphic basement geology of Mainland Orkney and Graemsay. *Scottish Journal of Geology*, 39, 145-149.
- STRACHAN, R., HOLDSWORTH, R., KRABBENDAM, M. & ALSOP, G. 2010. The Moine Supergroup of NW Scotland: insights into the analysis of polyorogenic supracrustal sequences. *Geological Society, London, Special Publications*, 335, 233-254.
- STRACHAN, R., SMITH, M., HARRIS, A. & FETTES, D. 2002. The northern Highland and Grampian terranes. *The Geology of Scotland. Geological Society, London*, 81, 148.
- SUN, S.-S. & MCDONOUGH, W.-S. 1989. Chemical and isotopic systematics of oceanic basalts: implications for mantle composition and processes. *Geological Society, London, Special Publications*, 42, 313-345.
- SVENSEN, H. H., HAMMER, Ø. & CORFU, F. 2015. Astronomically forced cyclicity in the Upper Ordovician and U–Pb ages of interlayered tephra, Oslo Region, Norway. *Palaeogeography, Palaeoclimatology, Palaeoecology*, 418, 150-159.
- TARNEY, J. & JONES, C. 1994. Trace element geochemistry of orogenic igneous rocks and crustal growth models. *Journal of the Geological Society*, 151, 855-868.
- TORSVIK, T., SMETHURST, M., MEERT, J. G., VAN DER VOO, R., MCKERROW, W., BRASIER, M., STURT, B. & WALDERHAUG, H. 1996. Continental break-up and collision in the Neoproterozoic and Palaeozoic—a tale of Baltica and Laurentia. *Earth-Science Reviews*, 40, 229-258.
- VON BLANCKENBURG, F. & DAVIES, J. H. 1996. Feasibility of double slab breakoff (Cretaceous and Tertiary) during the Alpine convergence. *Eclogae Geologicae Helvetiae*, 89, 111-127.
- WATERS, C., BROWNE, M., JONES, N. & SOMERVILLE, I. Midland Valley of Scotland. 2011. Geological Society of London.
- WATSON, J. 1984. The ending of the Caledonian orogeny in Scotland President's anniversary address 1983. *Journal of the Geological Society*, 141, 193-214.
- WILSON, G., EDWARDS, W., KNOX, J., JONES, R. & STEPHENS, J. 1935. The geology of the Orkneys: Mem. *Geol. Surv. Gt. Britain*.
- WINCHESTER, J. A. 1974. The zonal pattern of regional metamorphism in the Scottish Caledonides. *Journal of the Geological Society*, 130, 509-524.
- WINTER JOHN, D. 2010. Principles of Igneous and Metamorphic Petrology.

Appendix

1. Table with geochemical data from rock samples

SAMPLE	Ag	As	Cd	Co	Cu	Li	Mo	Ni	Pb	Sc	Tl	Zn	Ba	Ce	Cr	Cs	Dy	Er	Eu	
DESCRIP	ppm	ppm	ppm	ppm	ppm	ppm	ppm	ppm	ppm	ppm	ppm	ppm	ppm	ppm	ppm	ppm	ppm	ppm	ppm	
A.B. 16-04	<0.5	<5	<0.5	2	7	<10		1	1	31	2	<10	16	964	34.9	20	1.57	1.09	0.37	0.49
A.B. 16-05	<0.5	<5	<0.5	7	8	20		1	7	14	4	10	68	1410	127.5	20	3.42	2.3	1.02	1.34
A.B. 16-06	<0.5	<5	<0.5	4	5	<10		1	6	19	4	<10	14	1230	39.3	20	1.14	2.28	1.27	0.64
A.B. 16-07	<0.5	<5	<0.5	2	3	10	<1		1	27	2	<10	43	808	72	10	1.96	0.91	0.4	0.63
A.B. 16-09	<0.5	<5	<0.5	2	3	<10	<1	<1		33	1	<10	20	1260	28.7	10	1.46	0.74	0.31	0.45
A.B. 16-11	<0.5		5 <0.5	1	5	<10	<1		1	30	1	<10	6	1035	15.7	10	1.58	1.76	0.87	0.65
A.B. 16-16	1.4	181	<0.5	5	10	10		5	14	426	4	<10	76	1855	28.3	50	1.01	1.6	0.88	0.3
A.B. 16-17	0.9	31	<0.5	2	8	10		2	6	229	1	<10	65	359	31.7	10	0.58	1.69	1.1	0.1
A.B. 16-18	0.6	35	<0.5	1	9	<10		1	5	71	1	10	15	1570	43.7	10	0.5	1.88	1.2	0.14
A.B. 16-19	<0.5		102 <0.5	10	11	80		8	19	40	3	<10	63	>10000	14.3	20	0.32	1.65	1.1	0.38
A.B. 16-20	1.1	110	<0.5	7	9	80		10	16	107	2	<10	59	3270	12.7	30	0.47	1.3	0.72	0.33
A.B. 16-21	<0.5		115 0.5	8	9	70		8	20	118	2	<10	94	3170	11.8	20	0.32	1.38	0.79	0.39
A.B. 16-22	0.6	64	<0.5	3	6	20		2	2	68	2	<10	15	902	22.5	10	0.08	2.31	1.27	0.66
A.B. 16-24	1.1	102	<0.5	2	13	170		5	4	230	<1		9	>10000	2.3	20	0.4	0.1	0.12	0.11
A.B. 16-29	<0.5	<5	<0.5	6	8	20	<1		5	20	4	<10	68	1380	110	20	1.8	2.28	1.01	1.18

Gd	Hf	Ho	La	Lu	Nb	Nd	Pr	Rb	Sm	Sn	Sr	Ta	Tb	Th	Tm	U	V	W	Y
ppm	ppm	ppm	ppm	ppm	ppm	ppm	ppm	ppm	ppm	ppm	ppm	ppm	ppm	ppm	ppm	ppm	ppm	ppm	ppm
1.86	1	0.17	17.4	0.04	5.8	14.5	3.95	104.5	3.08	1	355	1.8	0.28	8.78	0.05	1.27	7	1	4.5
3.29	5.1	0.37	76	0.1	12	40.9	12.45	81.5	5.92	2	1030	0.8	0.42	19.15	0.12	2.19	46	1	10.1
2.33	7.5	0.45	17.8	0.18	8.4	15.6	4.32	86.3	3.13	1	254	0.5	0.38	5.23	0.21	1.3	32	1	12.4
1.64	3.9	0.15	43.9	0.05	7.9	21.7	6.73	74.8	3.15	1	654	0.4	0.21	15.5	0.07	1.37	21	1	4.7
1.15	2.6	0.12	14.8	0.05	4.2	9.7	2.89	106.5	1.66	1	410	<0.1	0.18	6.45	0.04	1.17	8	1	3.7
1.36	1.8	0.34	8.5	0.12	2.9	6	1.72	125.5	1.35	1	345	0.2	0.28	4.4	0.13	1.44	8	1	10.1
1.71	4.3	0.34	14.9	0.14	7.8	11.4	3.12	78.6	2.4	1	588	0.5	0.27	6.66	0.13	7.05	32	16	8.6
1.52	2.2	0.39	16.2	0.19	10.3	11.8	3.37	111.5	1.96	2	129.5	0.9	0.28	9.15	0.19	6.02	<5	2	11.5
1.72	3	0.38	22.2	0.18	13.2	13.7	4.3	132	2.31	2	122	1.3	0.31	12.1	0.19	6.23	8	3	10.5
1.61	1.6	0.36	8.3	0.2	1.8	7.3	1.78	24.3	1.81	1	769	0.1	0.29	3.5	0.2	4.43	40	5	13.6
1.44	1.8	0.29	7.9	0.1	3.3	7.8	1.88	34.8	1.91	1	300	0.1	0.25	5.06	0.11	11.35	30	5	8.4
1.7	2	0.27	6.3	0.09	2.2	6.7	1.52	34.6	1.38	1	309	0.1	0.26	4.66	0.11	9.08	29	6	8.2
2.24	1.1	0.46	11.6	0.19	1.3	11.2	2.65	15.6	2.2	1	4330	<0.1	0.38	3.6	0.18	11.85	21	7	13.1
0.24	1.1	0.04	1.2	0.03	1.4	1.4	0.32	20.8	0.44	1	627	<0.1	0.05	3.48	0.02	6.37	12	3	1.4
2.97	5.3	0.42	68.2	0.15	11.8	36.6	11.1	77.1	5.18	2	932	0.7	0.45	19.4	0.15	2.41	40	2	10.5

Yb	Zr	SiO2	Al2O3	Fe2O3	CaO	MgO	Na2O	K2O	Cr2O3	TiO2	MnO	P2O5	SrO	BaO	LOI	Total	Pass75um
ppm	ppm	%	%	%	%	%	%	%	%	%	%	%	%	%	%	%	%
0.29	23	75.3	14.5	1.16	1	0.09	3.66	5.39	<0.01	0.06	0.01	0.02	0.04	0.1	0.23	101.56	89.6
0.82	223	66.5	16.25	3.3	3.28	1.1	4.57	2.73	<0.01	0.48	0.04	0.23	0.11	0.15	1.23	99.97	
1.44	285	77.7	11.65	2.97	1.36	0.24	2.63	3.99	<0.01	0.43	0.03	0.07	0.03	0.13	0.13	101.36	
0.49	144	71.1	14.65	1.89	1.78	0.38	4.46	3.09	<0.01	0.25	0.02	0.11	0.08	0.08	0.38	98.27	
0.32	69	74.4	14.3	1.33	0.84	0.08	3.76	4.89	<0.01	0.12	0.01	0.05	0.06	0.13	0.27	100.24	
0.82	37	74.2	13.9	0.6	1.04	0.07	3	5.85	<0.01	0.05	0.01	0.03	0.04	0.11	0.74	99.64	
1.04	151	84.9	6.93	2.08	0.02	0.14	0.09	4.03	0.01	0.33	0.01	0.11	0.07	0.2	1.26	100.18	
1.23	59	85.9	7.09	1.07	0.02	0.01	0.4	5.65	<0.01	0.05	0.02	0.02	0.01	0.04	0.56	100.84	
1.27	65	79.3	9.65	1.17	0.01	0.01	0.17	8.12	<0.01	0.06	0.01	0.03	0.02	0.17	0.5	99.22	
1.15	64	83.8	2.06	4.84	0.19	0.14	0.23	1.16	<0.01	0.1	0.07	0.06	0.08	4.22	2.86	99.81	
0.73	69	91.4	2.69	2.86	0.17	0.08	0.07	1.57	<0.01	0.17	0.04	0.09	0.03	0.34	1.5	101.01	
0.69	71	88	2.76	3.97	0.31	0.13	0.19	1.64	<0.01	0.12	0.18	0.18	0.03	0.34	2.34	100.19	
1.51	44	29.4	1.24	2.03	34.3	1.89	0.02	0.79	<0.01	0.09	0.18	0.11	0.51	0.09	29.1	99.75	
0.13	37	92	2.03	1.08	0.07	0.03	0.04	0.92	<0.01	0.1	0.01	0.04	0.08	2.03	0.62	99.05	
0.95	211	69.1	16.2	3.28	2.38	1.04	4.74	2.92	<0.01	0.44	0.04	0.21	0.11	0.15	0.48	101.09	